DESIGNING AND ASSESSING MODEL INDEPENDENT TESTS OF DAMA'S MODULATION SIGNAL

Madeleine J. Zurowski

Under the supervision of
Prof Elisabetta Barberio
A/Prof Phillip Urquijo
Prof Rachel Webster

madeleine.zurowski@unimelb.edu.au

MOTIVATION

Lots of past + ongoing work to understand what DAMA have observed.

On the surface, this is "disproved as dark matter" by "model independent" results.

COSINE-100 team find no evidence of dark matter, casting more doubt on DAMA/LIBRA results

Is the end in sight for famous dark matter claim?

New data cast more doubt on controversial result from the DAMA experiment and an alternative explanation of it emerges

A Famous Dark Matter Signal Is Probably Coming From Something Else

An underground experiment in South Korea has turned up nothing, suggesting an intriguing observation fro[m] was a red herring.

By Isaac Schultz | Yesterday 4:

DARK UNIVERSE | NEWS

ANAIS challenges DAMA dark-matter claim

24 March 2021

Mar 4, 2021, 02:00am EST

Goodbye, DAMA/LIBRA: World's Most Controversial Dark Matter Experiment Fails Replication Test

Experiment Casts Doubt on Potential Dark Matter Find

May 27, 2021 • Physics 14, s71

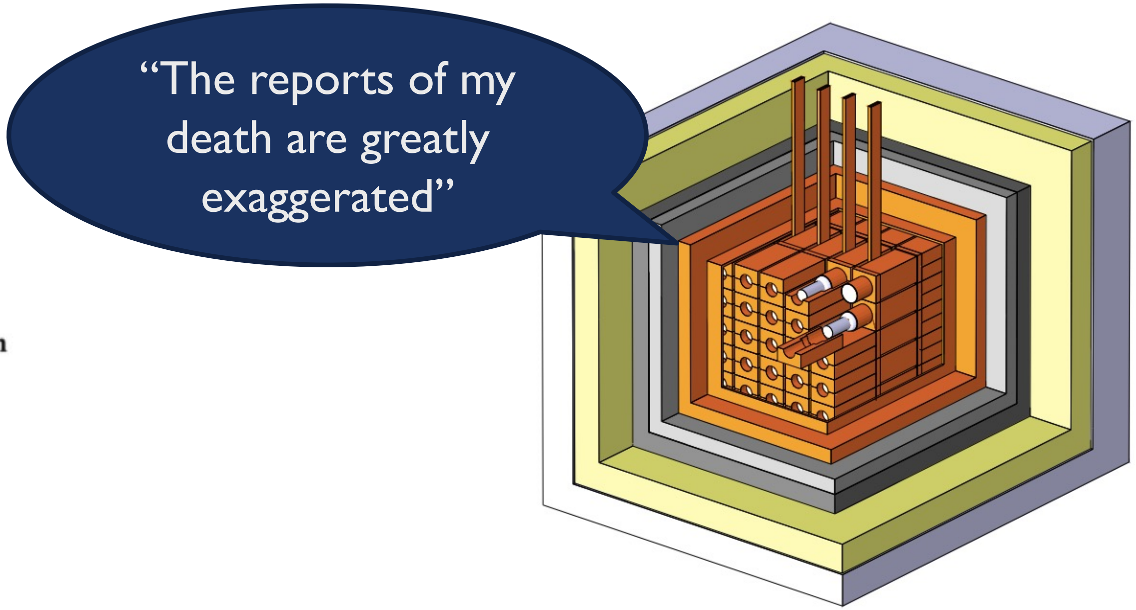

To conclusively say if DAMA is "dead" need to understand how stringent these results are, and necessary steps to design a model independent test.

OUTLINE

- Brief background on dark matter and the DAMA observation
- Assessing performance: explanation of interaction rates and sensitivity formalism
  - Introduction + use of versatile fitting/sensitivity tool
- Model independent tests of DAMA
- Event rate detector dependence
- Discussion of the SABRE detector
  - Background reduction techniques
  - Event reconstruction
  - Digitisation process
  - Future projections

DM EVIDENCE

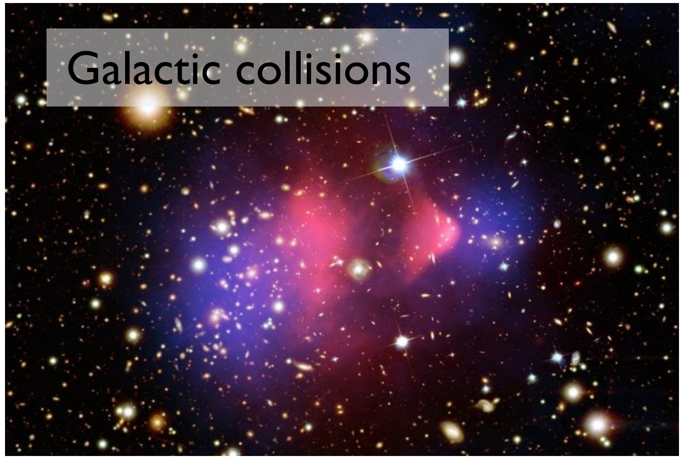
Galactic collisions

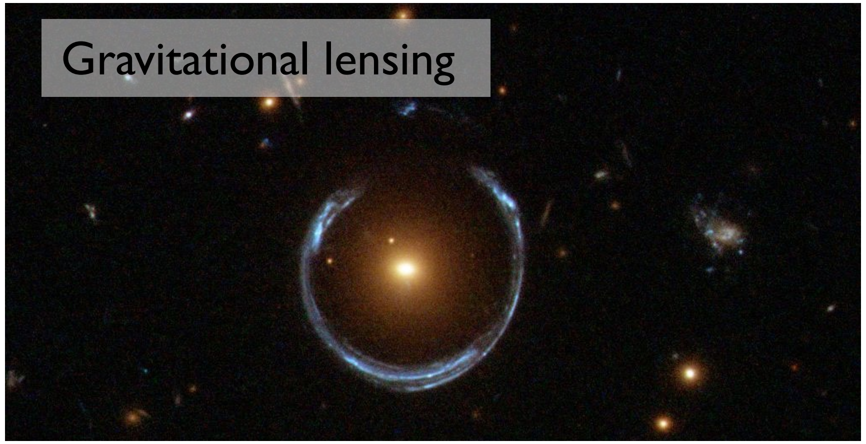
Gravitational lensing

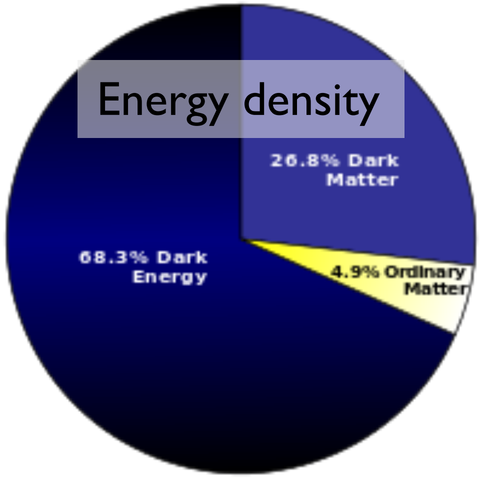
Energy density
26.8% Dark Matter
68.3% Dark Energy
4.9% Ordinary Matter

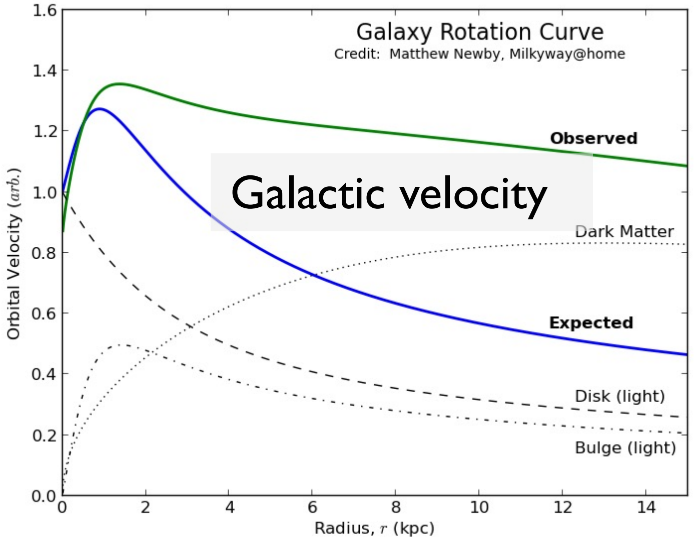
Galaxy Rotation Curve
Credit: Matthew Newby, Milkyway@home
Observed
Galactic velocity
Dark Matter
Expected
Disk (light)
Bulge (light)
Orbital Velocity (arb.)
Radius, r (kpc)
0.0
0.2
0.4
0.6
0.8
1.0
1.2
1.4
1.6
0
2
4
6
8
10
12
14

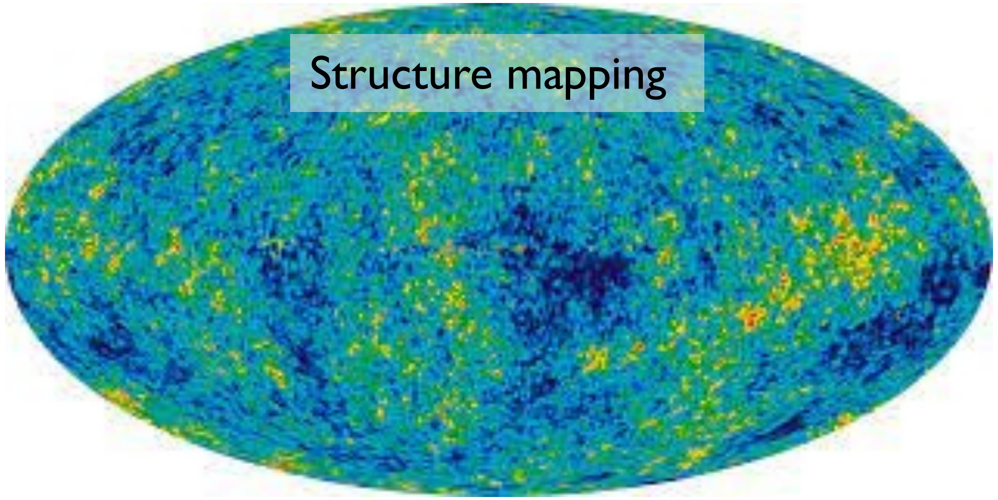
Structure mapping

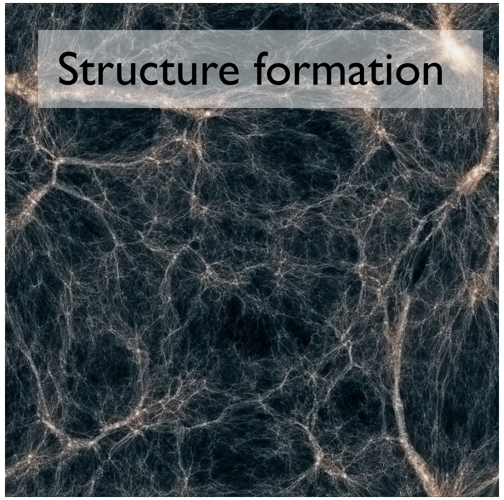
Structure formation

MODULATING SIGNAL

Astrophysical predictions of DM distribution imply a modulating signal due to Earth's rotation around the Sun.

$$R(E) = R_0(E) + R_m \cos(\omega(t - t_0))$$

- Period should be 1 year
- Phase should produce a peak in June
- Signal should appear in low energy range
- Events should be single hit

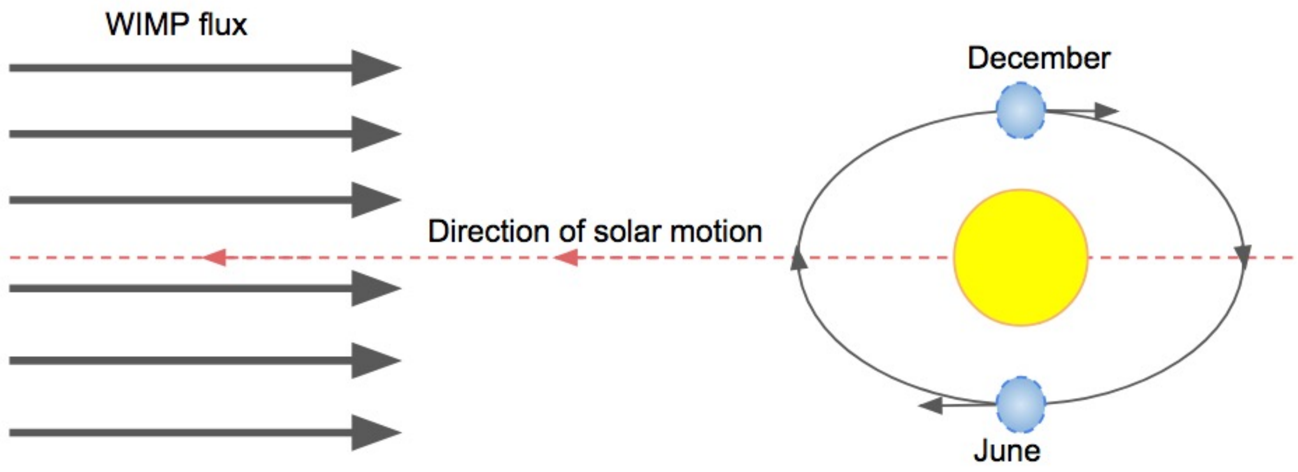

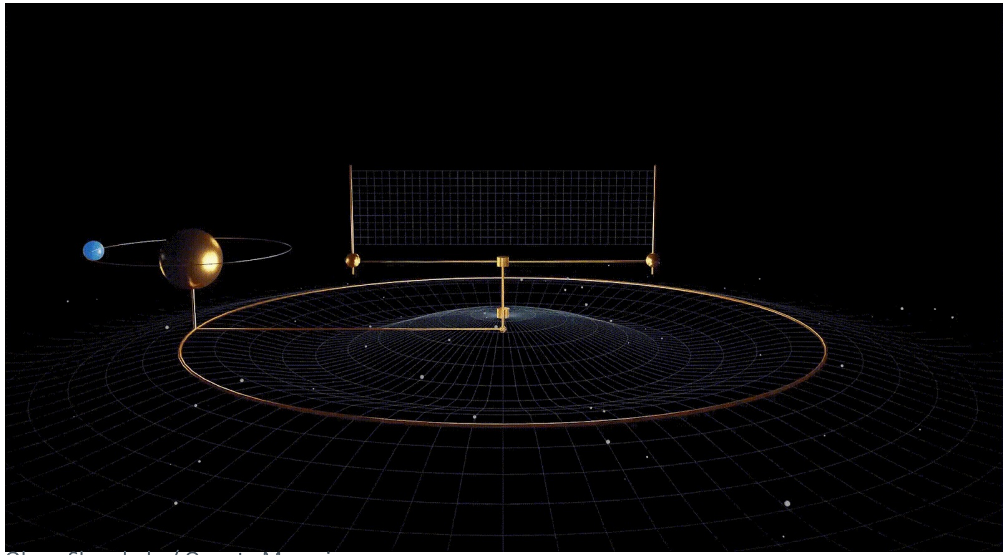

Olena Shmahalo / Quanta Magazine

DAMA RESULTS

250 kg NaI(Tl) detector based in LNGS consistently observed modulation rate compatible with DM expectations for ~20 years w/ ~13σ CL

- R_m: 0.01058±0.00090 cpd/kg/keV
- Phase: 144.5±5.1 days
- Period: 0.999±0.001 yr
- Modulation present in 1-6 keV

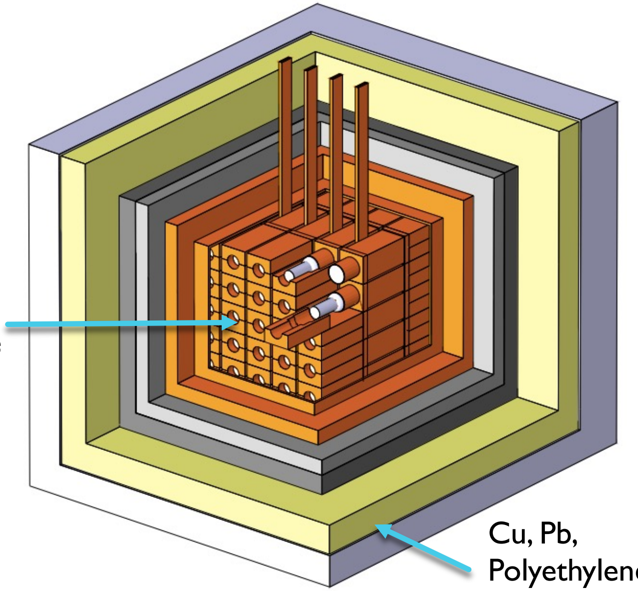

No direct fitting to constant rate, but upper limit given of ~0.8 cpd/kg/keV

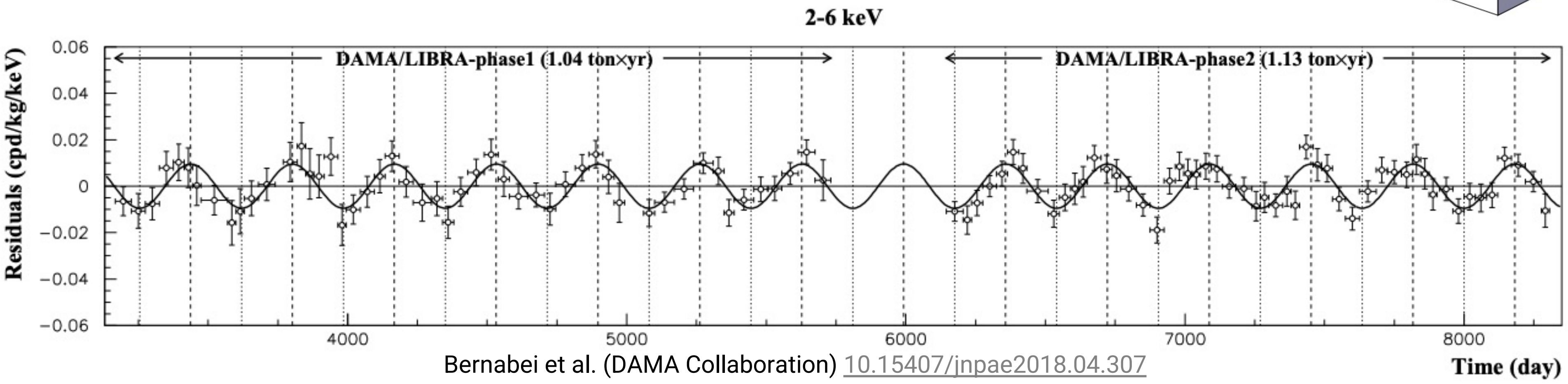

Bernabei et al. (DAMA Collaboration) 10.15407/jnpae2018.04.307

EXPERIMENTAL TENSION

Interpretation as DM is strongly constrained by null results from different targets

Target	Experiment/s
O	CRESST
F	PICO, PICASSO
Ne	NEWS-G
Na	DAMA
Si	DAMIC
Ar	DEAP, DarkSide
Ca	CRESST
Ge	CDMS, EDELWEISS
I	DAMA
Xe	XENON, LUX, PandaX
W	CRESST

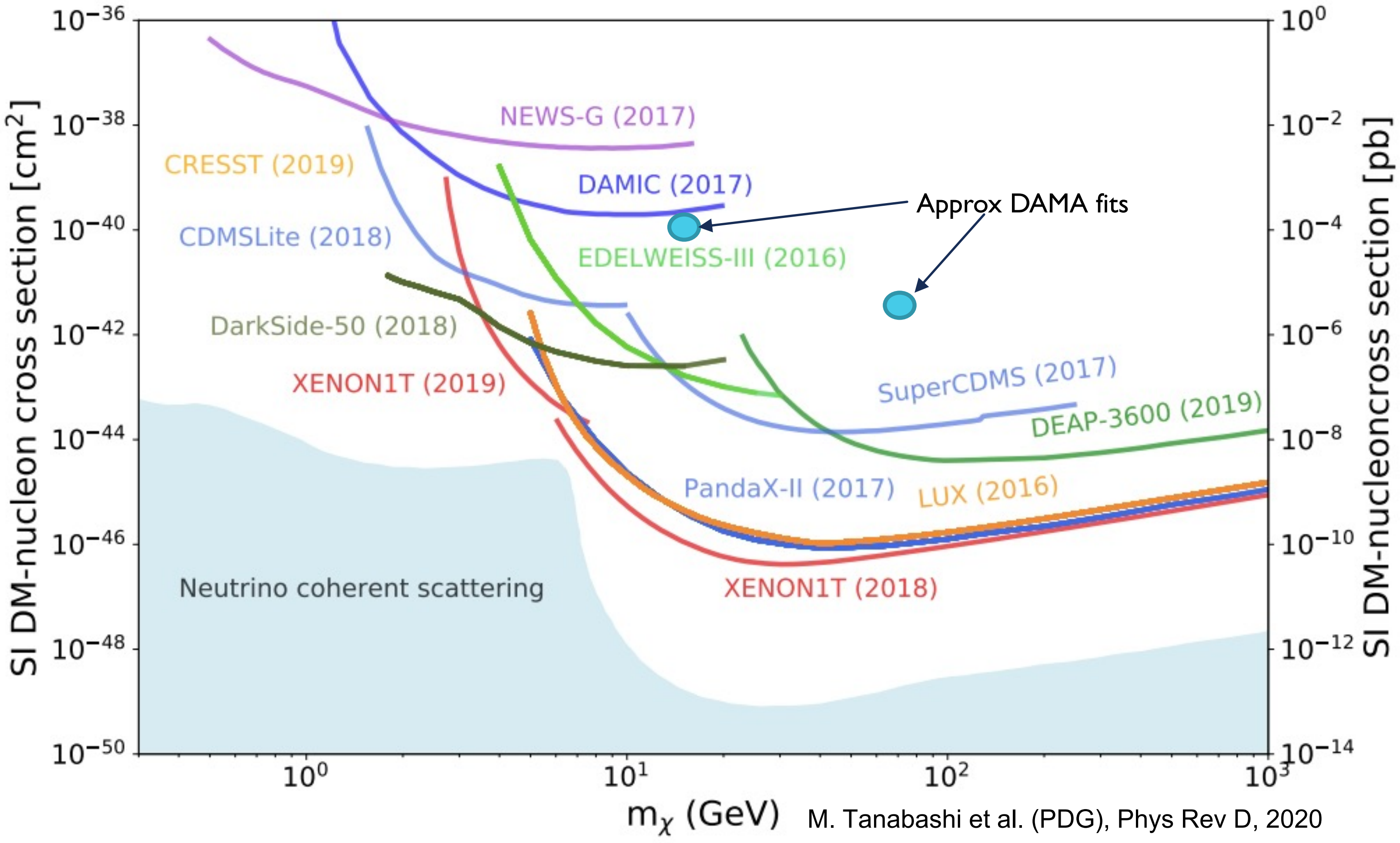

M. Tanabashi et al. (PDG), Phys Rev D, 2020

EVENT RATES

Limits are typically set by assessing how well the signal can be distinguished from detector backgrounds.

Two components to interaction rates with DM used for limit setting:

- Rate of DM interaction with SM
  Dictated by target, model choice, velocity distribution
- Rate of observation of events
  Dictated by observation process and detector setup

Can have significantly different energy scales, depending on type of detector.

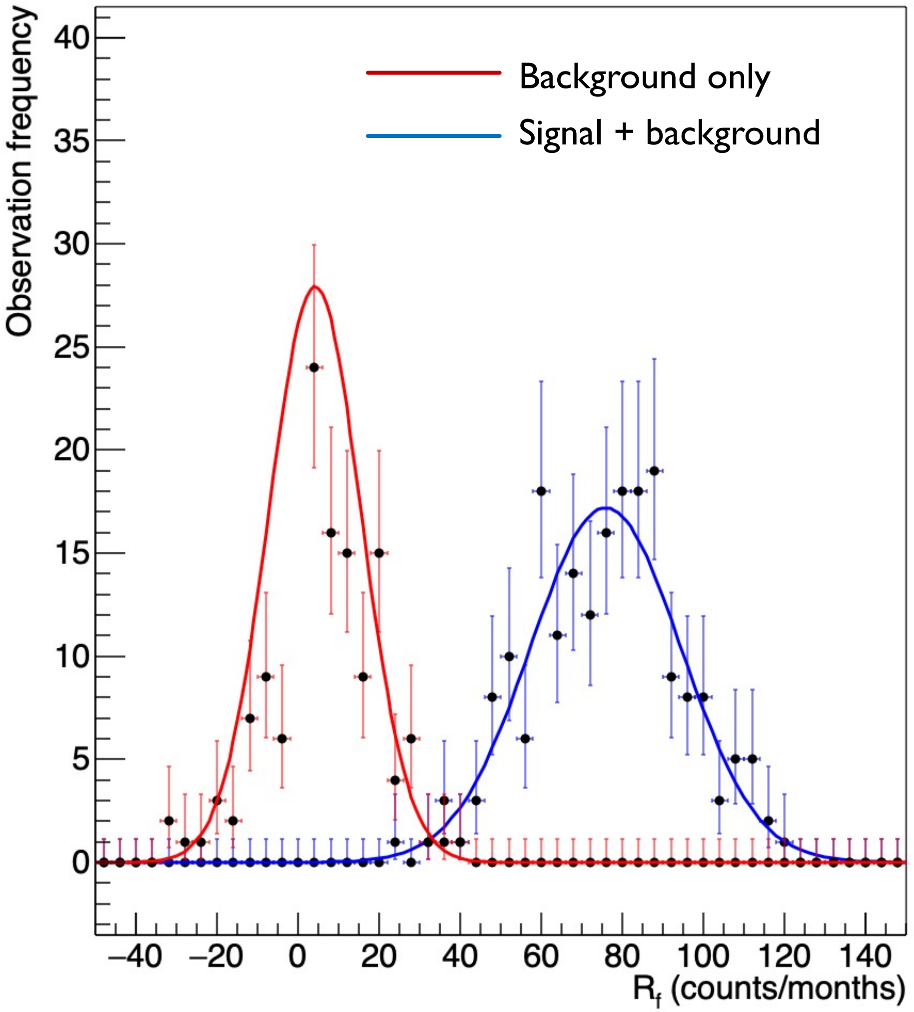

INTERACTION RATE

Number of nuclear recoils as a function of nuclear recoil energy E_R

$$\frac{dR}{dE_R} = N_T \frac{\rho}{m_\chi} \frac{\sigma_0 m_T}{2\mu_N^2} \sum_{i,j} \sum_{a,b=0,1} \hat{c}_i^{(a)} \hat{c}_j^{(b)} \left(F_{ij}^{(ab),1}(q) \int \frac{f_{lab}(\vec{v})}{v} d^3v + F_{ij}^{(ab),2}(q) \int v f_{lab}(\vec{v}) d^3v \right) .$$

DM and target properties

- Target density
- Target mass
- DM density
- DM mass
- DM cross section

DM interaction model

- Coupling constants
- DM Form factors
- Nuclear response functions

DM velocity distribution

OBSERVATION RATE

Number of events observed as a function of observation energy E_{ee} (electron equivalent keV for scintillator detectors)

$$\frac{dR}{dE'} = \epsilon(E') \frac{1}{(2\pi)^{1/2}} \int_0^\infty \frac{dR}{dE_R} \frac{dE_R}{dE_{ee}} \frac{1}{\Delta E_{ee}} \exp\left[\frac{-(E' - E_{ee})^2}{2(\Delta E_{ee})^2}\right] dE_{ee}$$

Efficiency/threshold ($\epsilon(E')$)

Imperfect/realistic detector setup
e.g., PMT QE ~30%

Interaction rate ($\frac{dR}{dE_R}$)

As per last slide

Quenching factor ($\frac{dE_R}{dE_{ee}}$)

Transformation from nuclear recoil energy to observable energy

Resolution ($\frac{1}{\Delta E_{ee}} \exp\left[\frac{-(E' - E_{ee})^2}{2(\Delta E_{ee})^2}\right]$)

Ability to resolve fine details in energy spectrum

SENSITIVITY COMPUTATION

MJZ, Barberio, Busoni JCAP12 (2020) 014

*we'll come back to the accuracy of this later

DAMA searches explicitly for modulating signal (not constant excess) over a ~constant background*
Need to understand how well statistical fluctuations in a background model mimic modulation.
Simulate this by randomly sampling from Poissonian over detector live time, and fitting to $R_c + R_f \cos(\omega t)$.

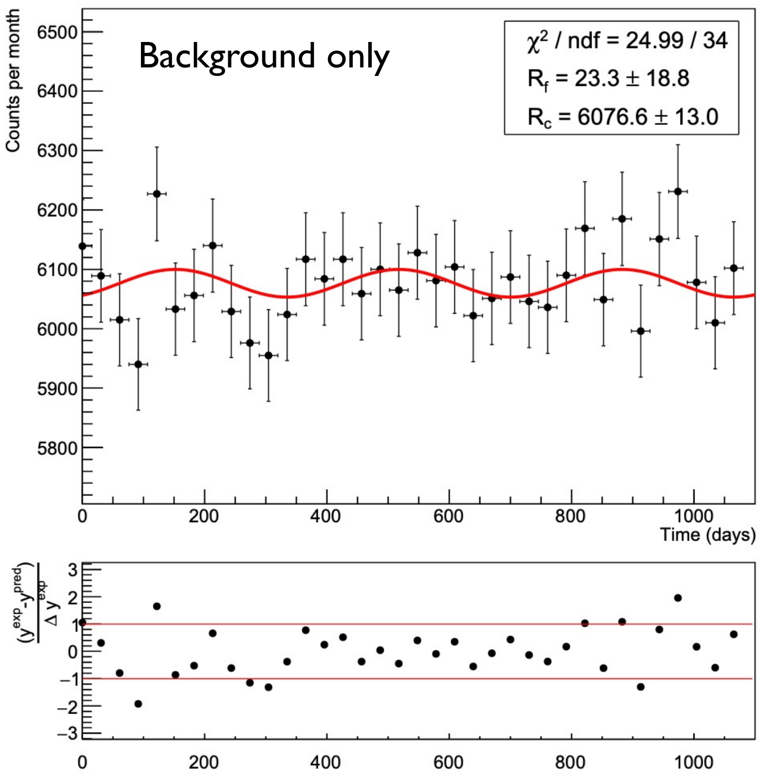

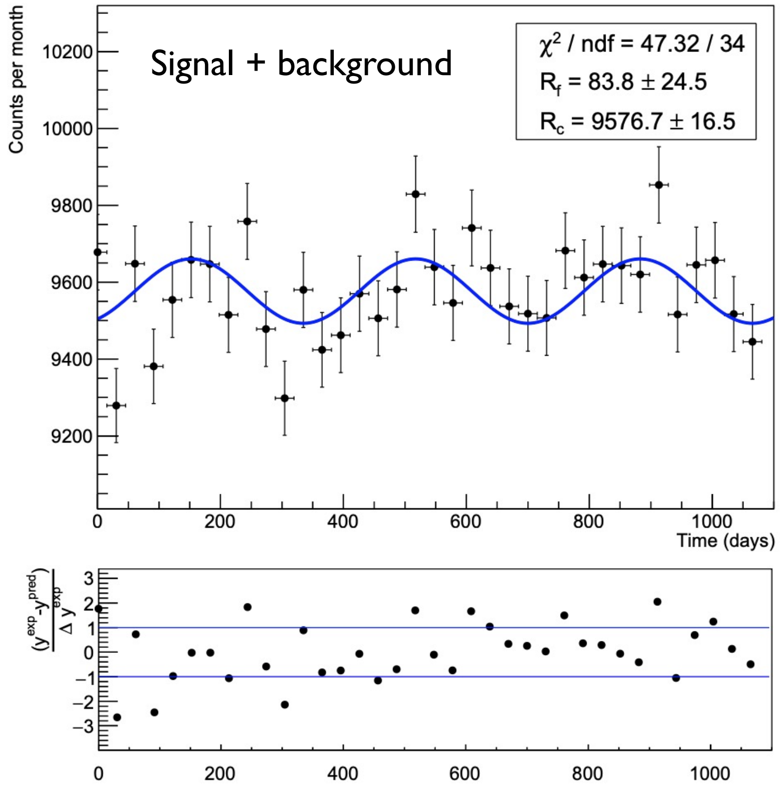

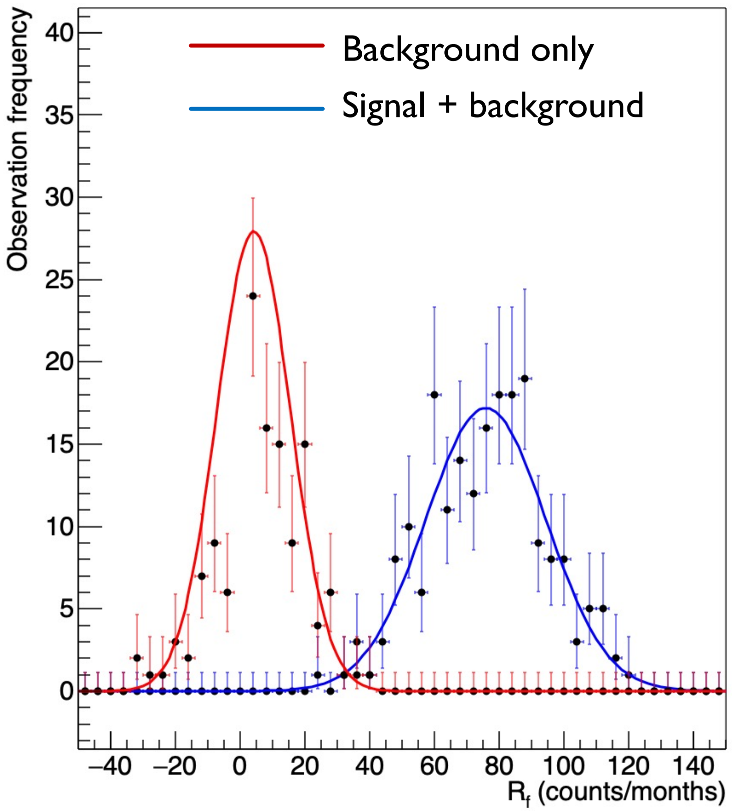

SENSITIVITY COMPUTATION

MJZ, Barberio arxiv:2107.07674, accepted by EPJC

Poisson simulations are based on expected number of observed interactions:

- Background only: $N_b = M_E \times \Delta T \times \Delta E \times R_b$
- Signal + background: $N_{sb} = M_E \times \Delta T \times \Delta E \times (R_b + R_0 + R_m \cos(\omega t))$

Where

- M_E= exposure mass
- ΔT= data taking time bins
- ΔE= energy bin widths
- R_b= background rate in energy/time bin
- R_0= constant signal rate in energy/time bin
- R_m= modulating signal rate in energy/time bin

This can be used to compute limits in both a model dependent and independent way:

Model dependent - R_0 and R_m computed by assuming model, mass and cross section

Model independent - R_0 and R_m taken from measurement by a detector (e.g., DAMA)

SENSITIVITY COMPUTATION

[1] MJZ, Barberio, Busoni JCAP12 (2020) 014
[2] MJZ, Barberio arxiv:2107.07674, EPJC
[3] Barberio, Duffy, Lawrence, MJZ (in prep.)

Desirable to have flexible calculation for various models, targets, and velocity distributions [1,2,3]
Set up so each step/calculation is agnostic of others, allows for testing of various model dependencies

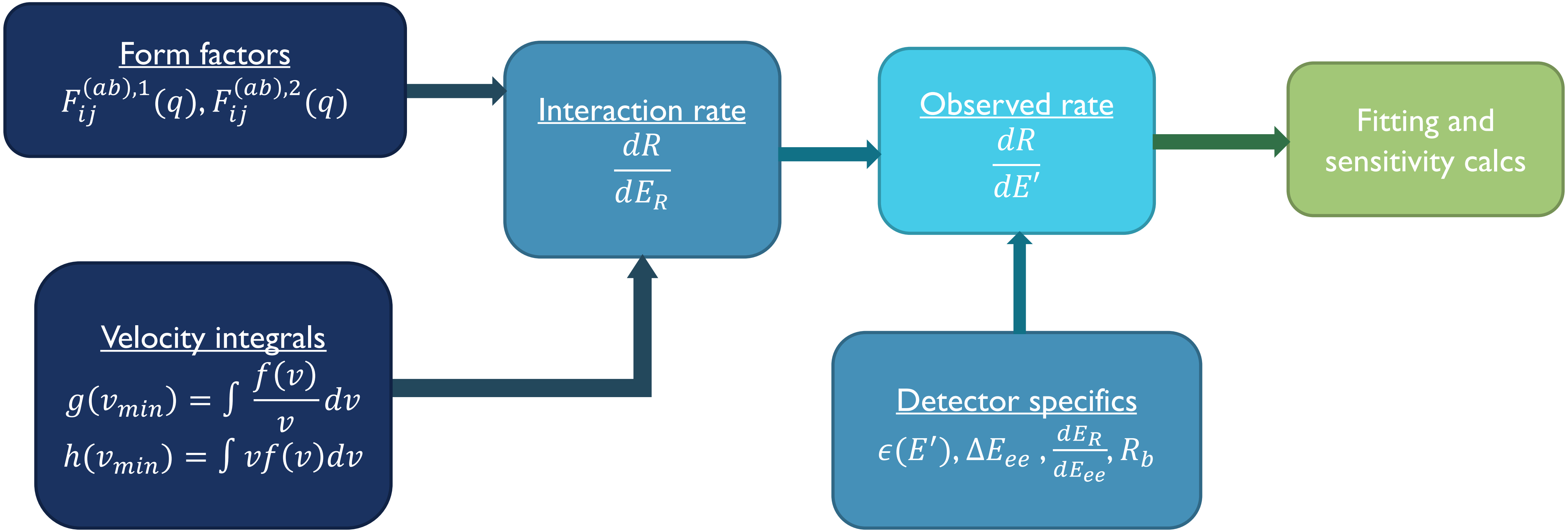

SENSITIVITY COMPUTATION

[1] Kang, Scopel, Tomar, PRD 99, 103019 (2019)
[2] MJZ, Barberio, Busoni JCAP12 (2020) 014
[3] MJZ, Barberio arxiv:2107.07674, EPJC
[4] Barberio, Duffy, Lawrence, MJZ (in prep.)

Allows for tests of influence of different pSIDM models and velocity distributions on fits to DAMA and SABRE sensitivity [2,4]

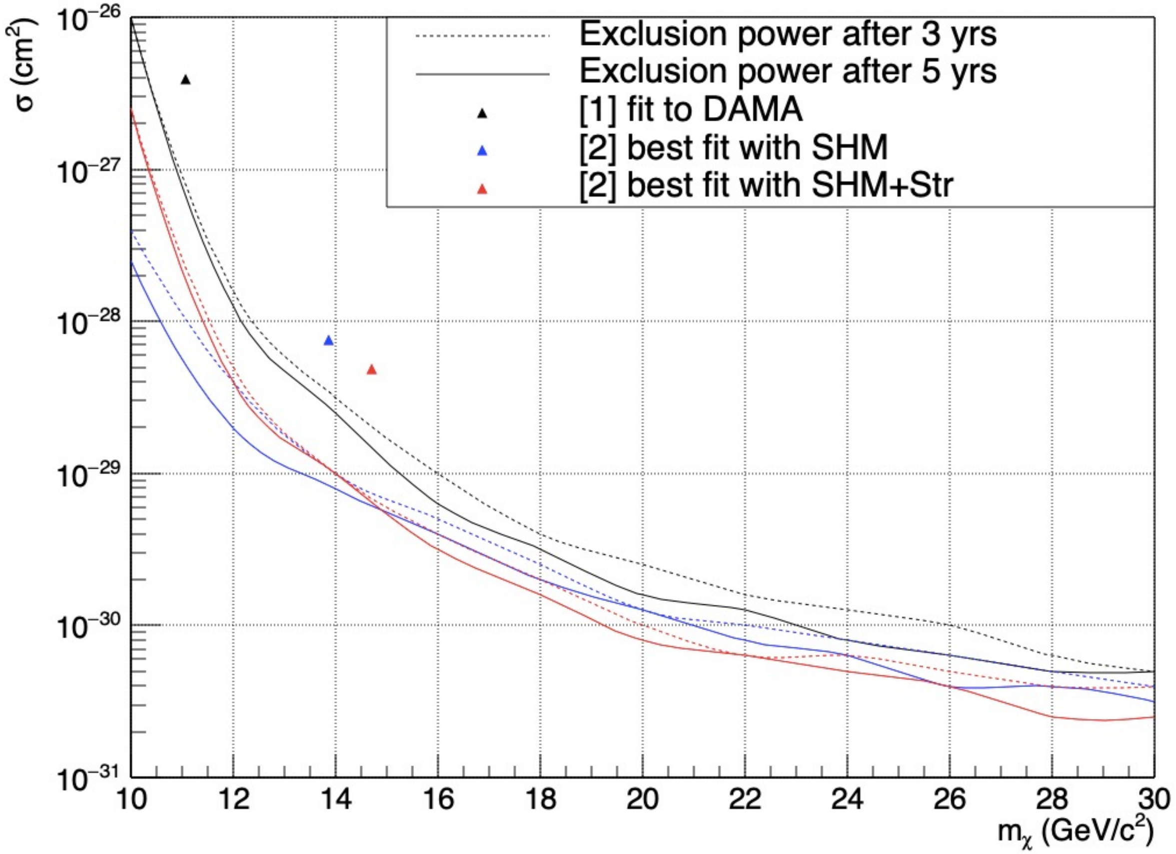

Allows for tests of influence of background models on excluding DAMA [3]

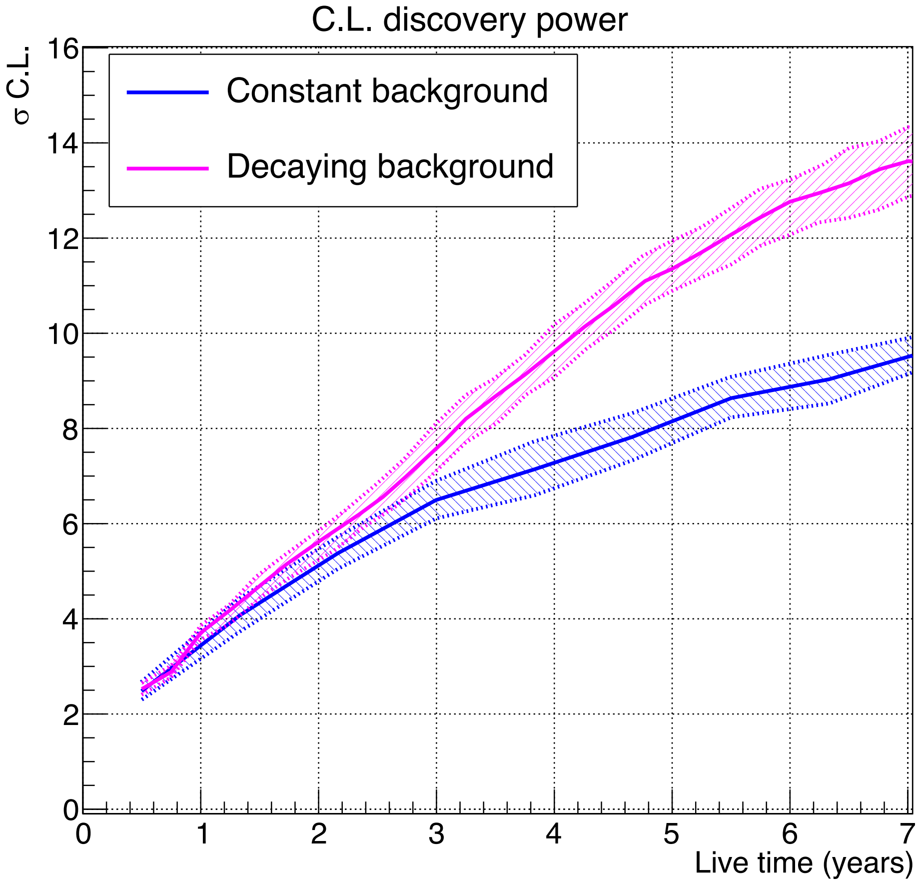

MODEL DEPENDENCE

[1] Kang, Scopel, Tomar, PRD 99, 103019 (2019)

Proton-philic inelastic spin dependent WIMP [1]

Target	A	Spin	Experiment/s
~~O~~	~~16~~	~~-~~	~~CRESST~~
~~F~~	~~19~~	~~p~~	~~PICO, PICASSO~~
~~Ne~~	~~20~~	~~-~~	~~NEWS-G~~
Na	23	p	DAMA
~~Ar~~	~~40~~	~~-~~	~~DEAP, DarkSide~~
~~Ca~~	~~40~~	~~-~~	~~CRESST~~
~~Ge~~	~~73~~	~~n~~	~~CDMS, EDELWEISS~~
I	127	p	DAMA
~~Xe~~	~~131~~	~~n~~	~~XENON, LUX, PandaX~~
~~W~~	~~184~~	~~-~~	~~CRESST~~

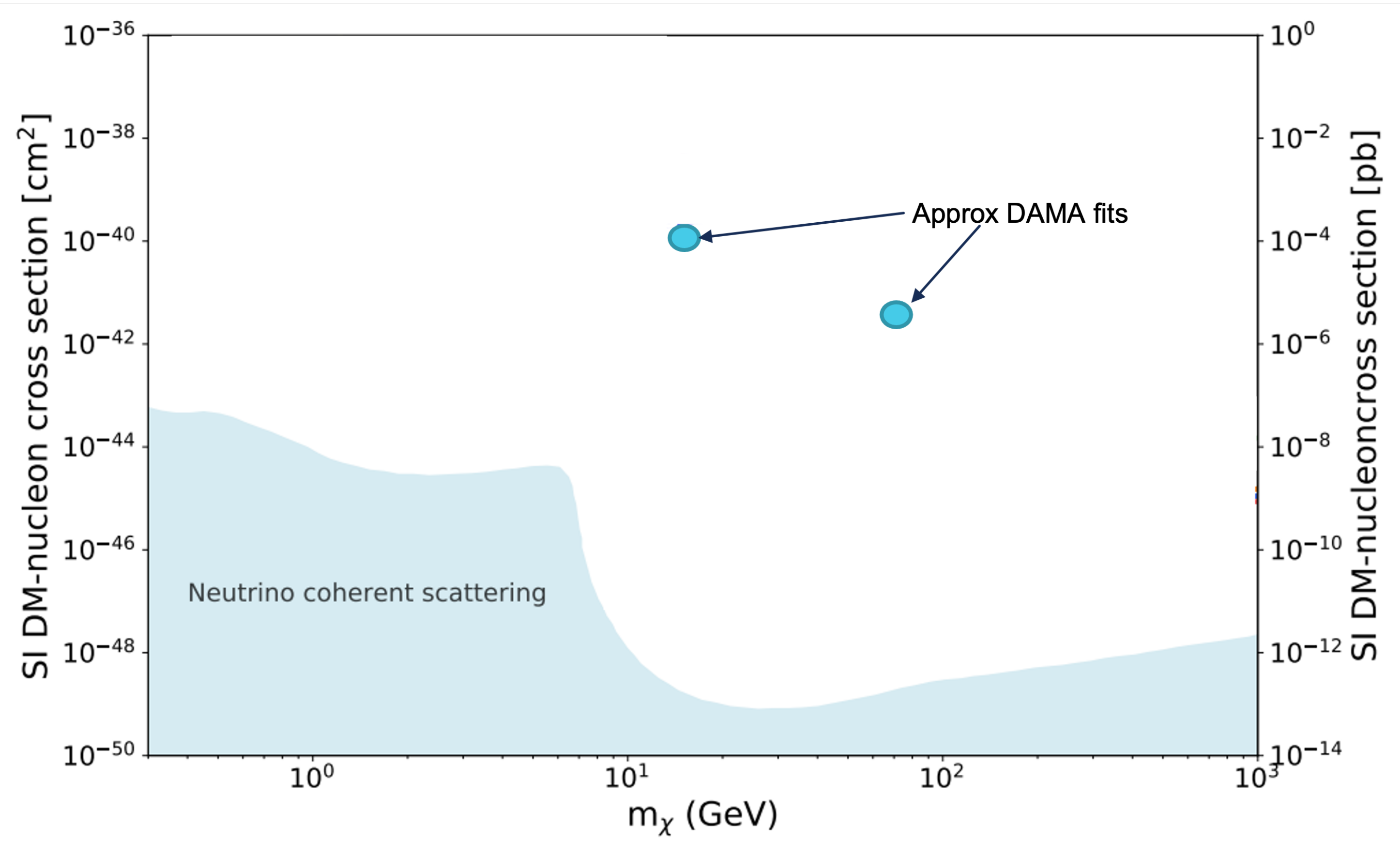

VELOCITY DISTRIBUTIONS

Velocity distribution gives the expected modulation fraction. Strongly dependent on DM and target masses through v_{min}

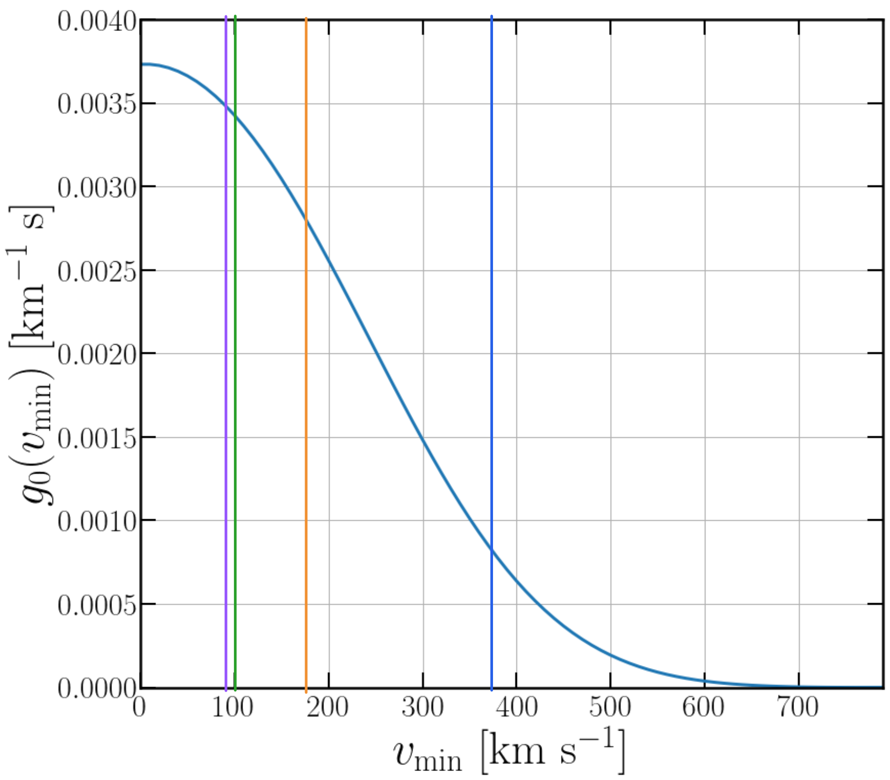

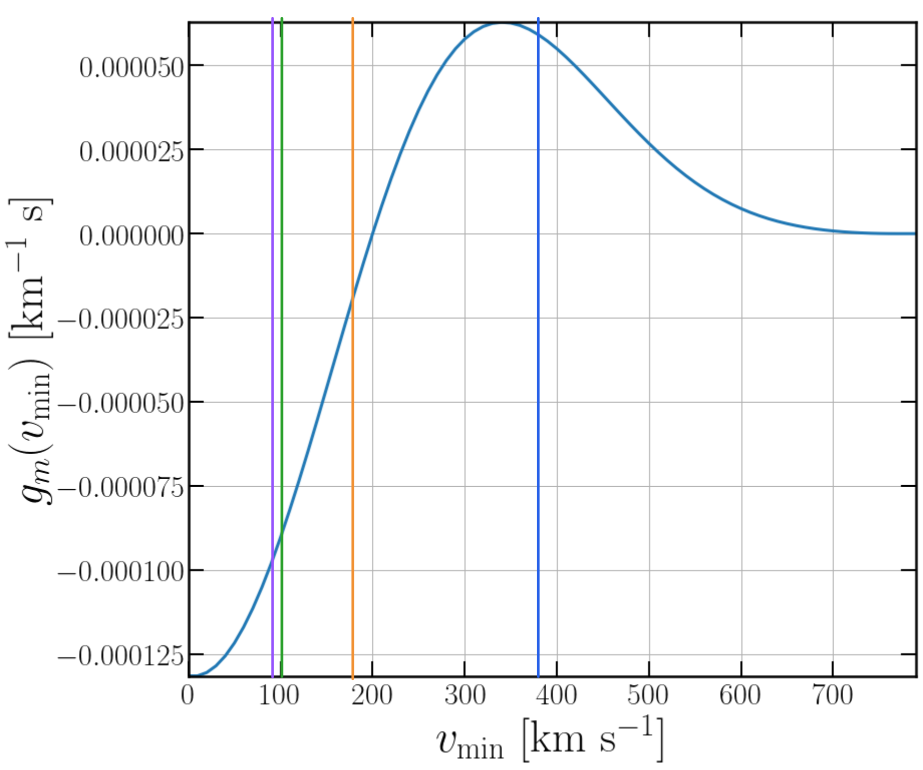

$$g(v_{\rm min}) = \int v \; f_{lab}(\vec{v}) dv \; d\Omega,$$

$$h(v_{\rm min}) = \int v^3 \; f_{lab}(\vec{v}) dv \; d\Omega.$$

$$v_{\rm min} = \sqrt{\frac{m_\chi E (m_\chi + m_T)^2}{2 m_\chi^2 m_T^2}}$$

For m_χ= 70 GeV/c^2:

Target	v_{min}
Ge	103 km/s
Xe	89 km/s
I	180 km/s
Na	374 km/s

VELOCITY DISTRIBUTIONS

Lawrence et al. (in prep)

Realistic galaxy simulations suggest the presence of substructure that influences the expected modulation

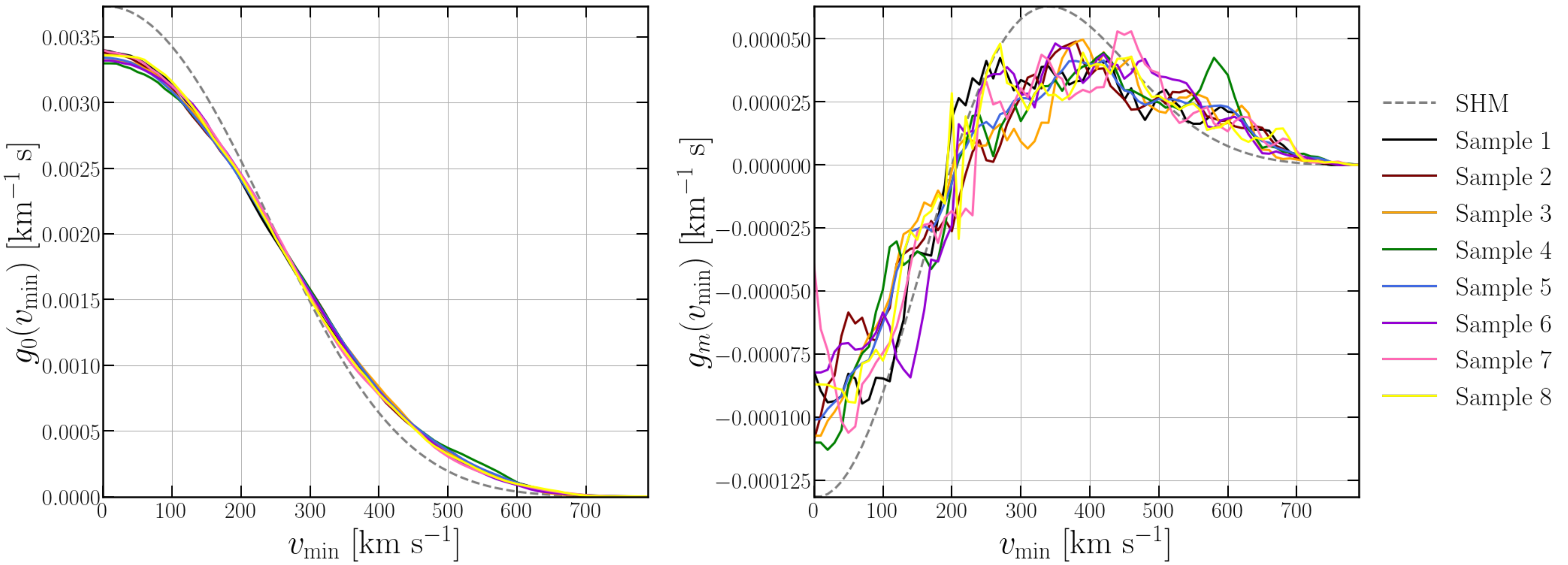

VELOCITY DISTRIBUTIONS

For different DM masses, the consideration of more realistic velocity distributions change the modulation energy spectrum, and can maximise the modulation for Na and I compared to other targets.

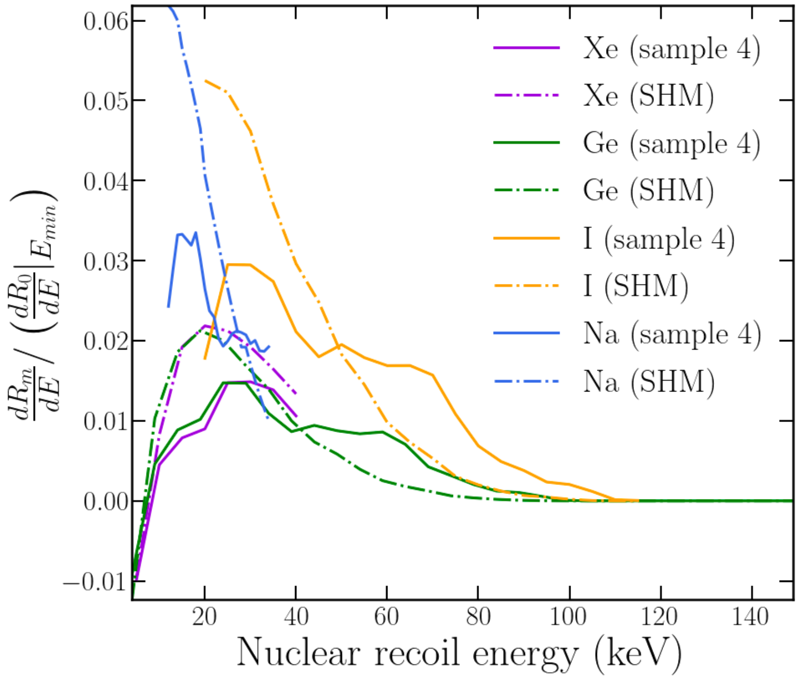

m_χ=10 GeV/c^2

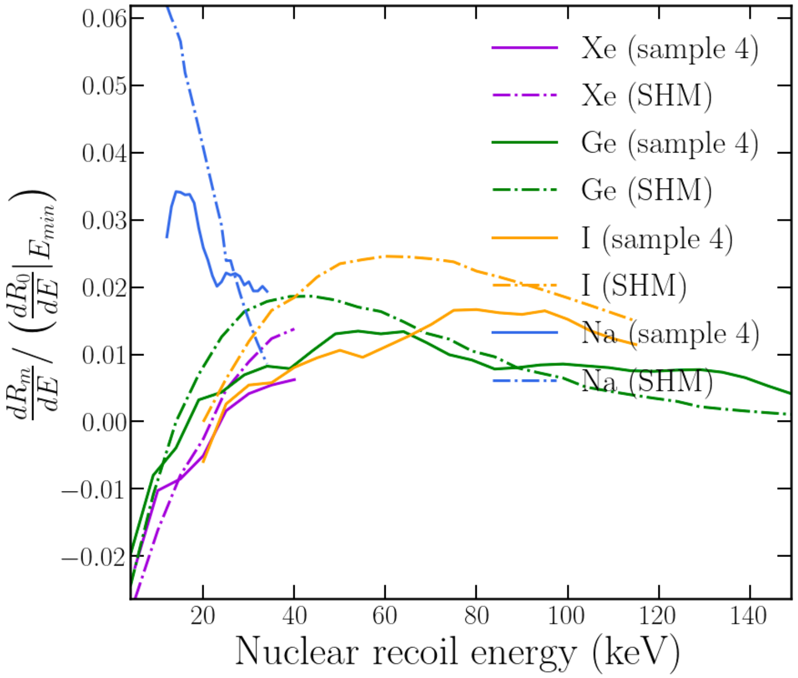

m_χ=50 GeV/c^2

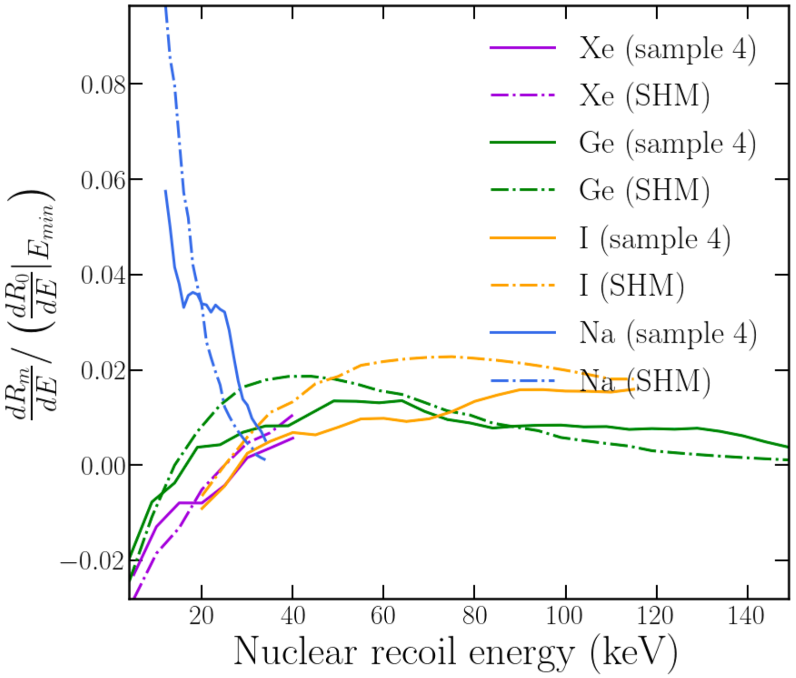

m_χ=100 GeV/c^2

REQUIREMENTS FOR MODEL INDEPENDENCE

Such a large collection of model possibilities, need to assess using the same target and as similar a set up as possible

$$\frac{dR}{dE'} = \epsilon(E')\frac{1}{(2\pi)^{1/2}}\int_0^\infty \boxed{\frac{dR}{dE_R}}\frac{dE_R}{dE_{ee}}\frac{1}{\Delta E_{ee}}\exp\left[\frac{-(E'-E_{ee})^2}{2(\Delta E_{ee})^2}\right]dE_{ee}$$

Interaction rate the same for all NaI detectors. No need to choose a model, just perform Boolean check.

Test for a modulation that has the same ratio of R_m/R_0 as DAMA (exact value may change based on set up)
Cannot construct a true model independent test from constant constraints alone
Need to assume a model to map DAMA modulation onto constrained parameter space

NAI DETECTORS

[1] Bernabei et al. PPNP114 103810 (2020)
[2] Adhikari et al. EPJC 78, 107 (2018)
[3] Amare et al. PRD 103, 102005 (2021)

DAMA[1]

Background ~0.8 cpd/kgk/keV

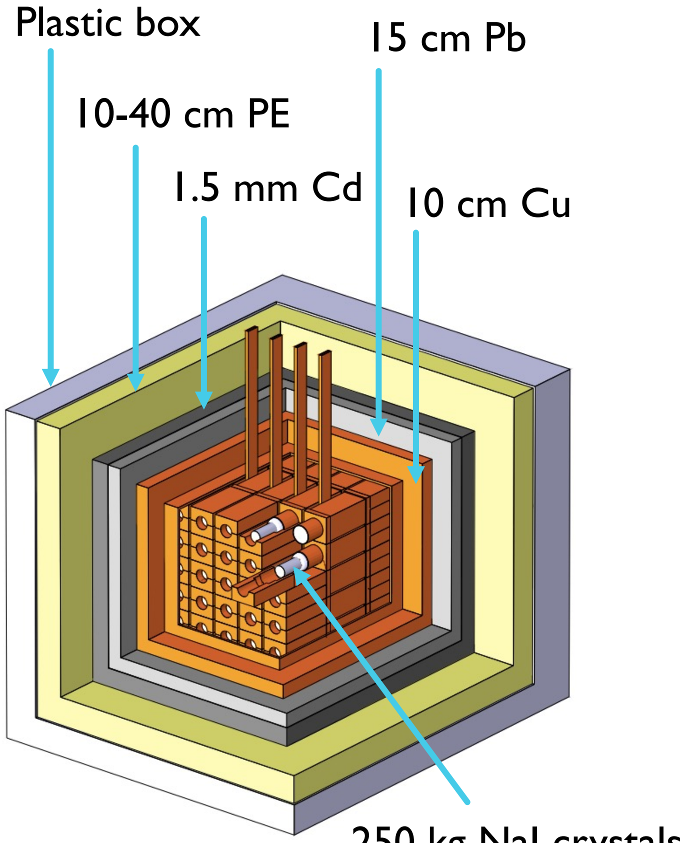

COSINE[2]

Background ~2.9 cpd/kg/keV

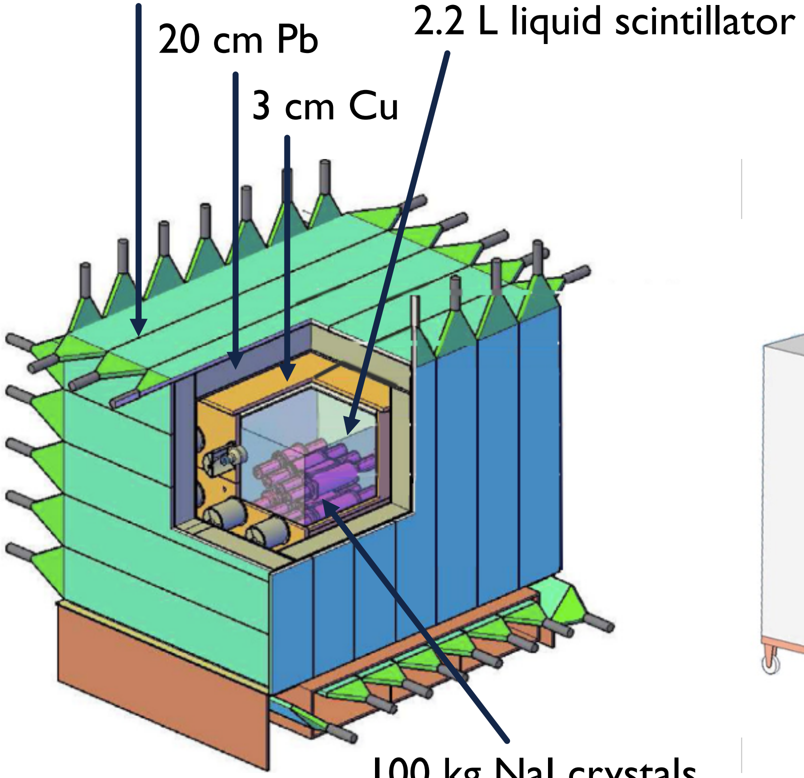

ANAIS[3]

Background ~3.2 cpd/kg/keV

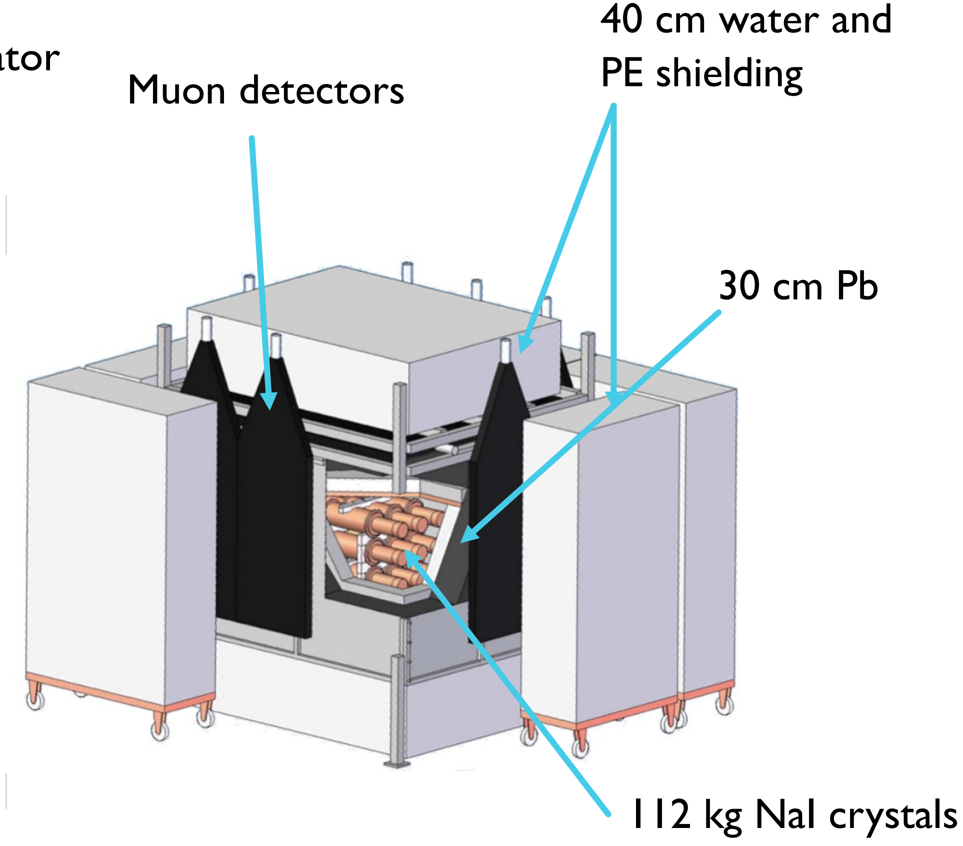

RECENT RESULTS

Most "damning" NaI constraints to date are based on lack of constant excess ⇒ <u>model dependent</u> test
But! This region already strongly constrained by DAMA from its first data taking.

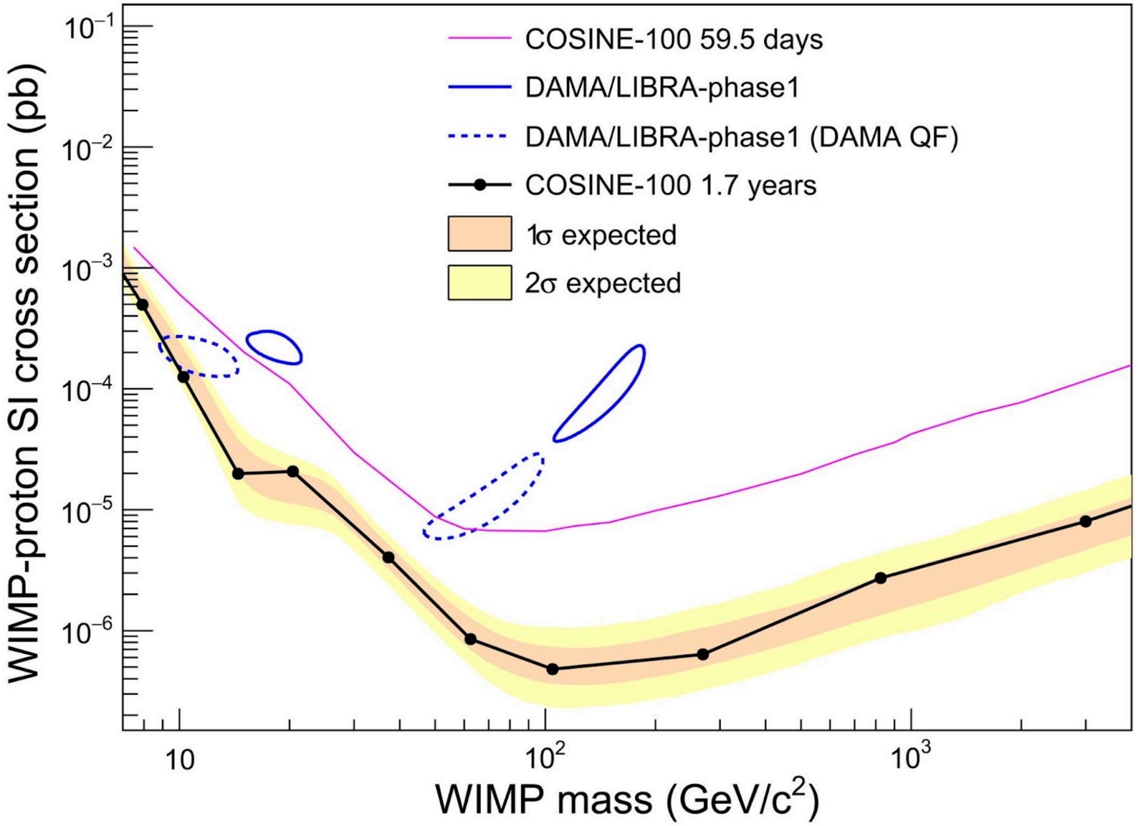

Adhikari et al. (COSINE Collaboration) 10.1126/sciadv.abk2699

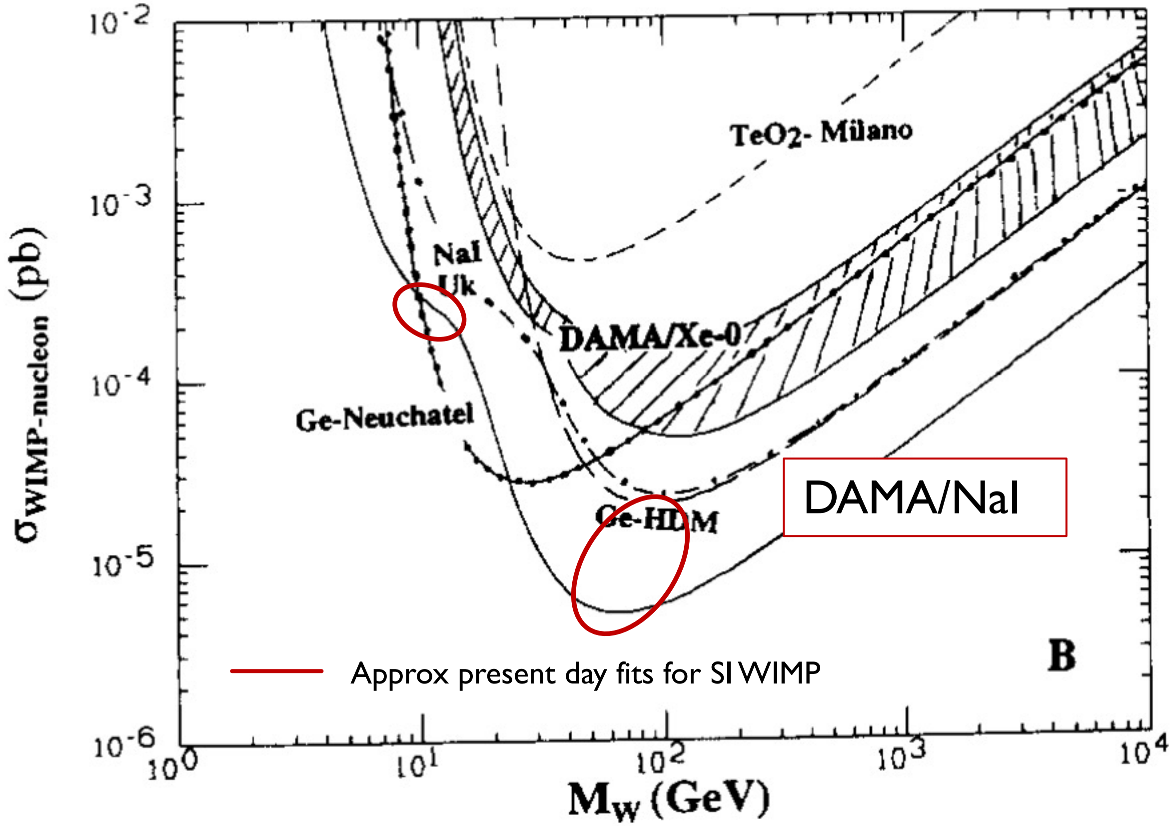

Bernabei et al. (DAMA Collaboration) 10.1016/S0370-2693(96)80020-7

RECENT RESULTS

[1] Bernabei et al. PPNP114 103810 (2020)
[2] Adhikari et al. arxiv:2111.08863
[3] Amare et al. PRD 103, 102005 (2021)

For modulation searches, both COSINE and ANAIS are beginning to reach strong sensitivity, but at present both still compatible with DAMA and null hypothesis within 3σ due to high backgrounds

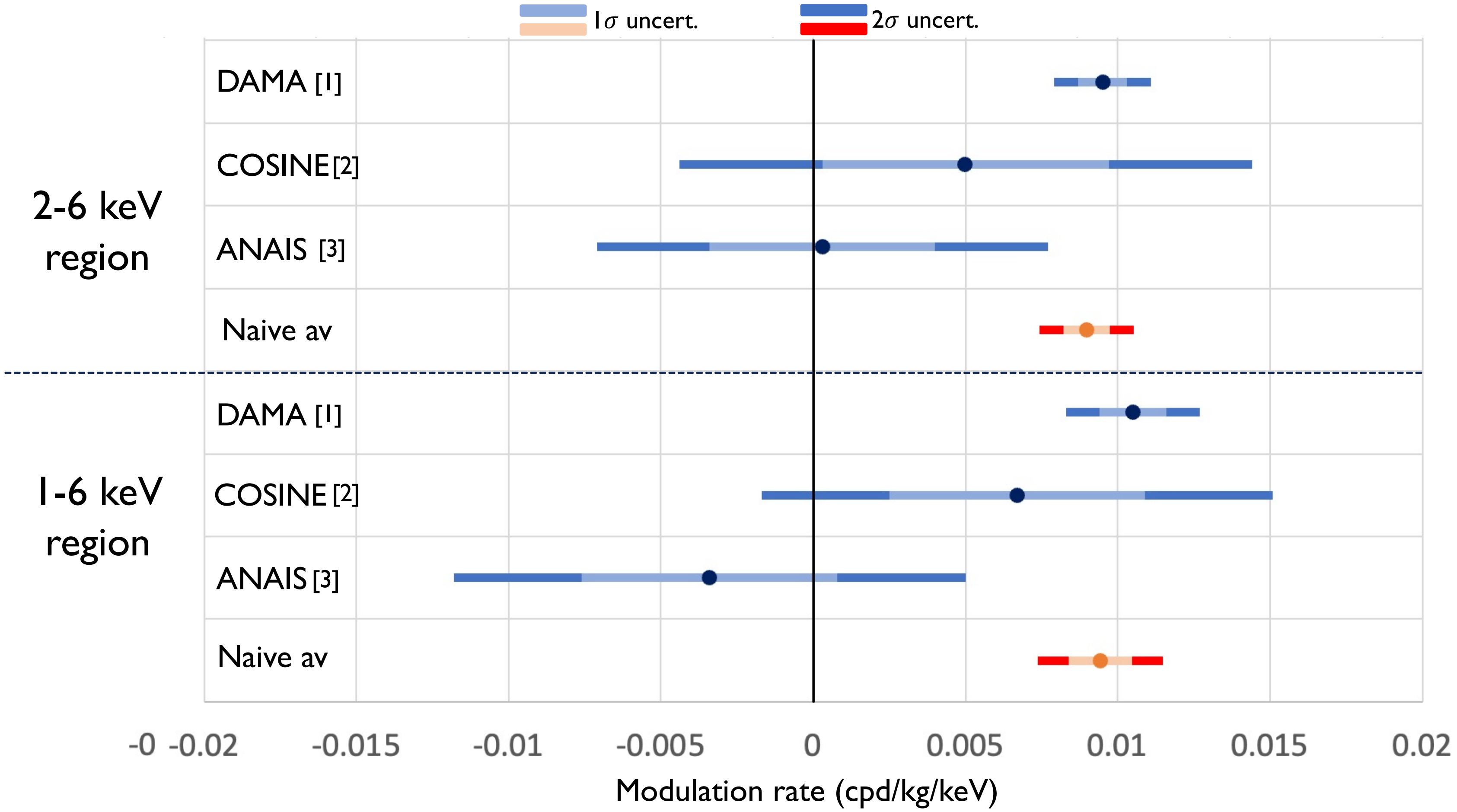

Naïve average = weighted average assuming no correlation

DETECTOR DEPENDENCIES

Difficulty with model independent tests is then slight differences between detector setups.
Need to understand if these can introduce 'hidden' model dependence – i.e., will these changes appear more extreme for different models/masses of DM?

Potential differences of interest:

- Na quenching factor
- Radioactive backgrounds
- Electronic backgrounds
- Background modelling
- Location specifics
- Energy thresholds

Radioactive backgrounds, Electronic backgrounds, Background modelling → Background modelling and mitigation

QUENCHING FACTOR

Purpose is to converts nuclear recoil energy (signal) into electron equivalent energy (used to calibrate detector).

$$E_{ee} = Q(E_{NR})E_{NR}$$

Ionisation from recoiling nucleus

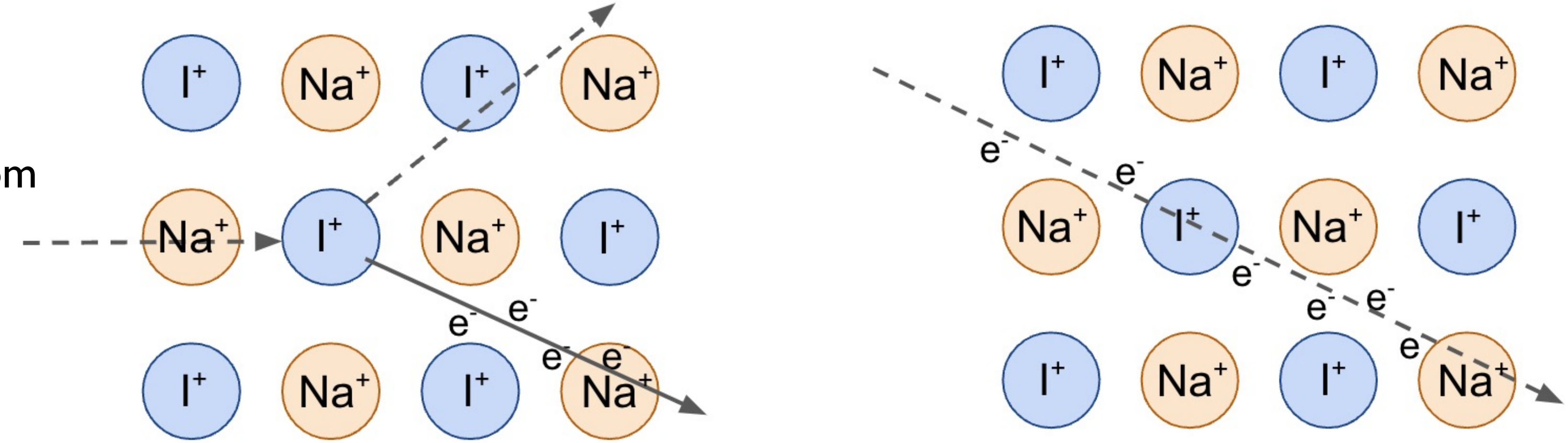

Ionisation from external particle

Possible that this effect depends strongly on optical properties of crystal so different growth methods can impact results. Interesting to think about as:

- Differences observed in QF measurements by different groups
- Would change both amplitude and position of signal
- Depends on the nucleus DM interacts with so impacts different masses in different ways

QUENCHING FACTOR MEASUREMENTS

[1]L.J. Bignell et al 2021 JINST 16 P07034
[2]T. Stiegler et al. 2017 arxiv:1706.07494
[3]J. Xu et al. 2015 10.1103/physrevc.92.015807
[4]H. Joo et al. 2019 10.1016/j.astropartphys.2019.01.001

Why are the DAMA quenching factors different to those measured since?

Possible solutions:

1. DAMA are using an inaccurate QF
2. QF is something that changes crystal to crystal

Particular solution will influence how data should be interpreted and compared.

Also possibility that (1) and (2) are both true - still inconsistencies at low energy

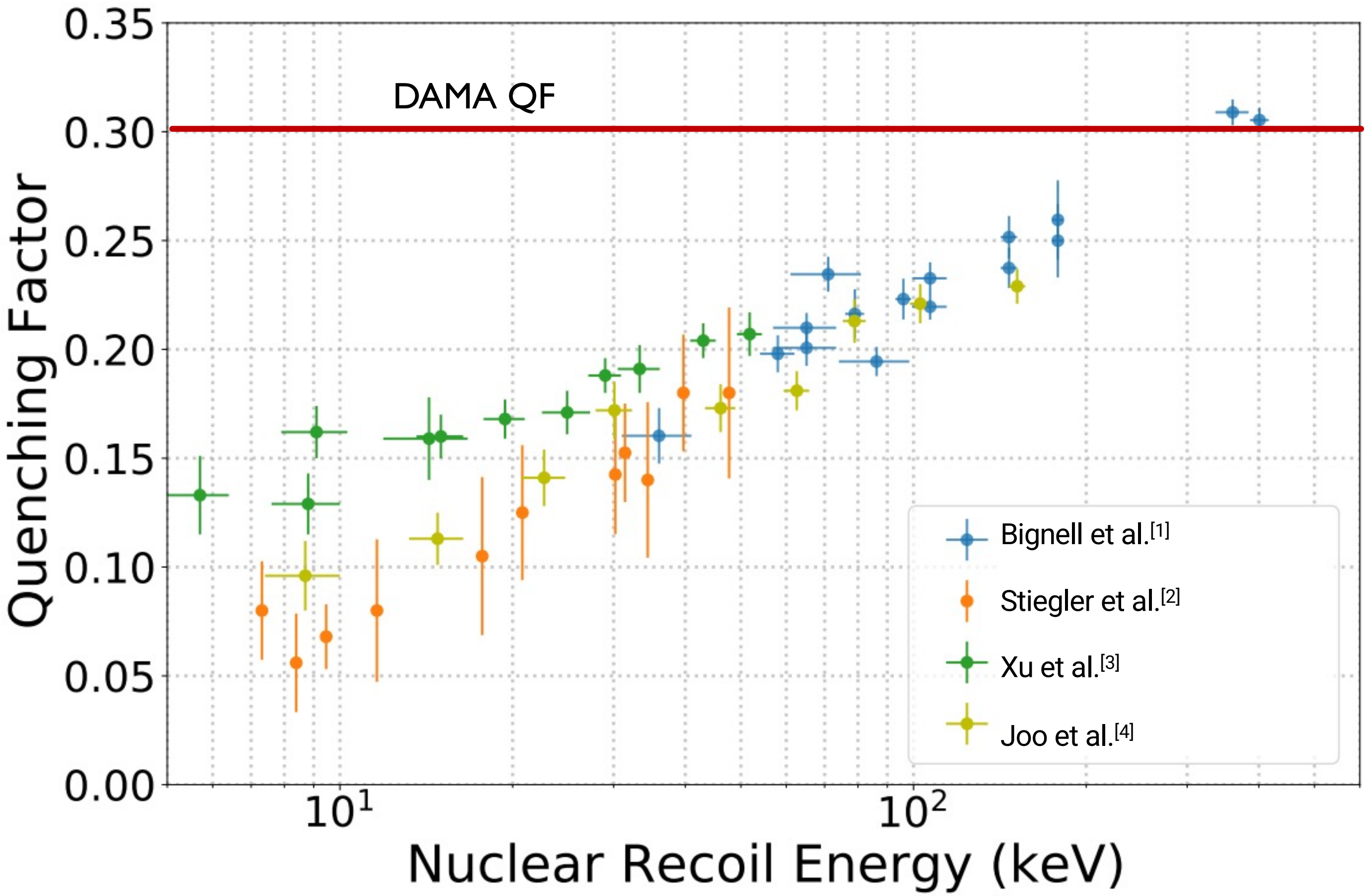

QUENCHING FACTOR IMPACT

[1] Adhikari et al. JCAP 11 (2019)

Can use results presented by COSINE [1] to understand how different QF combinations impact exclusion of DAMA

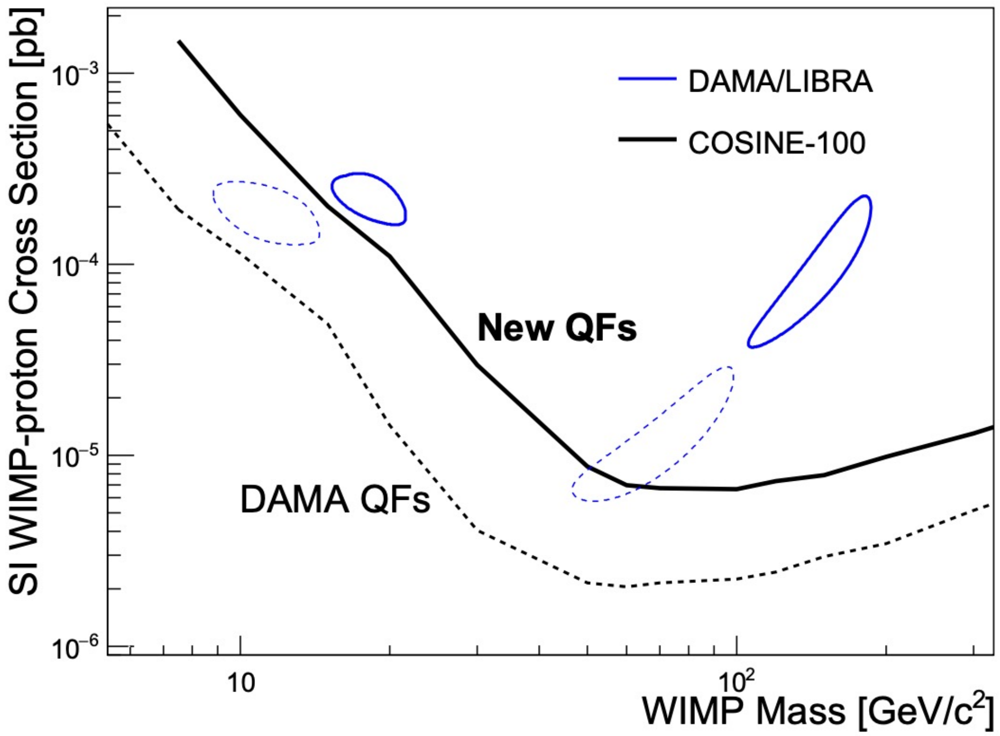

Assuming detectors have the same QF (either the solid or dotted lines)

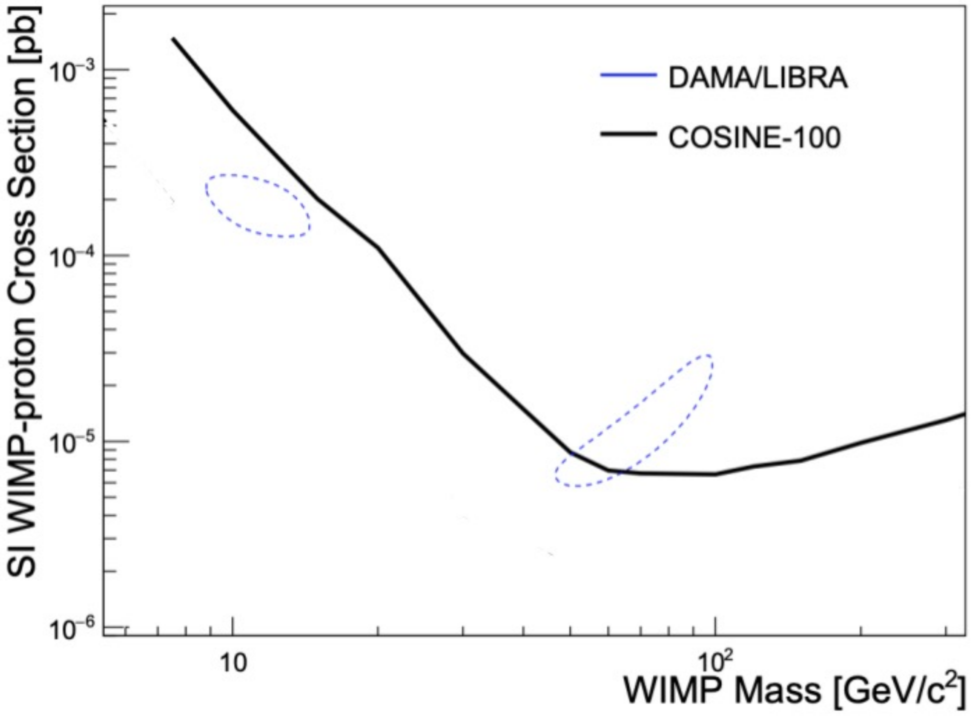

Assuming detectors have different QFs

QUENCHING FACTOR IMPACT

Change of QF has a strong influence on observable rate.

Changing relationship between NR and observed energy means the 1-6 keV_{ee} observable region of interest is "accessing" different parts of the recoil energy spectrum.

This will affect all DM interaction models, where the degree of extremity is dictated by the shape of the recoil spectrum

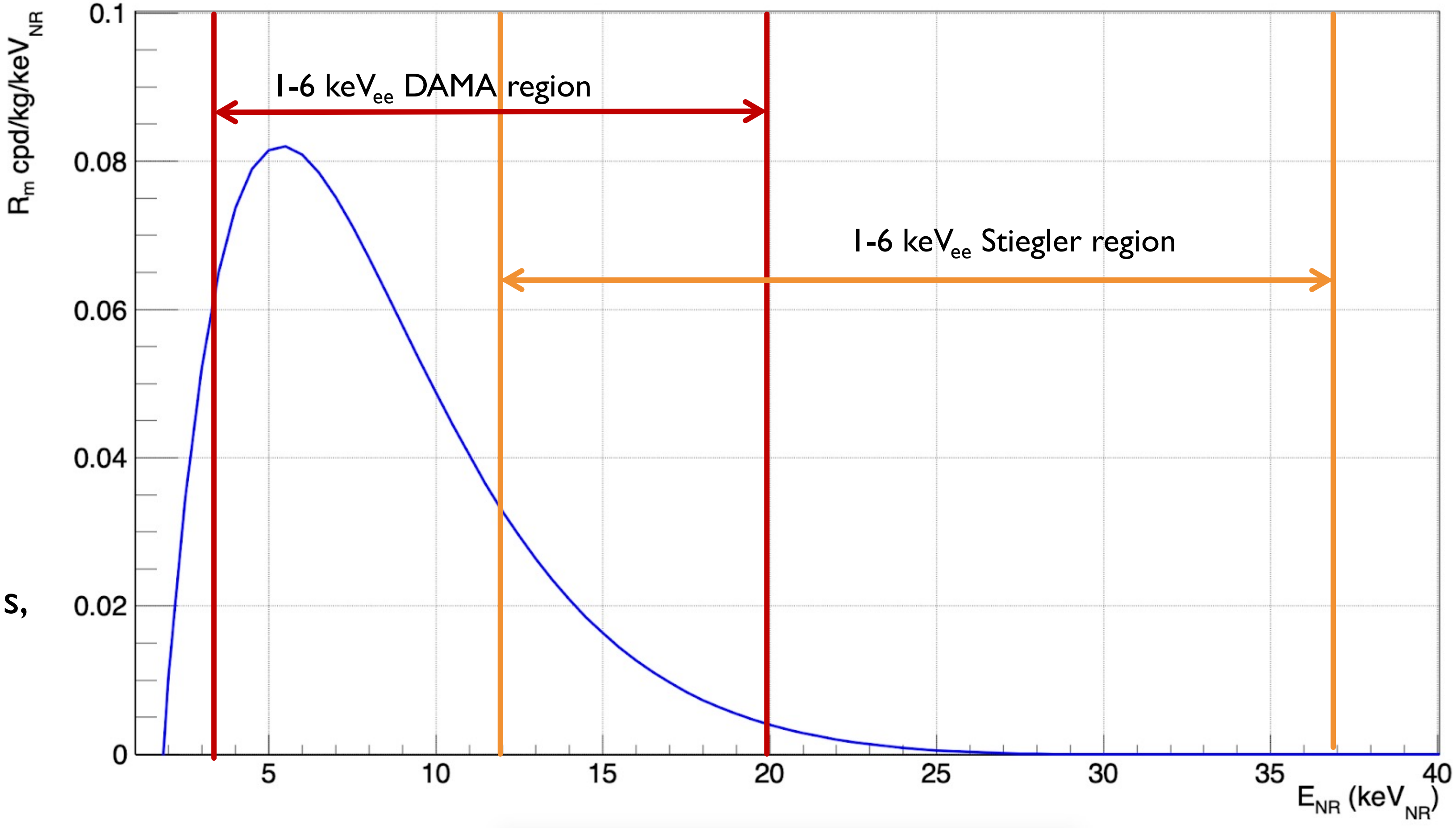

QUENCHING FACTOR IMPACT

[1] Stiegler et al. 2017 arxiv:1706.07494
[2] Adhikari et al. Astropart Phys 2021 102581
[3] Bernabei et al. JINST 2012

Detector differences can still change the observed modulation even if interaction rate is the same
e.g., for low mass spin independent DM, m_χ= 10 GeV/c^2, σ_χ=1.15x10^{-39} cm^2, change to QF drastically changes the observable signal, both in value and shape in region of interest.

⇒ Even for a same target test, no guarantee the modulation will look the same

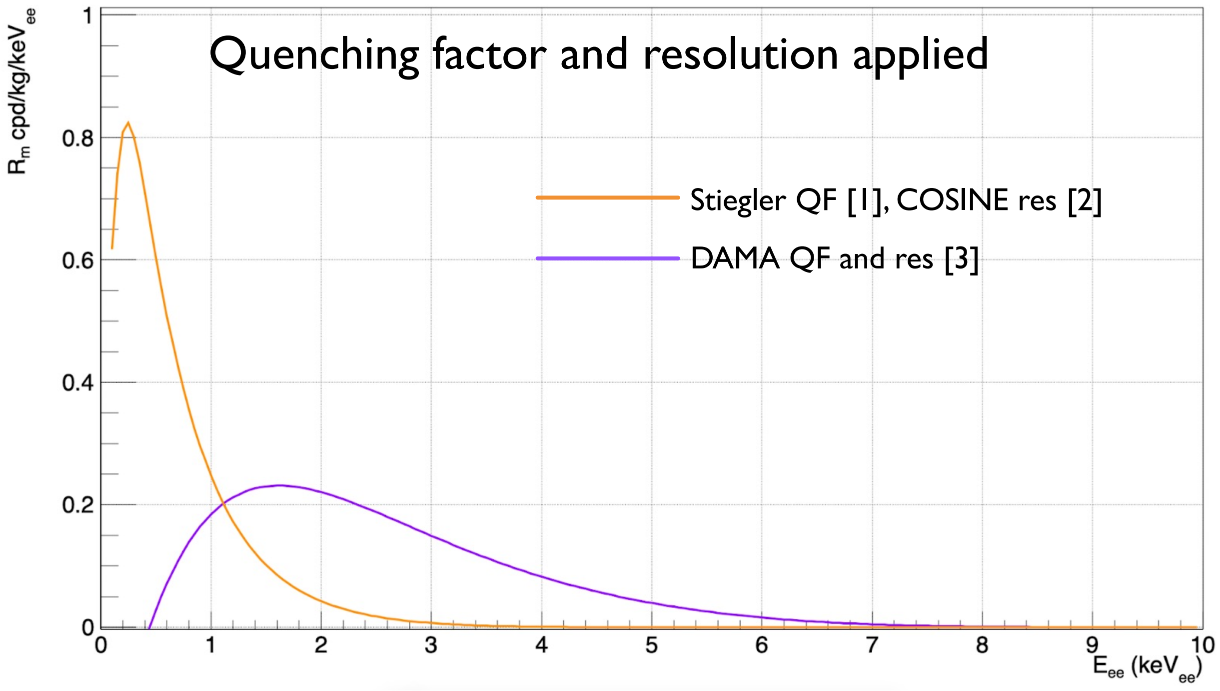

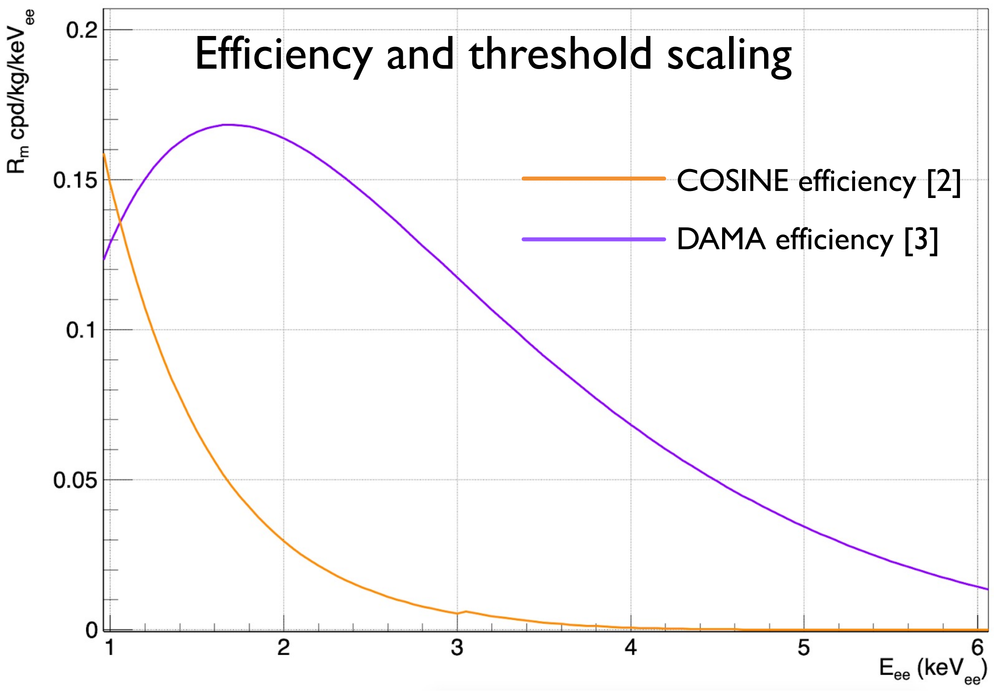

QUENCHING FACTOR IMPACT

[1] Bernabei et al. PPNP114 103810 (2020)
[2] Adhikari et al. arxiv:2111.08863
[3] Amare et al. PRD 103, 102005 (2021)
[4] Xu et al. 2015 PRC 92.015807
[5] Stiegler et al. 2017 arxiv:1706.07494
[6] Bignell et al 2021 JINST 16 P07034

This toy model w/ different QFs can produce modulation amplitudes more consistent with other observations

Effect is strongly dependent on DM model and mass ⇒ <u>model independent test is impossible</u>

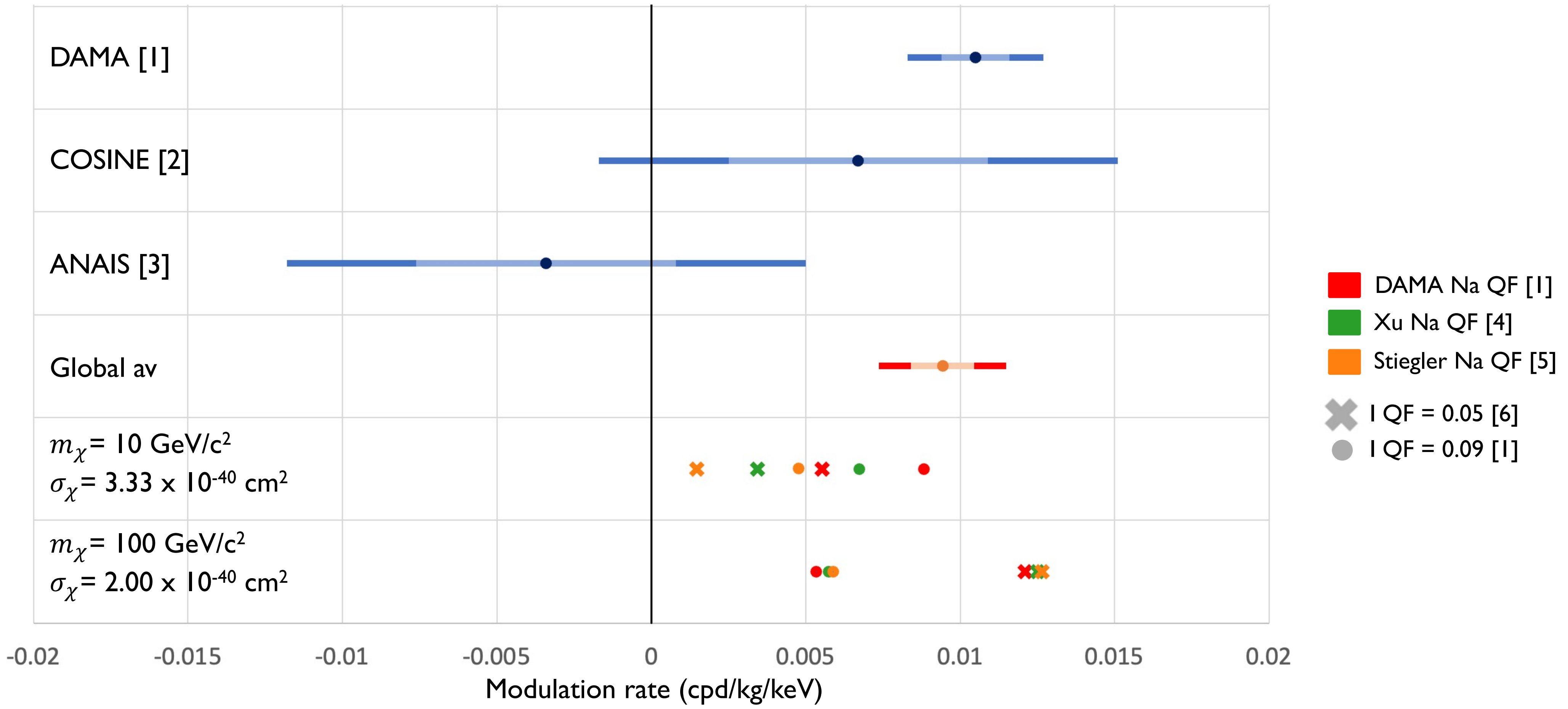

BACKGROUND MODELS

[1] Adhikari et al. arxiv:2111.08863
[2] Buttazzo et al JHEP04(2020)137

COSINE and Buttazzo et al. demonstrated influence of improperly modelled backgrounds:

1. Introduction of bias from simplistic time dependence [1]

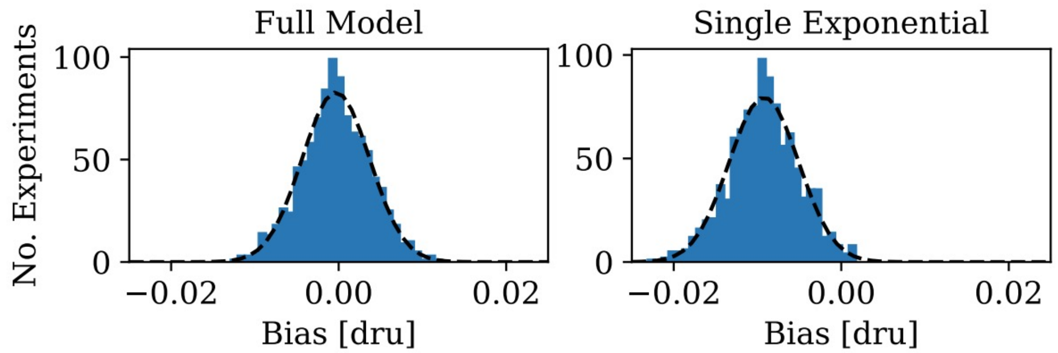

2. Introduction of modulation from assumption of constant and subtracting averaged rate [2]

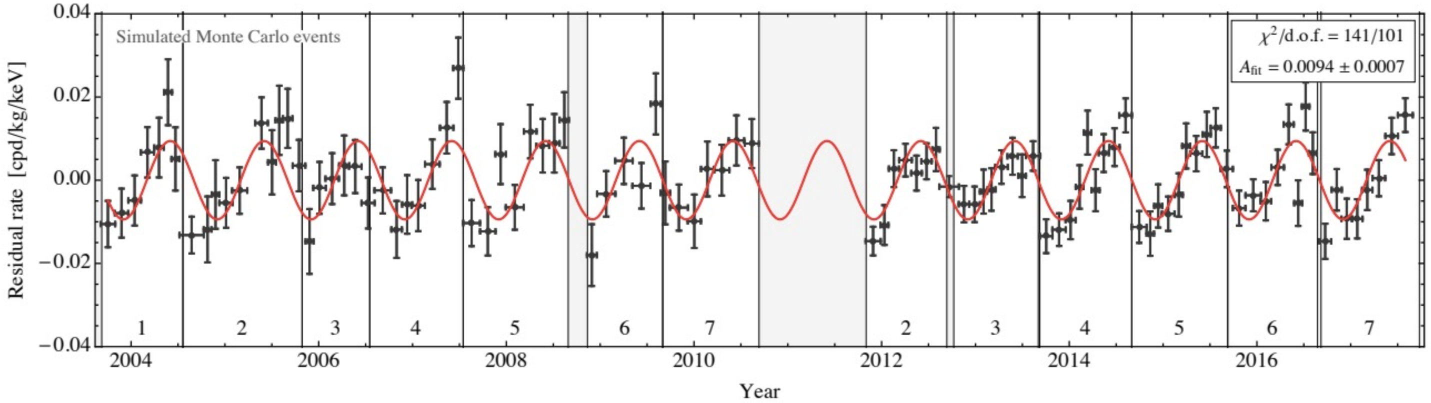

BACKGROUND MODELS

[1] Amare et al. Phys. Rev. D 103, 102005 (2021)
[2] Bernabei et al. PPNP114 103810 (2020)

Clear that background modelling is difficult especially in the low energy region due to PMT noise etc.

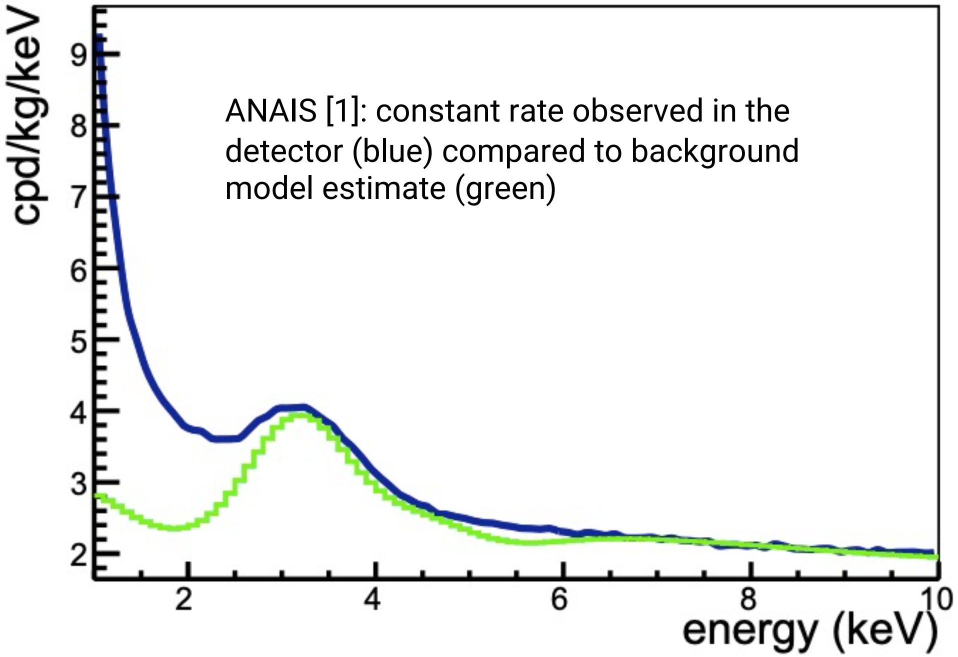

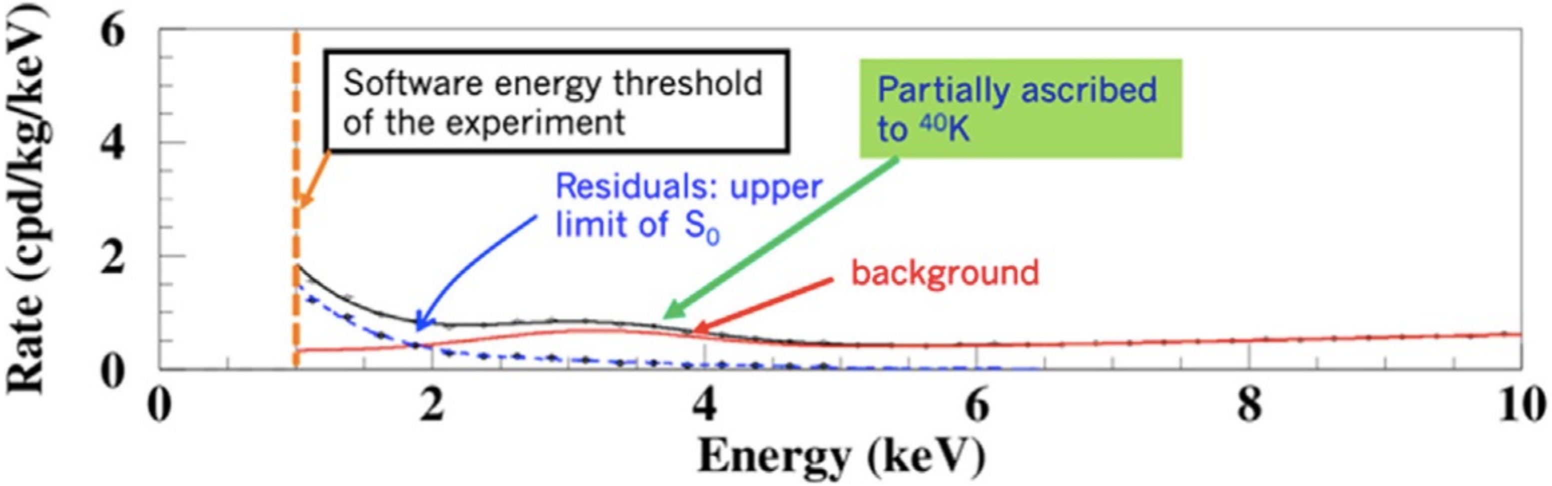

DAMA [2]: observed constant rate with extrapolated upper limits

⇒ need a low background, well modelled experiment to understand if modulation is real or an artifact of analysis

BACKGROUND MODELS

[1] Borexino collab. JCAP02(2019)046
[2] DAMA collab. Nucl. Phys. At. Energy 19 (2018)

Muons a particular issue for DM modulation searches as they have a similar phase due to seasonal dependence. Need to be carefully measured to understand their impact on the data.

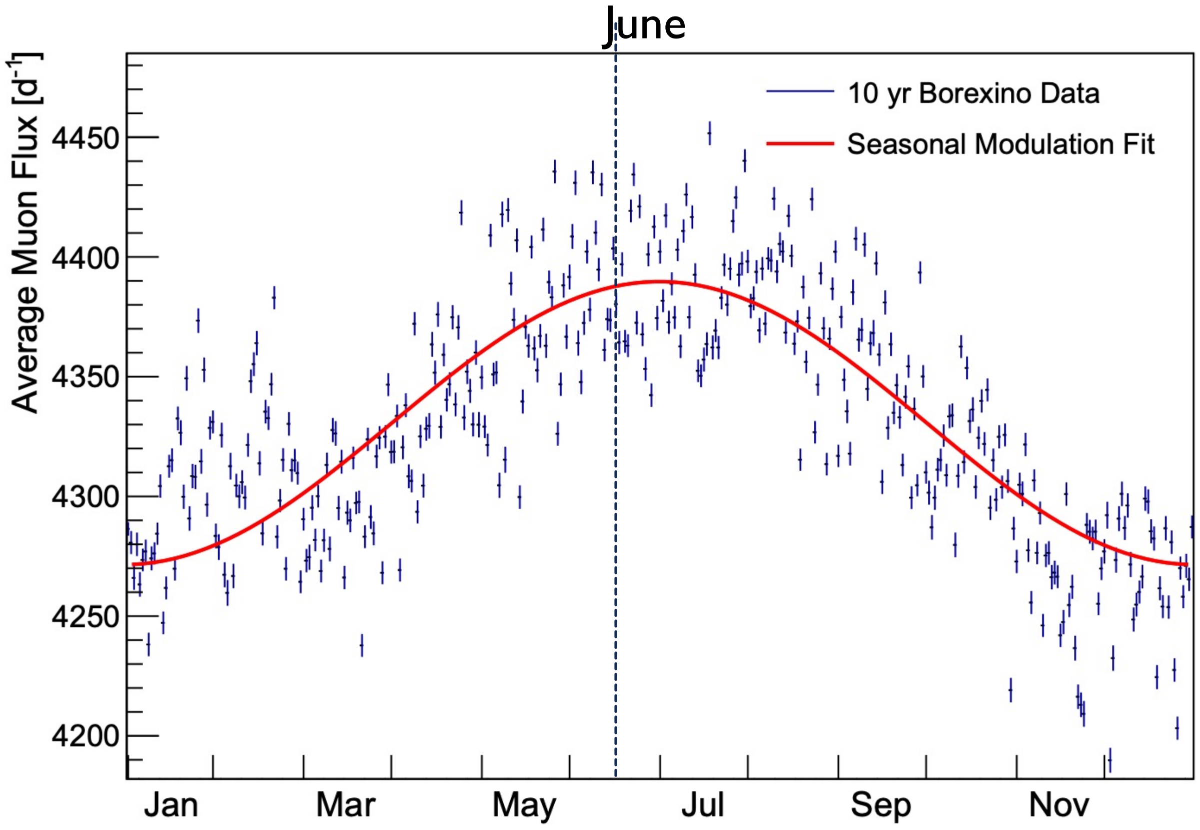

Average muon rate at Borexino over 10 yrs [1]

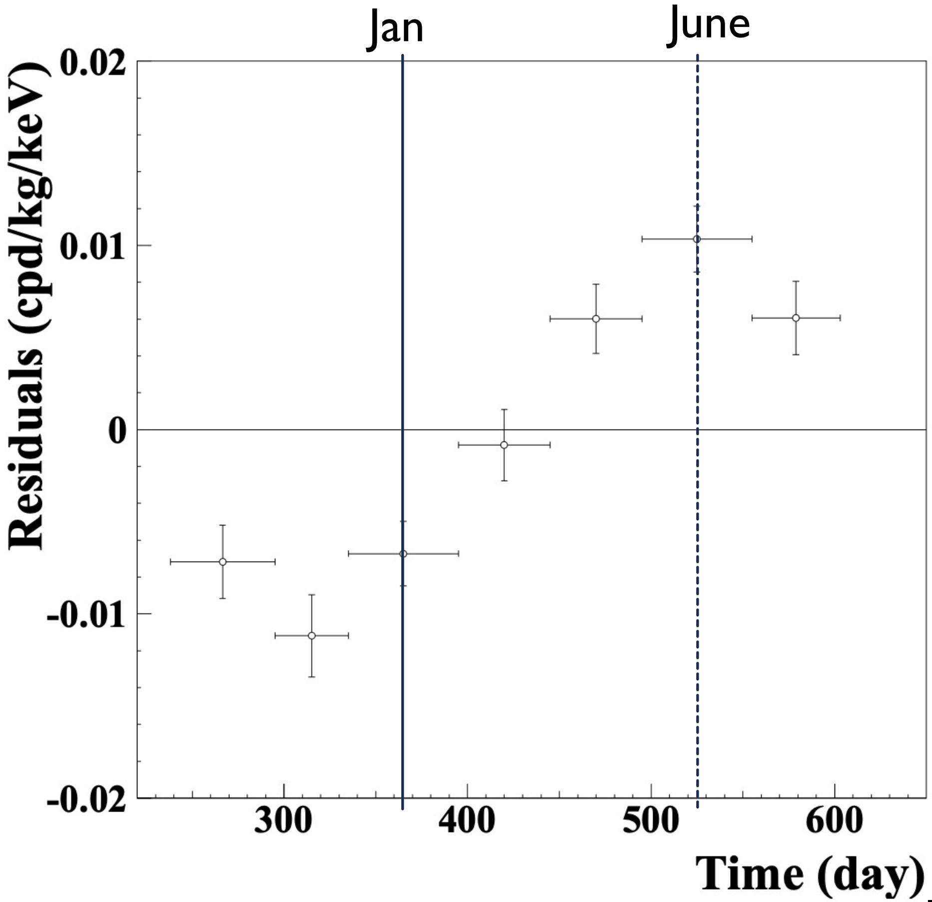

Average modulation at DAMA over 6 yrs[2]

DETECTOR DEPENDENCIES

Large uncertainties/inconclusive results:

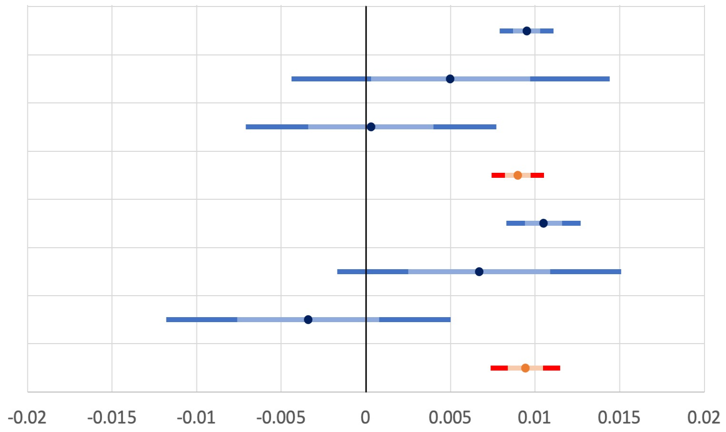

Potential detector difference:

- Na quenching factor
- Radioactive backgrounds
- Electronic backgrounds
- Background modelling
- Location specifics
- Energy thresholds

We need another model independent, well characterised setup to properly understand this landscape.

SABRE

Four key improvements on other NaI(Tl) detectors:

1. Ultra-high purity crystals
2. Active background rejection
3. Low energy threshold
4. Dual hemisphere data

Will provide unprecedented background and sensitivity

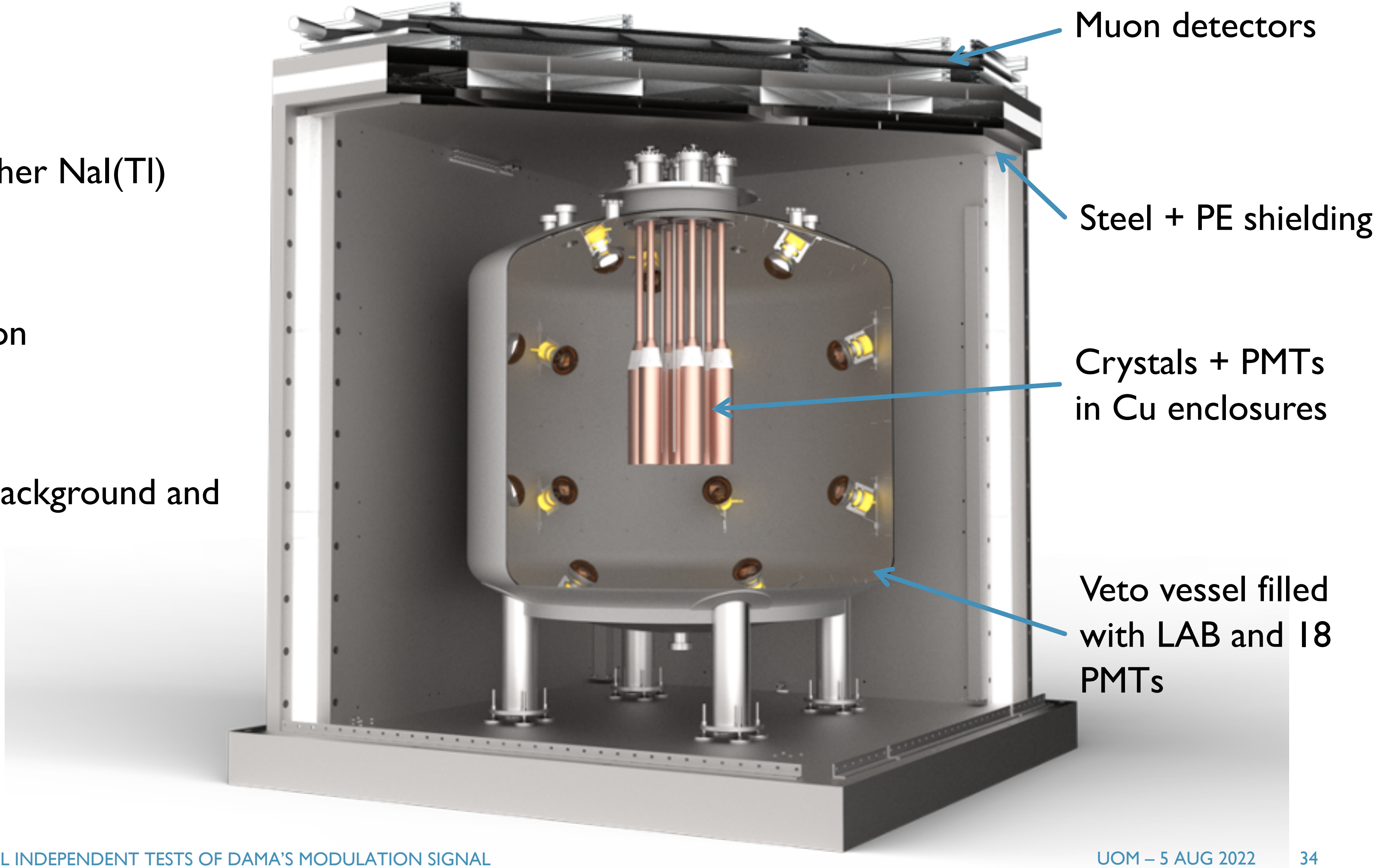

SABRE

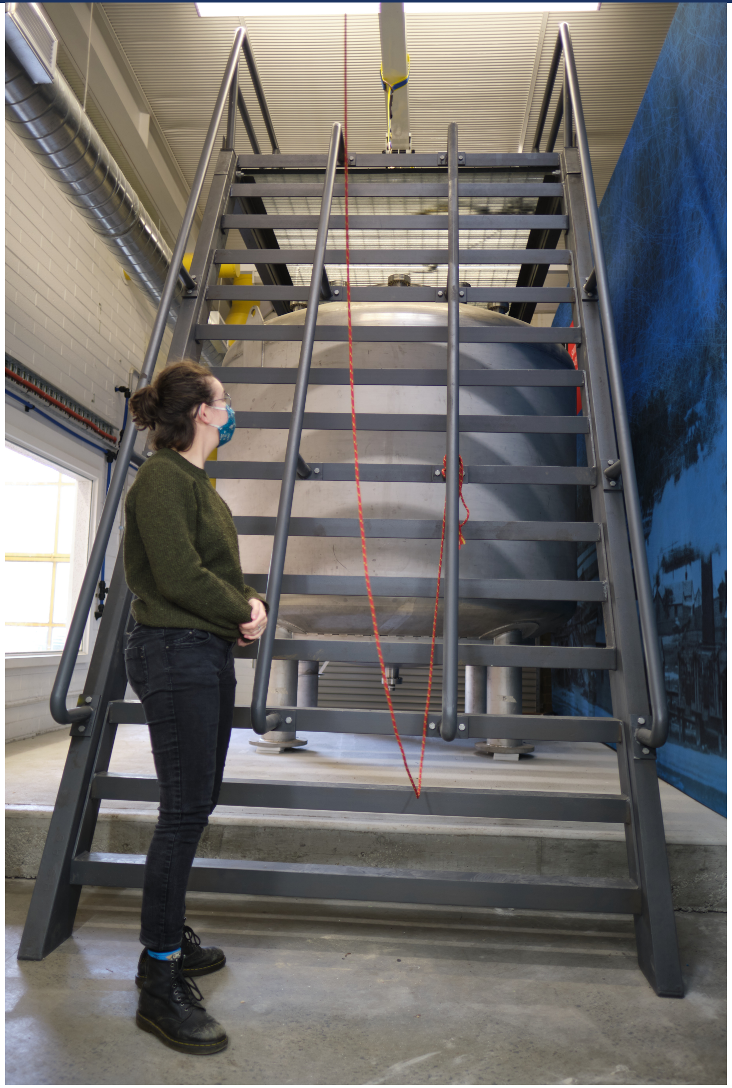

BACKGROUND REDUCTION

[1] F. Calaprice et al. arXiv: 2105.09225
[2] Burkhant Suerfu et al. Phys. Rev. Research **2**, 013223

Significant R&D undertaken with Princeton collaborators (Calaprice group) has produced lowest background NaI(Tl) ever [1,2].

Contaminant	Issue	Half life	Introduction	Current reduction method
Hydroxide (NaOH)	Causes sticking/cracking of crystal during growth	N/A	Reaction of NaI with water	$SiCl_4$ treatment
Potassium 40	Beta decay - 3 keV Auger electron	10^9 years	Similar properties to Na	Veto
Lead 210	Beta decay – 15 keV electron	22.3 years	Rn in water/atmosphere	None
Tritium (^3H)	Beta decay – 5 keV electron	12 years	Cosmogenic	Travel restrictions

NaOH (MSc), 40K, and 210Pb removal has all been addressed over my research (slight interruptions in latter two from COVID)

40K REDUCTION

Fractional crystallization utilises difference in solubility of materials

1. Mix solution to saturation at high temp
2. Cool and stir
3. Less soluble material forms a precipitate
4. Separation occurs via filtration

Na_2CO_3 and K_2CO_3 are ideal for this process (less hygroscopic than NaI)

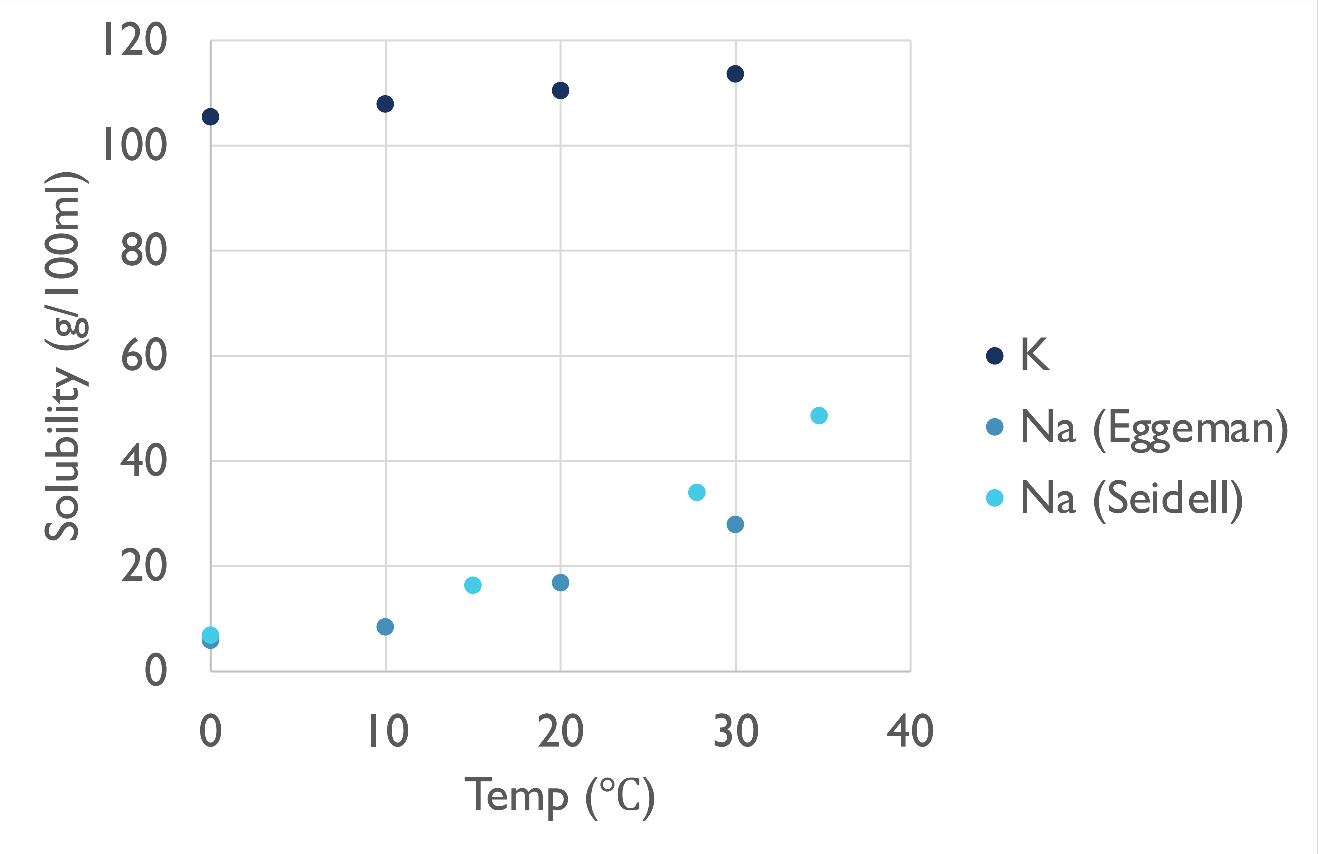

40K REDUCTION

Total yield of Na_2CO_3 was approx 30% - expected from solubility.

Levels of key contaminants are shown below for control solution (A0), then 1 and 2 crystallization cycles

Contaminant	A0 (ppm)	A1 (ppm)	A2 (ppm)
K39	0.260	0.625	0.318
Pb208	0.030	0.054	0.076
Rb85	0.040	0.008	<0.003
Th232	<0.003	<0.002	<0.003
U238	<0.003	<0.002	<0.003

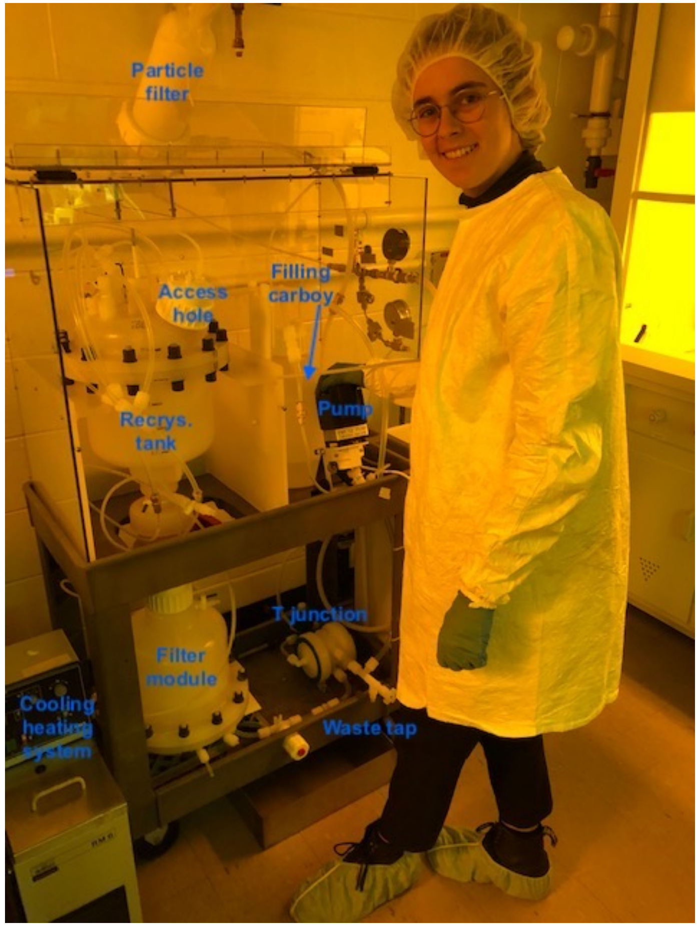

210PB REDUCTION

He bubbling suggested used to remove ^{208}Pb due to its lower melting temp, 330°C. Pb contamination will melt first then stripped away by gas

Resulting crystal demonstrated poor optical qualities but lead reduced, though potassium suffered a slight increase

Contaminant	Powder (ppm)	Crystal section (ppm)		
		1	2	3
K39	0.0075	0.0086	0.012	0.012
Pb208	0.0010	0.00035	0.00033	0.00024
Rb85	<0.0002	<0.0002	<0.0002	<0.0002
Th232	<0.0008	<0.0008	<0.0008	<0.0008
U238	<0.0001	<0.0001	<0.0001	<0.0001

BACKGROUND LEVELS

Crystal	^{nat}K (ppb)	^{238}U (ppt)	^{226}Ra (μBq/kg)	^{210}Pb (μBq/kg)	^{232}Th (μBq/kg)	R_b in 2-6 keV (cpd/kg/keV)	Active mass (kg)
DAMA [1]	13	0.7-10	8.7-124	5-30	2-31	<0.8	250
ANAIS [2]	31	<0.81	-	1530	0.4-4	3.2	112
COSINE [3]	<42	<0.12	8-60	10-420	7-35	2.7	~60
SABRE [4]	4.3±0.2	0.4	5.9±0.6	410±20	1.6±0.3	< 1 (goal)	~50 (goal)
PICOLON [5]	<20	-	13±4	<5.7	1.2±1.4	< 1 (goal)	~20 (goal)

[1] R. Bernabei et al., NIMA 592(3) (2008)
[2] J. Amare et al., EPJC 79 412(2019)
[3] P. Adhikari et al., EPJC 78 490 (2018)
[4] B. Suerfu et al., Phys. Rev. Research 2, 013223 (2020)
[5] K. Fushimi et al., PTEP 4 043F01 (2021)

ACTIVE VETO

SABRE also utilizes an external tagging system that identifies and reduces background during operation.

System has 4π coverage made up of:

- 12 kL linear alkyl benzene doped with PPO and Bis-MSB
- 18 Hamamatsu R5912 PMTs

Any radioactive decay with gamma >100 keV can be vetoed.

cpd/kg/keV per mBq/kg	238U	232Th	210Pb	85Kr	87Rb	40K
1-6 keV no veto	0.963	0.250	0.681	0.191	0.695	0.650
1-6 keV with veto	0.921	0.216	0.681	0.191	0.695	0.095
Veto effectiveness	4.3%	13.3%	0.0%	0.0%	0.0%	85.4%

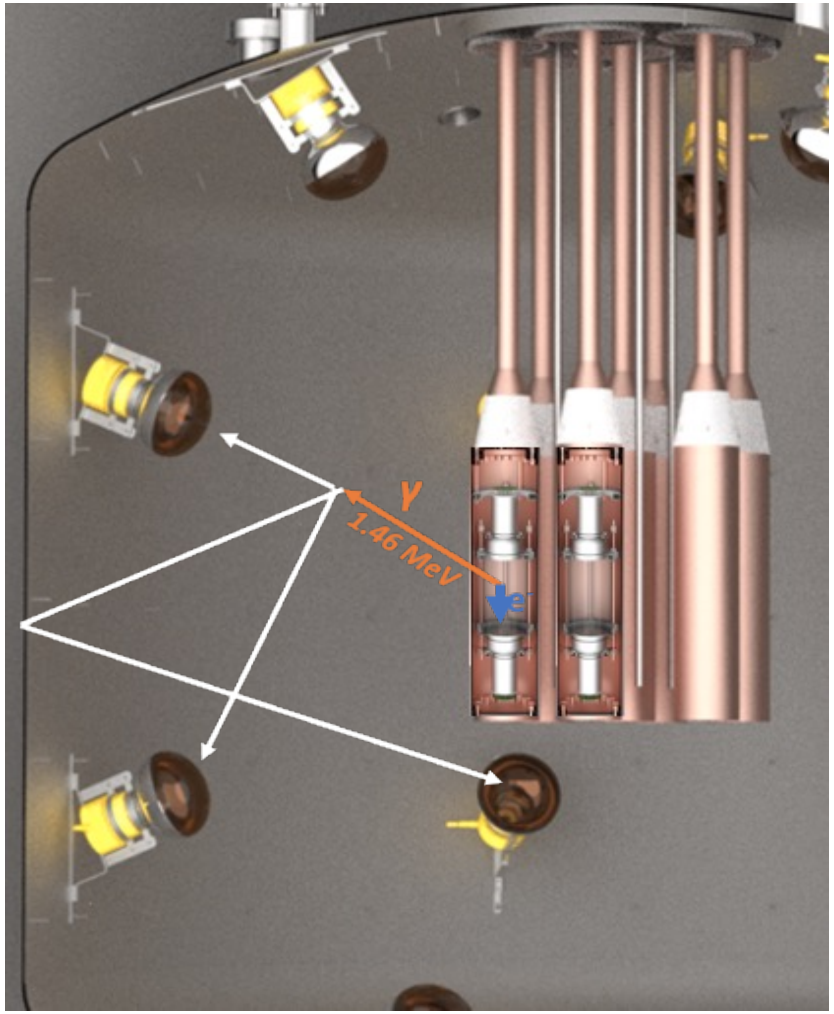

TOTAL BACKGROUND MODEL

[1] SABRE South Collab. arxiv:2205.13849

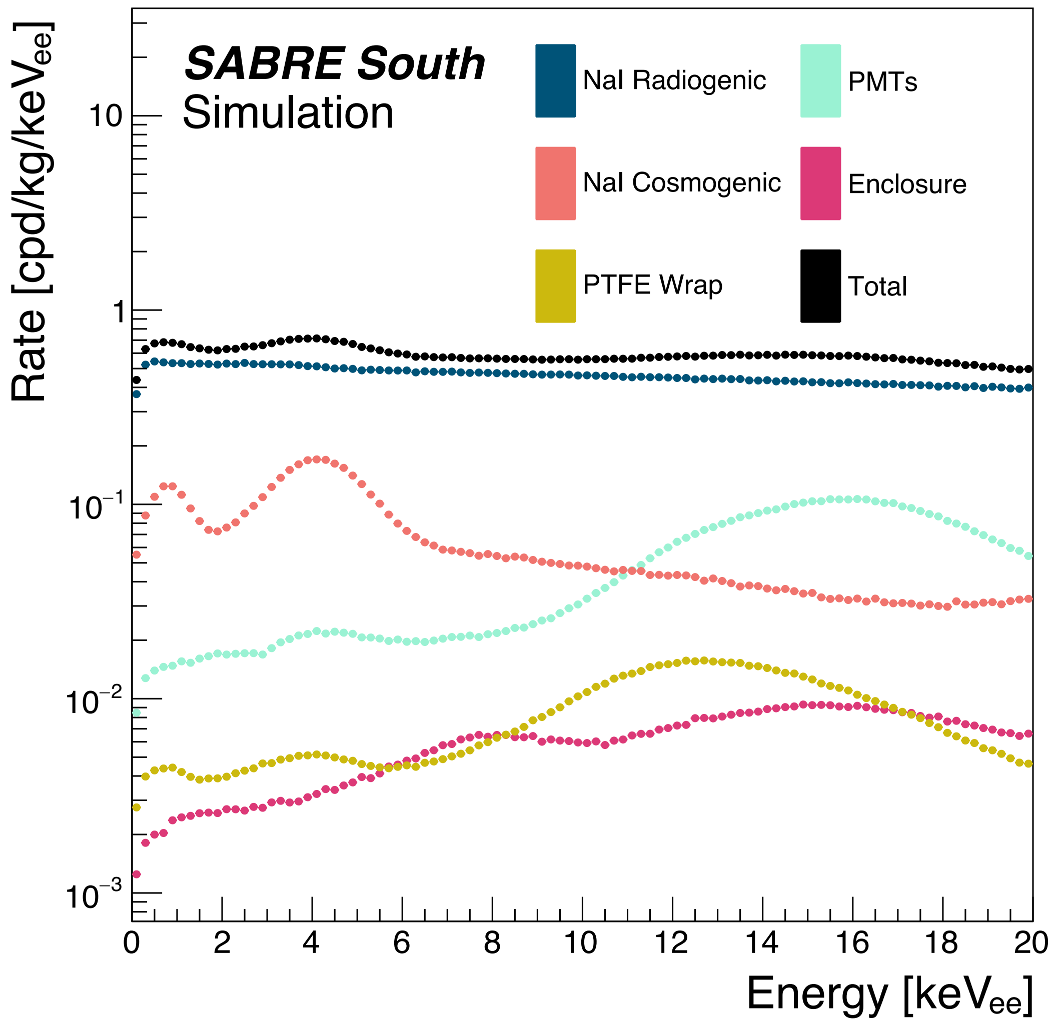

Component	Rate (cpd/kg/keV)	Veto efficiency (%)
Crystal intrinsic	$<5.2 \times 10^{-1}$	13
Crystal cosmogenic	1.6×10^{-1}	45
Crystal PMTs	3.8×10^{-2}	57
Crystal wrap	4.5×10^{-3}	11
Enclosures	3.2×10^{-3}	85
Conduits	1.9×10^{-5}	96
Steel vessel	1.4×10^{-5}	>99
Veto PMTs	1.9×10^{-5}	>99
Shielding	3.9×10^{-6}	>99
Liquid scintillator	4.9×10^{-8}	>99
External	5.0×10^{-4}	>93
Total	**0.72**	**27**

ACTIVE VETO

Barberio, Nuti, MJZ (in prep.)

Background simulations assume deposition in scintillator ⇒ detection of optical photon. Not the case!

Successful detection is dependent on

1. Number of photons generated by deposition of energy E
   - Light yield of LAB Poiss(n; LY x E)
2. Probability of photon generated at (x, y, z) reaching PMT_i.
   - Given by $P_{Di}(x, y, z)$ based on simulation
3. Probability of PMT_i detecting photon
   - QE_i

True detection probability is:

$$\mathrm{Poiss}(n; LY \times E) * \mathrm{Bi}(n, QE_i \times P_{Di}(x, y, z))$$

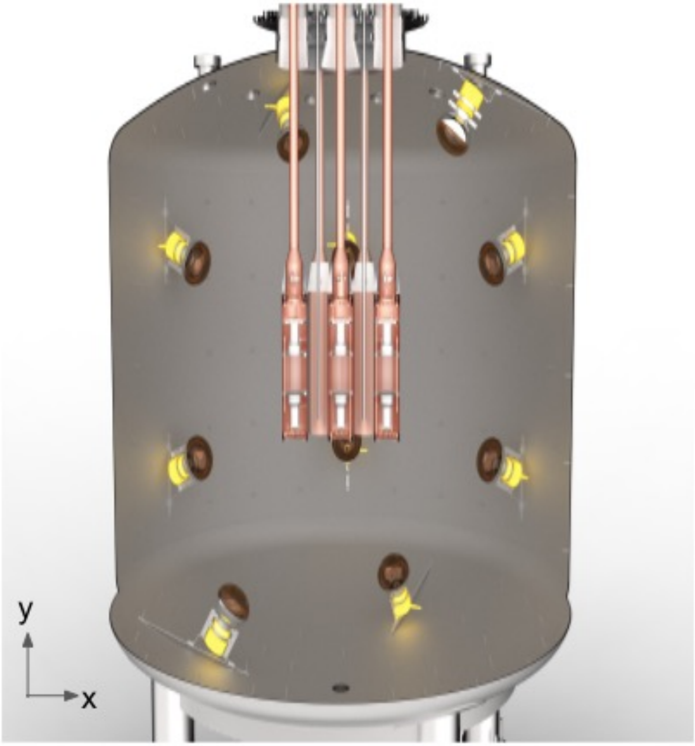

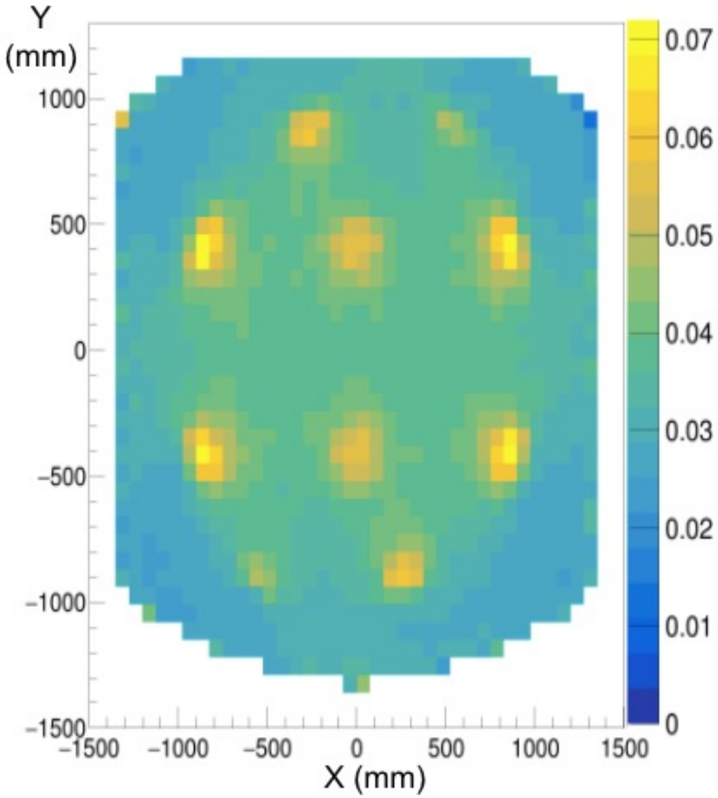

Probability of optical photon hitting PMT as a function of creation position

ACTIVE VETO

Barberio, Nuti, MJZ (in prep.)

Strong position dependence, but likely we can cut on a lower energy threshold than assumed for simulations (100 keV)

- Average $P_{Di}(x, y, z) \sim 0.04$
- Average QE ~ 0.3
- Light yield ~ 12 PE/keV

⇒ average number of detections is 0.144 PE/keV.

Likely PMT threshold is 6-8 PE, meaning veto threshold can be reduced to 50 keV, leading to:

- Reduced overall background
- Possible sensitivity to new physics using LS as detector

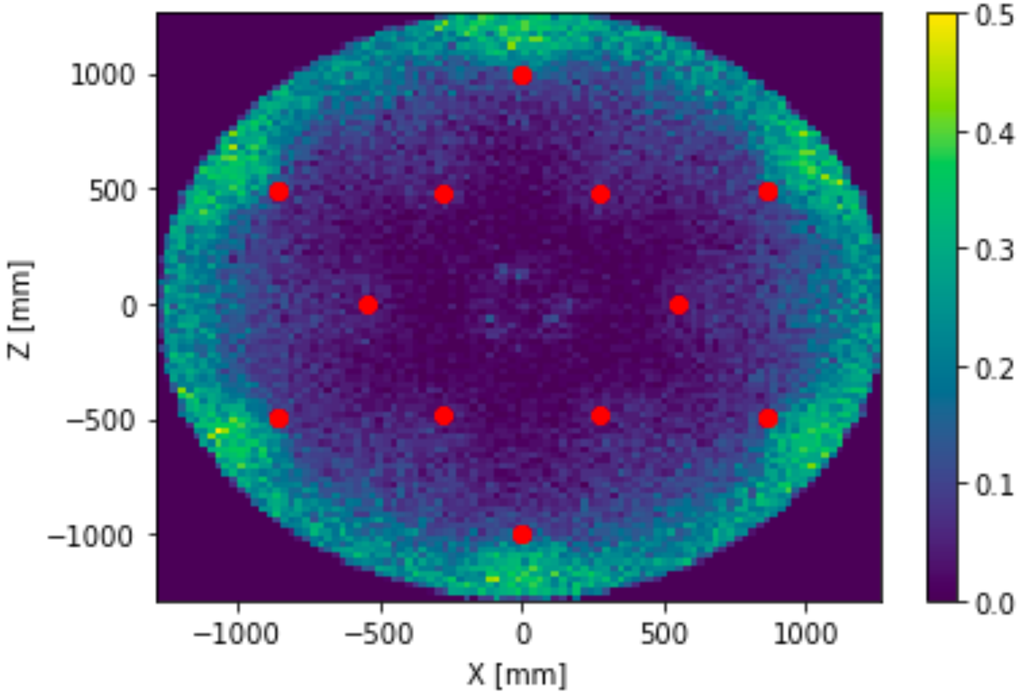

Fraction of 100 keV events undetected by PMTs

EVENT RECONSTRUCTION

Barberio, Nuti, MJZ (in prep.)

Detection probability maps can also be used to inform position reconstruction and particle ID in veto detector (tells us which PMTs will see which events)

Basic reconstruction: weighting (x, y, z) coordinate of PMT with number of detected photons

$$X = \frac{\sum_{i=0}^{17} X\_PMT_i \times \left(Q\_PMT_i^{\ 3}\right)}{\sum_{i=0}^{17} \left(Q\_PMT_i^{\ 3}\right)}$$

Cube power is included to remove biasing.

For 1 MeV events,
$X_{rec} - X_{true} = 5.75$ mm
$\Delta(X_{rec} - X_{true}) = 176.11$ mm

Less than ideal, but a good start!

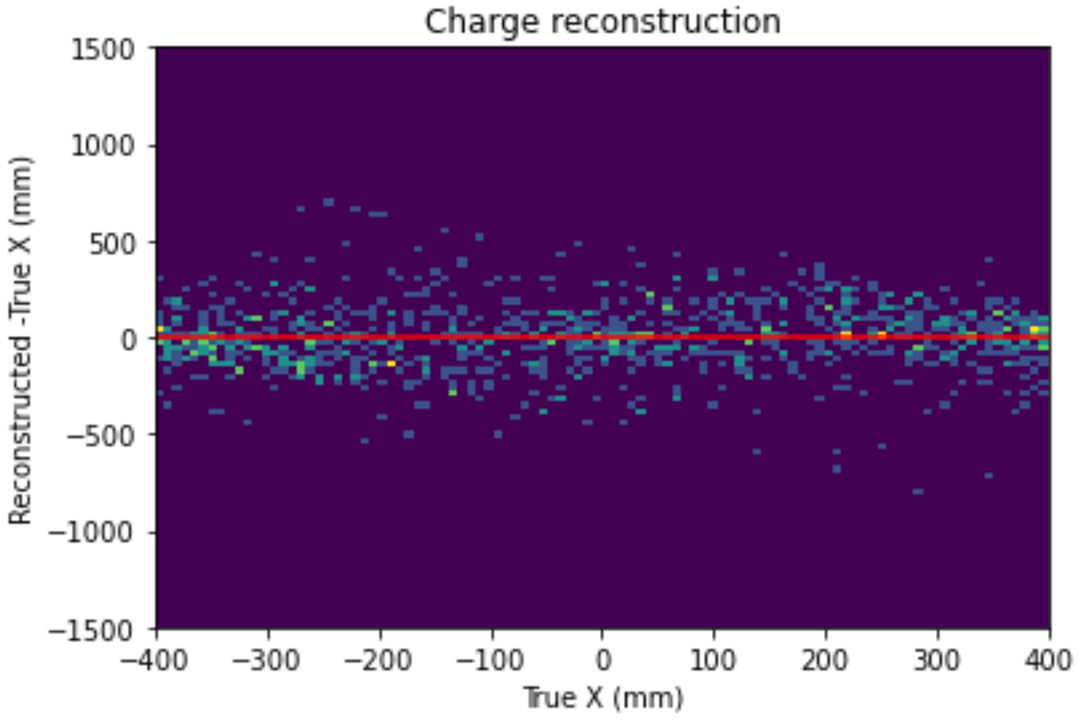

EVENT RECONSTRUCTION

Barberio, Nuti, MJZ (in prep.)

Another option is to invert existing probability maps – plot the number of generated photons required at each position to produce one hit in PMTs. This method is beneficial as gives both position and energy in one step

1. Construct this 3D map for each PMT
2. For an event, scale each of these with the number of observed photons at PMT
3. Find the position that has the ~ same number of photons generated in each plot

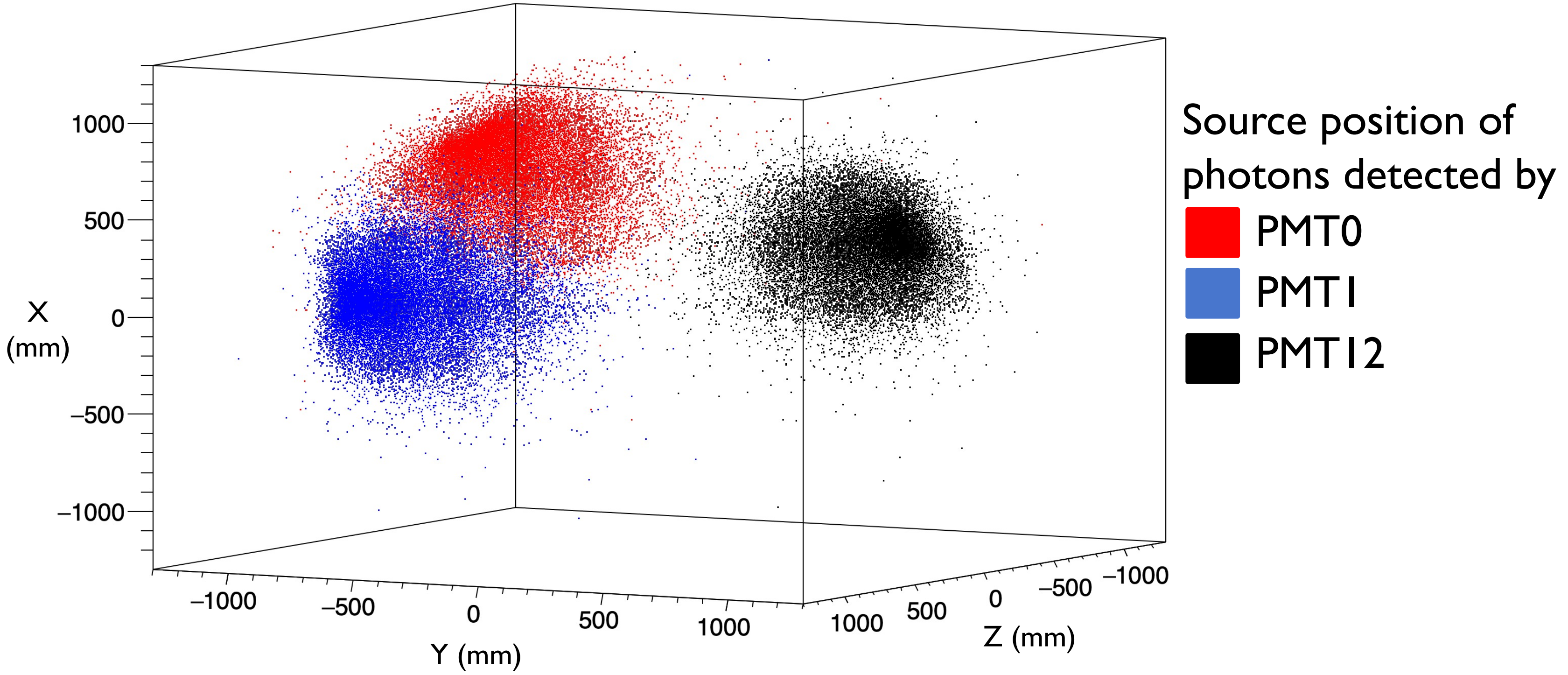

EVENT RECONSTRUCTION

Barberio, Nuti, MJZ (in prep.)

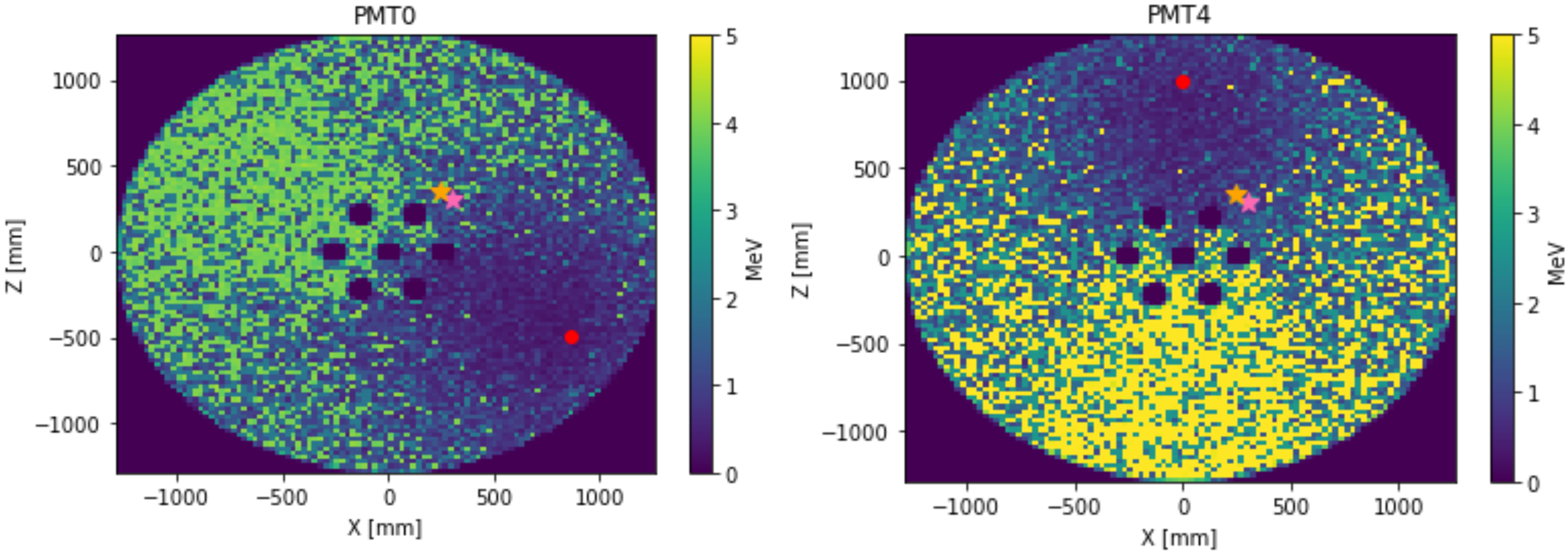

Energy deposition required to have the observed number of hits in both PMT0 and PMT4 (given by red dots). The true event position is shown in pink, and the reconstructed in orange.

EVENT RECONSTRUCTION

Li et al., Nucl Sci Tech (2021)32:49
Barberio, Nuti, MJZ (in prep.)

Can also use timing information to reconstruct position. Based on the requirement that hit time is ~ time of direct flight

$$\frac{|\vec{X}_T|}{|\vec{X}_R|} = \frac{t_i}{tof_i}$$

1. Take charge reconstruction as initial guess position, R_0
2. Compute the time of flight from this position to PMT_i, tof_i
3. Compare this to hit time for PMT_i, t_i
4. Construct the correction factor dr
5. Repeat steps 2-4 using R_0+dr as the new guess

$$d\vec{r} = \frac{1}{N_{PMTs}} \sum_i \left(\frac{t_i}{tof_i} - 1 \right) \vec{X}_R$$

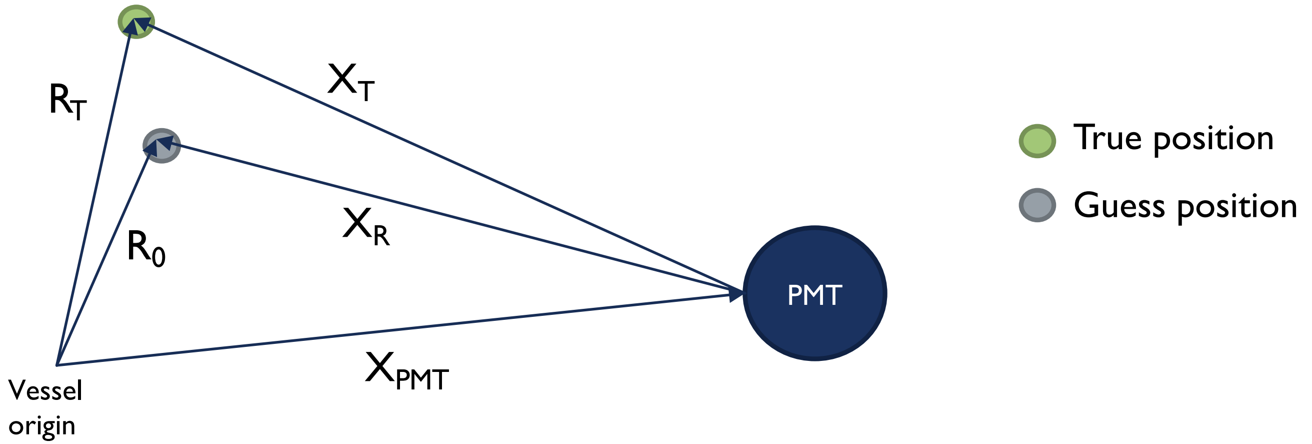

This requires a fully 'digitized' signal

WAVEFORM SIMULATION

Melbourne, Spinks, MJZ (in prep.)

Digitisation of optical simulations takes the list of photon arrival times output by Geant4 and simulates the physical process that produces a signal that can be analysed in the same way as actual data.

1. **Apply quantum efficiency and transit time**
   - Applies a probability cut to mimic QE
   - Adds cable length and PMT TT
2. **Convolution**
   - Determine each photoelectron (PE) charge
   - Convolve with SPE to get semicontinuous waveform
3. **Digitise**
   - Account for sample rate and resolution of DAQ
4. **Noise effects**
   - Add baseline fluctuations, shot noise, dark rate

Finalising development for use in analysis framework

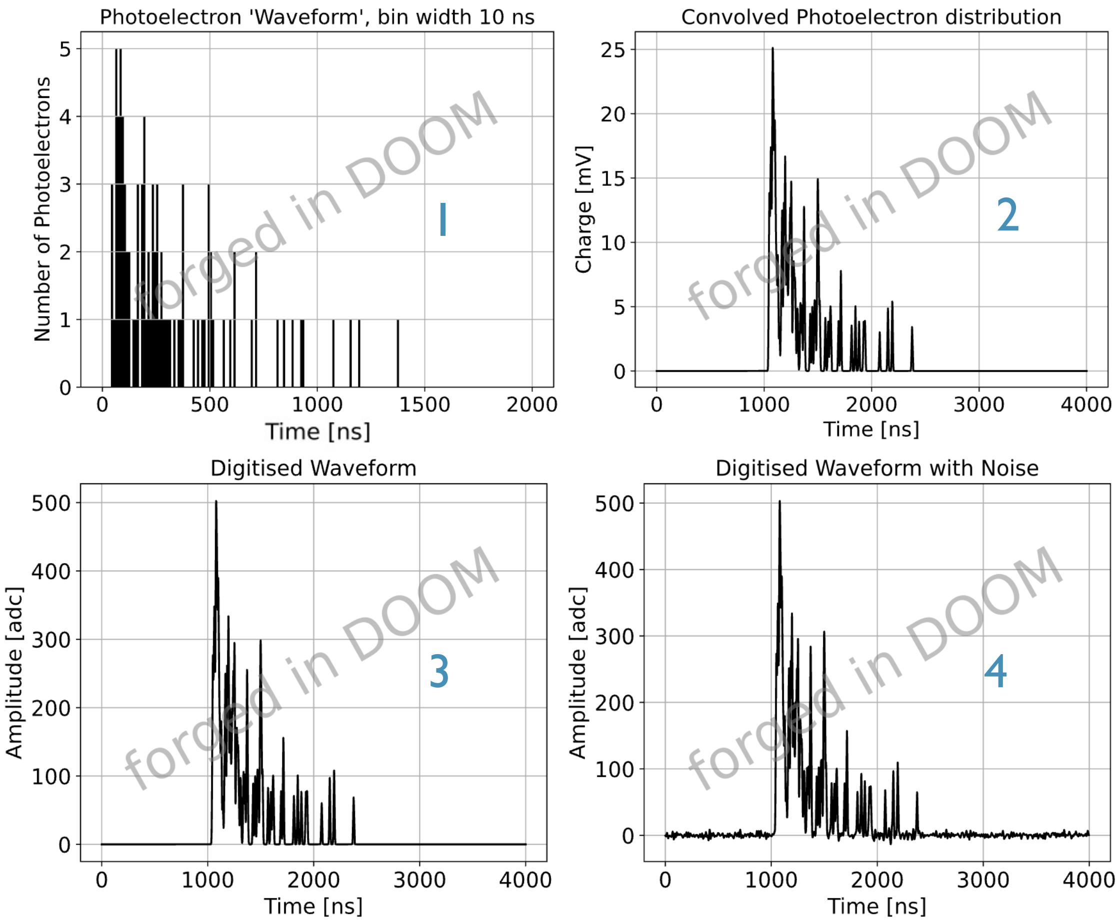

WAVEFORM SIMULATION

Melbourne, Spinks, MJZ (in prep.)

Preliminary validation ongoing using calibration data with 137Cs near a NaI crystal

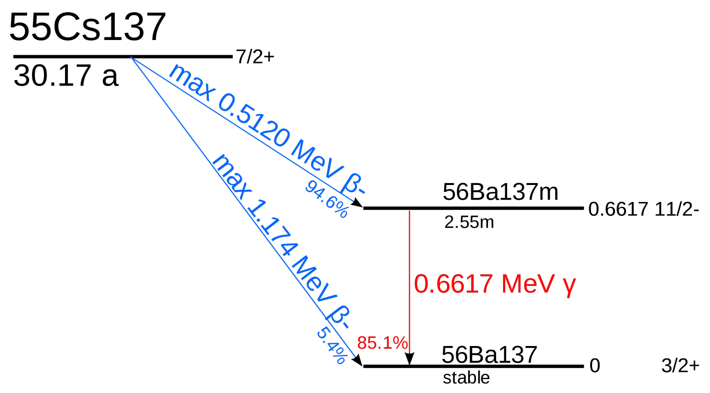

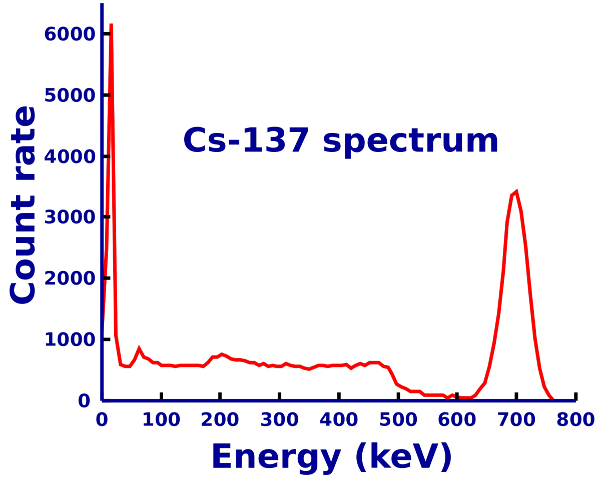

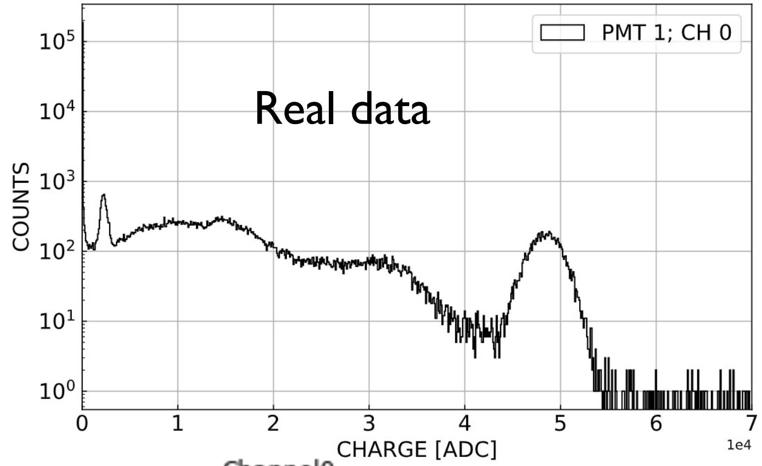

Still ironing out Geant4 issues, but results looking good so far!

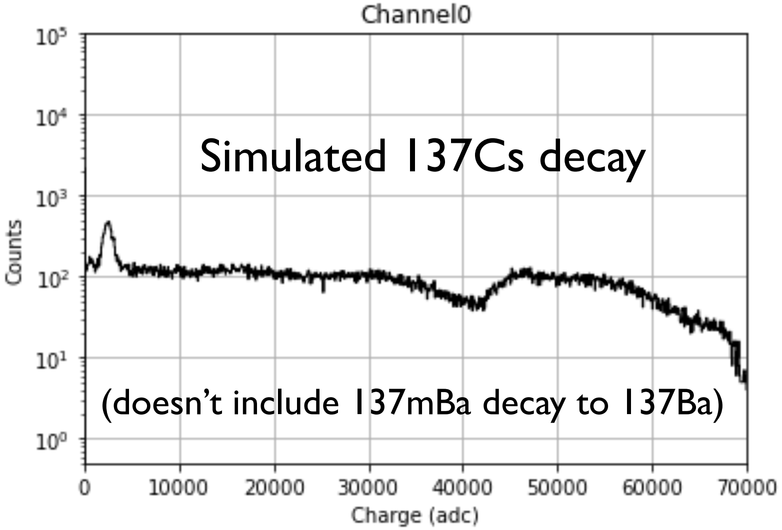

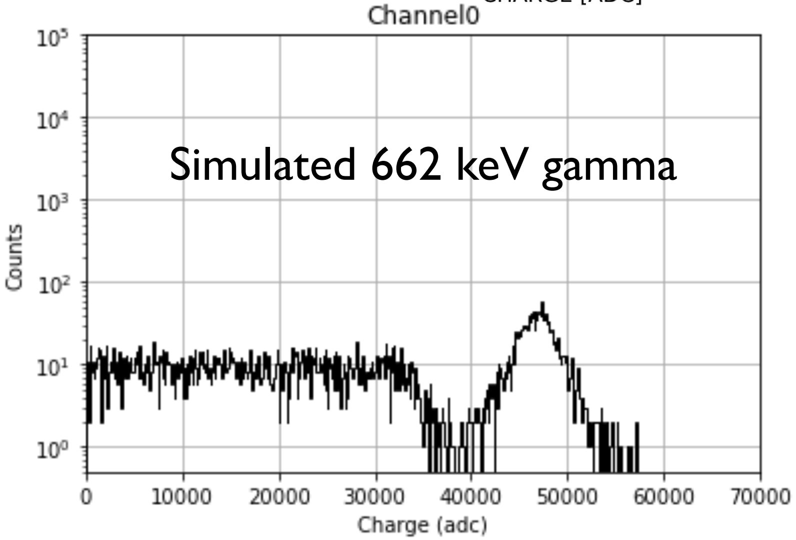

FUTURE PROJECTIONS

Based on these studies, SABRE South is expected to have a total mass of 50 kg, and background <0.7 cpd/kg/keV.

In the event of null results, we should reach 3σ exclusion in ~2yr of data taking, and 5σ approx 3 yrs after that.

In the event of a positive DAMA-like signal, SABRE will have a discovery power of 5σ within ~2yrs.

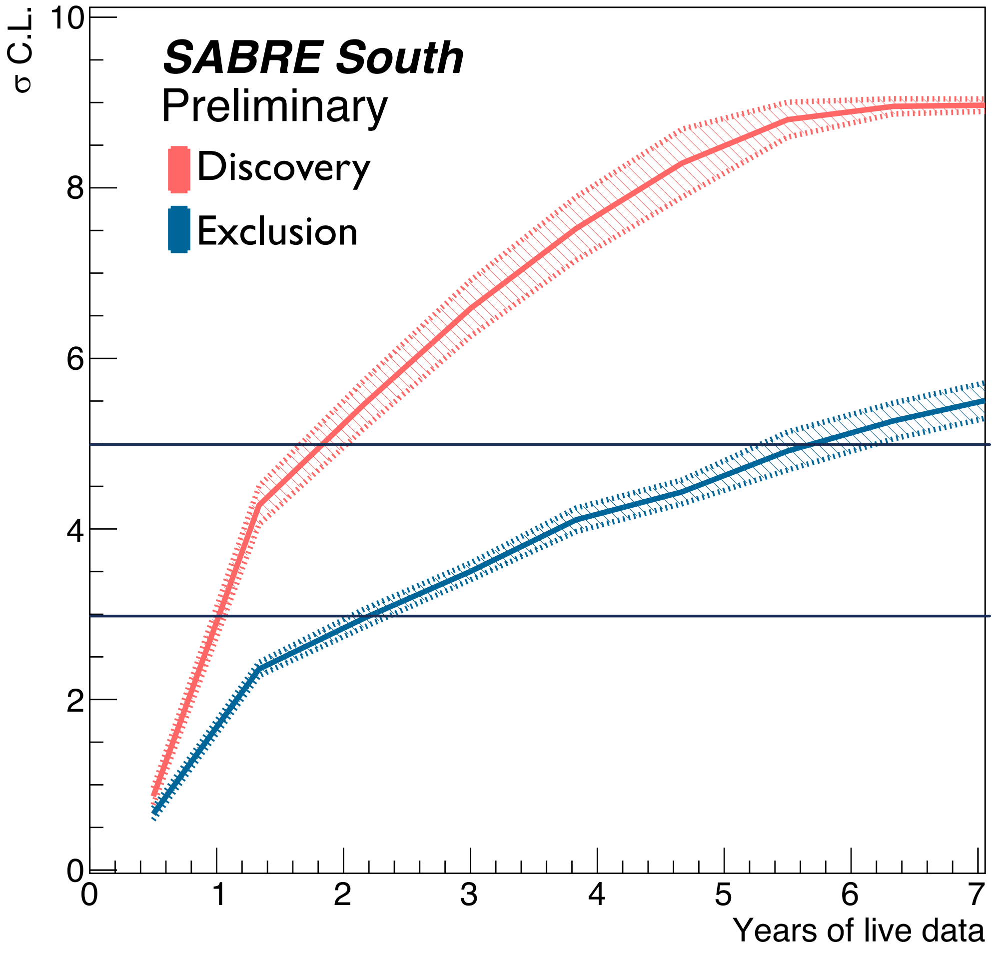

FUTURE PROJECTIONS

Additionally, can compare the ability to constrain generic new physics: minimum excess each setup could observe with 3σ as a function of live time.

Again, SABRE performs very well, very quickly.
This is due to its ultra low background compared to the other two experiments.

Further studies are in progress to examine how different, more intricate background models will influence experimental sensitivity, and what kind of new physics could be probed with such a set up.

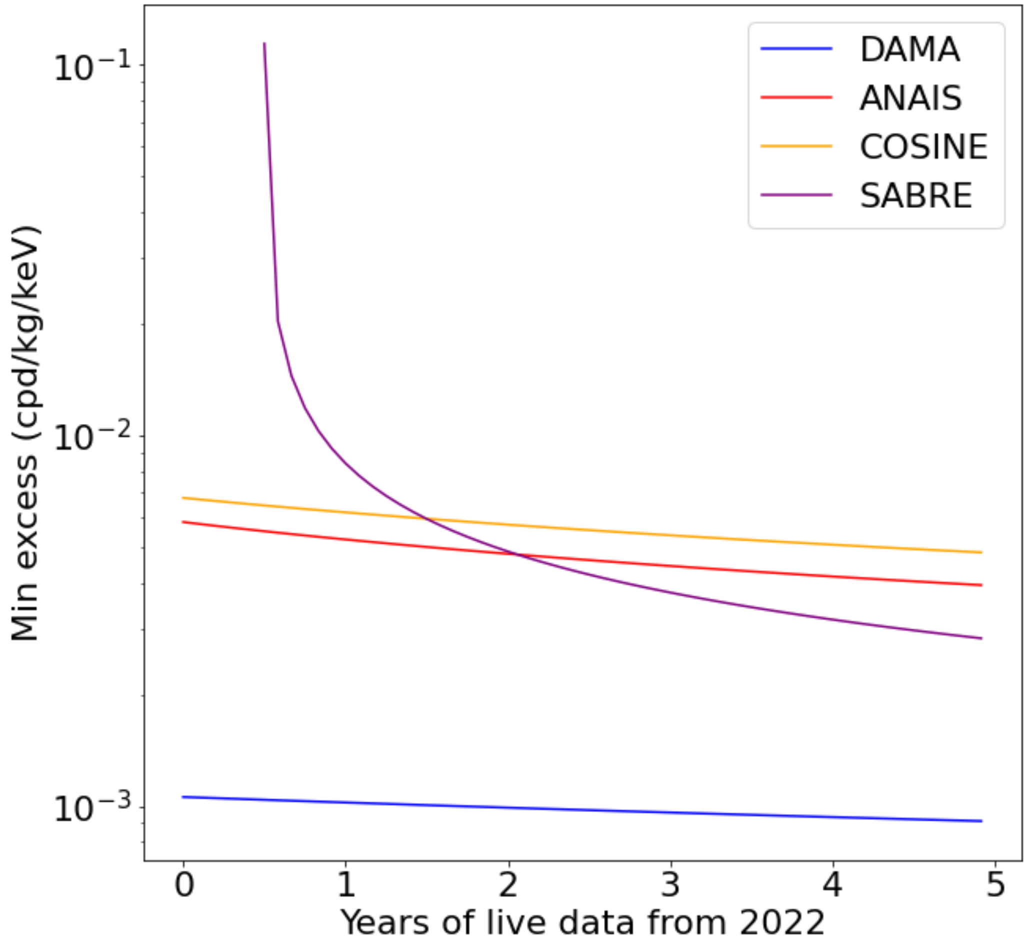

SUMMARY

PhD work has fallen into a few different categories:

- Understanding the need and performance of model independent tests of DAMA
  - Impact of different models and velocity distributions on observations
  - Requirements for a model independent test
  - Detector dependence on observation rate
- SABRE background model
  - Crystal purification techniques
  - MC modelling of contaminations
  - Crystal requirements
- Event reconstruction
  - Optical simulations
  - Position reconstruction
  - Waveform simulation
- Experimental projections
  - Ability of SABRE to constrain DAMA
  - Tests of new physics with SABRE

Key outputs/future work

- MJZ, Barberio, Busoni, JCAP12 (2020) 014
- MJZ, Barberio, arxiv:2107.07674 (presented at TAUP21)
- Barberio, Duffy, Lawerence, MJZ, (impact of vel. dist. in prep.)
- MJZ in SABRE South Collab. arxiv:2205.13849 (corresponding author)
- SABRE Technical Design Report (in prep, chapter editor)
- MJZ, Barberio (impact of QF in prep, presented at IDM22)
- Ongoing project with M. Mews
- Melbourne, Spinks, MJZ (waveform simulation, in prep)
- SABRE White Paper (in prep, chapter coordinator)

ACKNOWLEDGEMENTS

ARC CENTRE OF EXCELLENCE FOR DARK MATTER

SABRE South

Australian Government

Australian National University

SWINBURNE UNIVERSITY OF TECHNOLOGY

THE UNIVERSITY of ADELAIDE

THE UNIVERSITY OF MELBOURNE

SABRE North

INFN LNGS
Istituto Nazionale di Fisica Nucleare
Laboratori Nazionali del Gran Sasso

Pacific Northwest NATIONAL LABORATORY

PRINCETON UNIVERSITY

SAPIENZA UNIVERSITÀ DI ROMA

UNIVERSITÀ DEGLI STUDI DI MILANO

BACK UP SLIDES

PSIDM MODELS

[1] Kang, Scopel, Tomar, PRD 99, 103019 (2019)

Family of models presented to reduce experimental tension w/ DAMA

Case	Spin (j_χ)	m (GeV)	σ_0 (cm^2)	δ (keV)	Non zero $\hat{\mathbf{c}}_0$ components	
1	0	11.1	3.9×10^{-27}	22.8	$\hat{c}_7^0 = 0.68$	$\hat{c}_7^1 = 0.73$
2	1/2	11.6	4.7×10^{-28}	23.7	$\hat{c}_4^0 = -0.0014$ $\hat{c}_5^0 = -0.032$ $\hat{c}_6^0 = 0.692$	$\hat{c}_4^1 = -0.0015$ $\hat{c}_5^1 = -0.0166$ $\hat{c}_6^1 = 0.7217$
3	1	11.4	5.7×10^{-32}	23.4	$\hat{c}_4^0 = 0.0717$ $\hat{c}_5^0 = 0.1892$	$\hat{c}_4^1 = 0.0753$ $\hat{c}_5^1 = 0.9764$

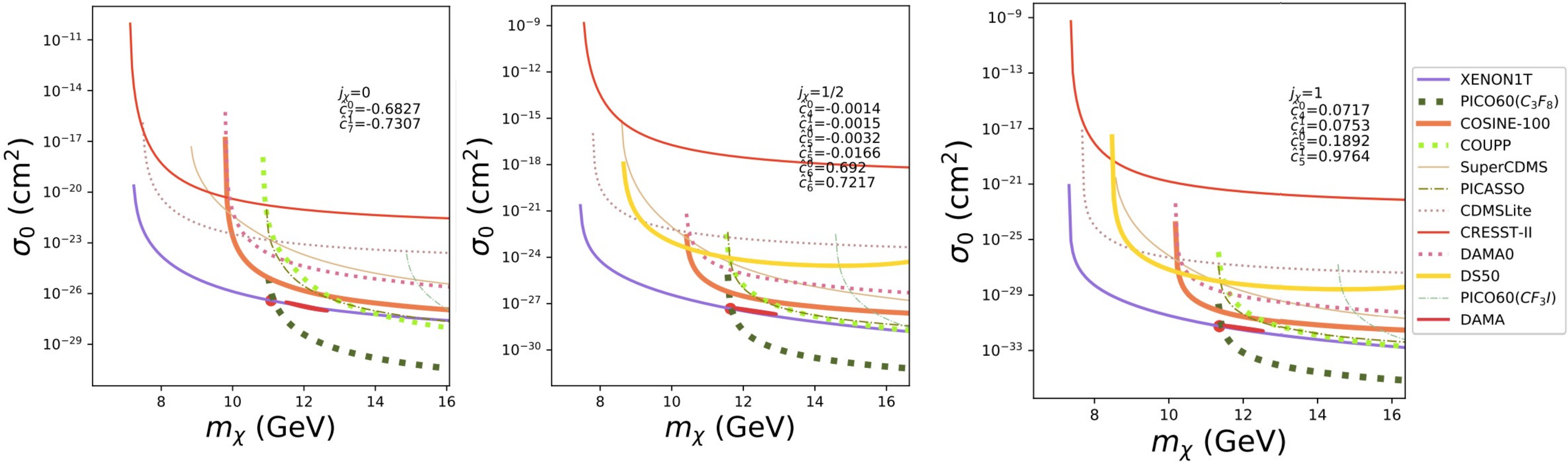

PSIDM MODELS

MJZ, Barberio, Busoni JCAP12 (2020) 014

Can take these models and find better fits (rather than the lowest tension)

Also examine influence of velocity distribution – inclusion of high velocity stream substructure increases mass and decreases cross section and mass splitting

Velocity distribution	Model	m_χ (GeV)	σ_0 (cm^2)	δ (keV)	χ^2/dof
SHM	1	13.87	7.53×10^{-29}	20.17	7.02/12
	2	13.47	2.09×10^{-29}	20.82	6.71/12
	3	13.17	2.45×10^{-33}	20.42	6.92/12
SHM+Stream	1	14.72	4.89×10^{-29}	19.81	7.31/12
	2	14.29	1.36×10^{-29}	20.67	6.89/12
	3	13.96	1.26×10^{-33}	19.70	7.18/12

NAOH REDUCTION

1. Fill $SiCl_4$ (2 mg/g NaI) and crystal crucible in gloveboxes
2. Pump apparatus to vacuum and purge w N2
3. Powder heated to 450°C over 20 hours
4. Heat to 700°C for 30 mins and open valve to allow vapour pressure of $SiCl_4$ to mix
5. Allow crystal to cool naturally

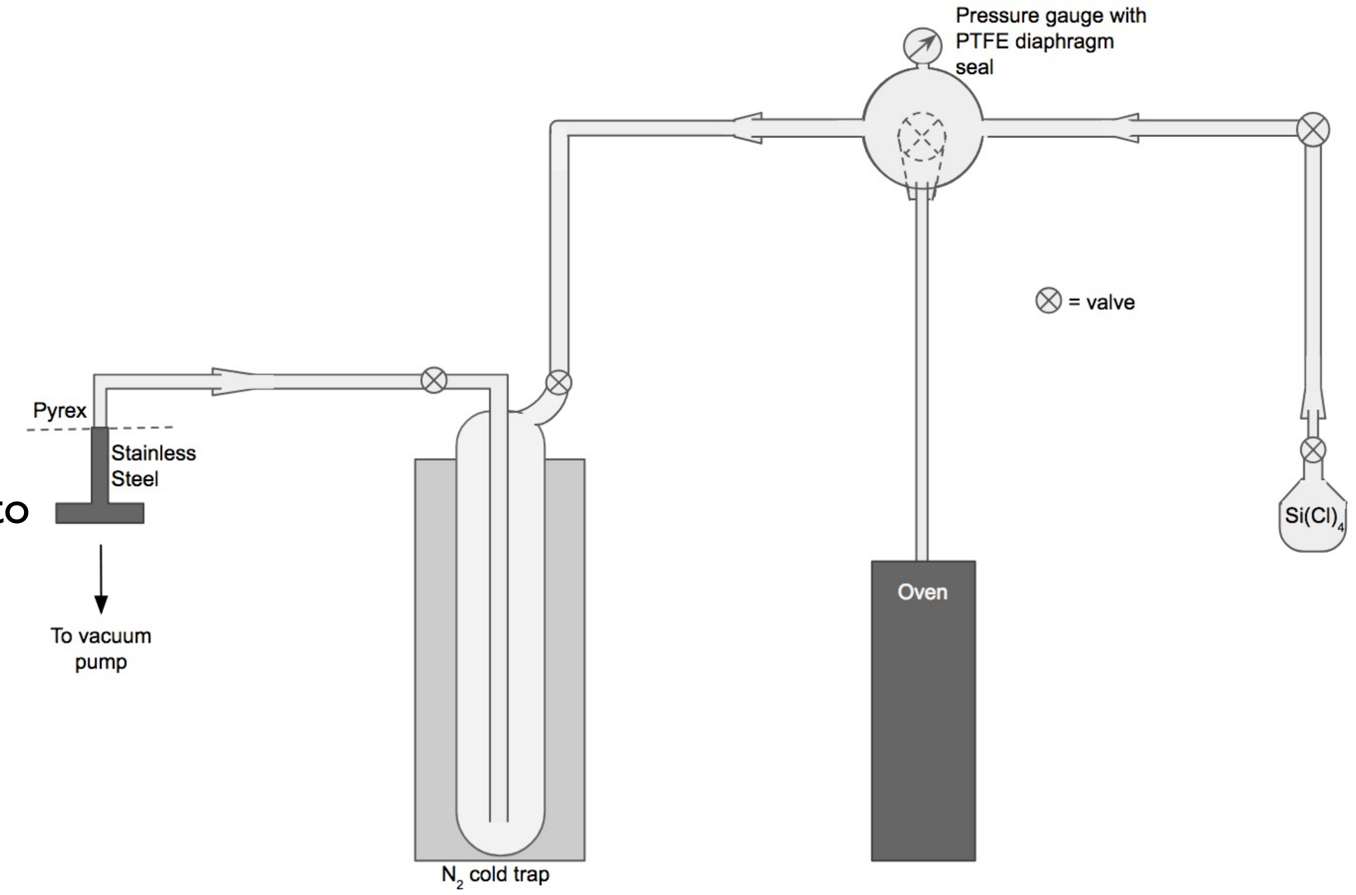

NAOH REDUCTION

Hydroxides 'wet' sides of growth container causing sticking, then cracking reducing optical qualities

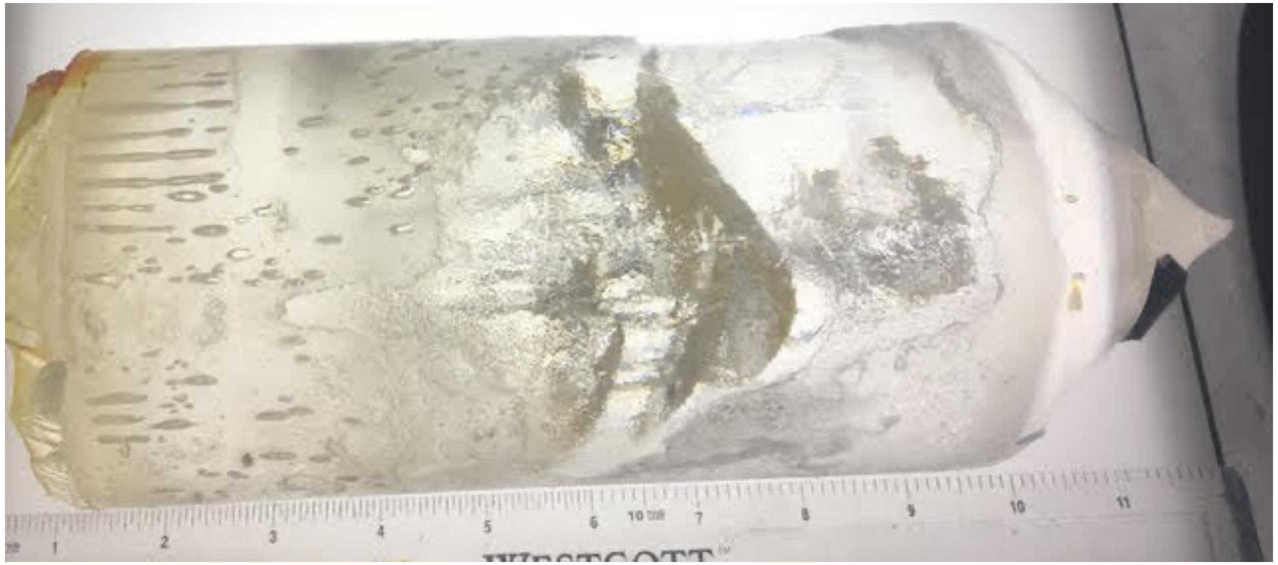

Can be reduced via introduction of Silicon tetrahalides SiX_4 where X is I or Cl

$$SiCl_4 + 2NaOH \rightarrow 2NaCl + 2HCl + SiO_2$$

NAOH REDUCTION

Test of this method with non-optical crystals (no thallium doping) indicated success in reducing sticking

Further tests are required to understand any negative effects on optical qualities

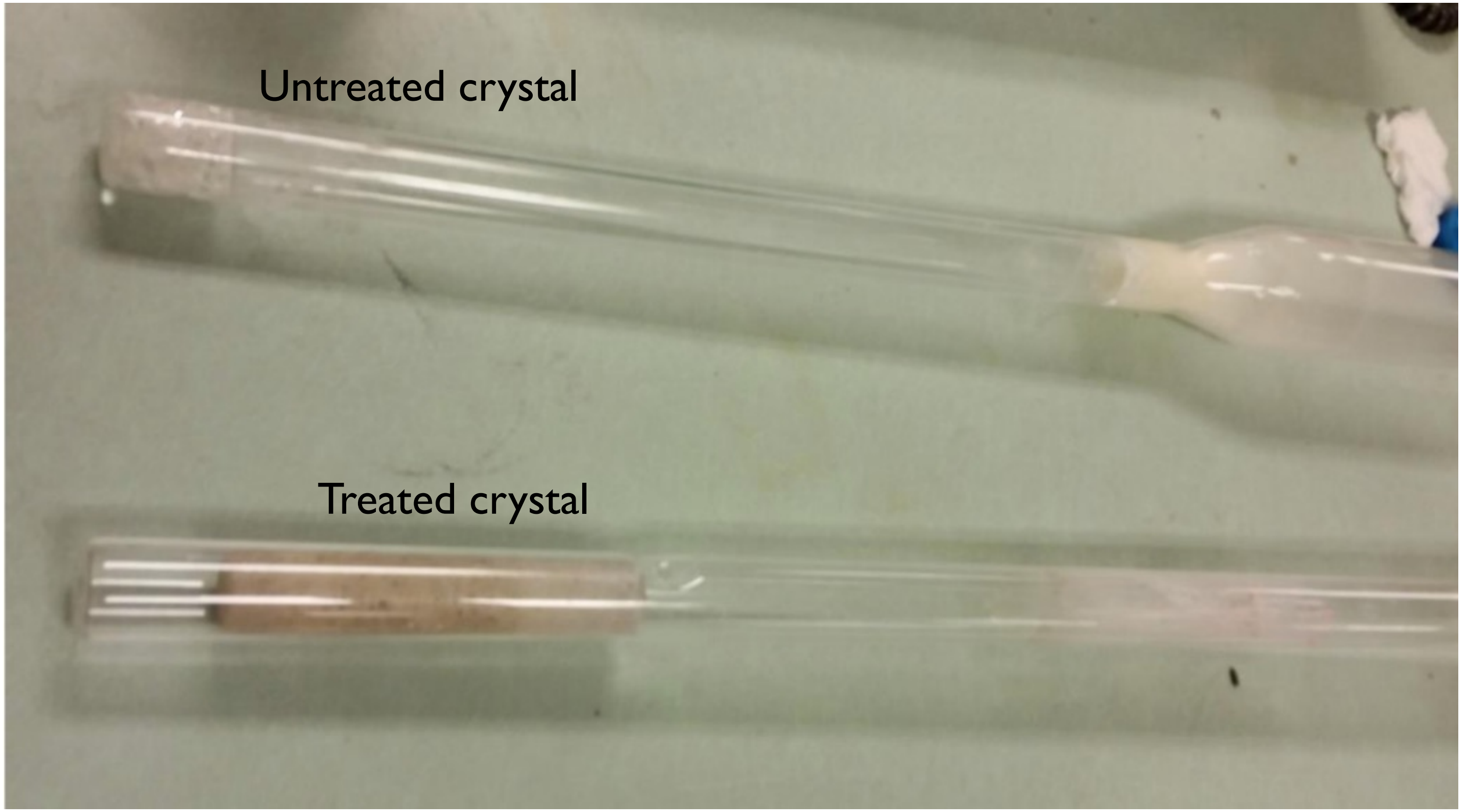

40K REDUCTION

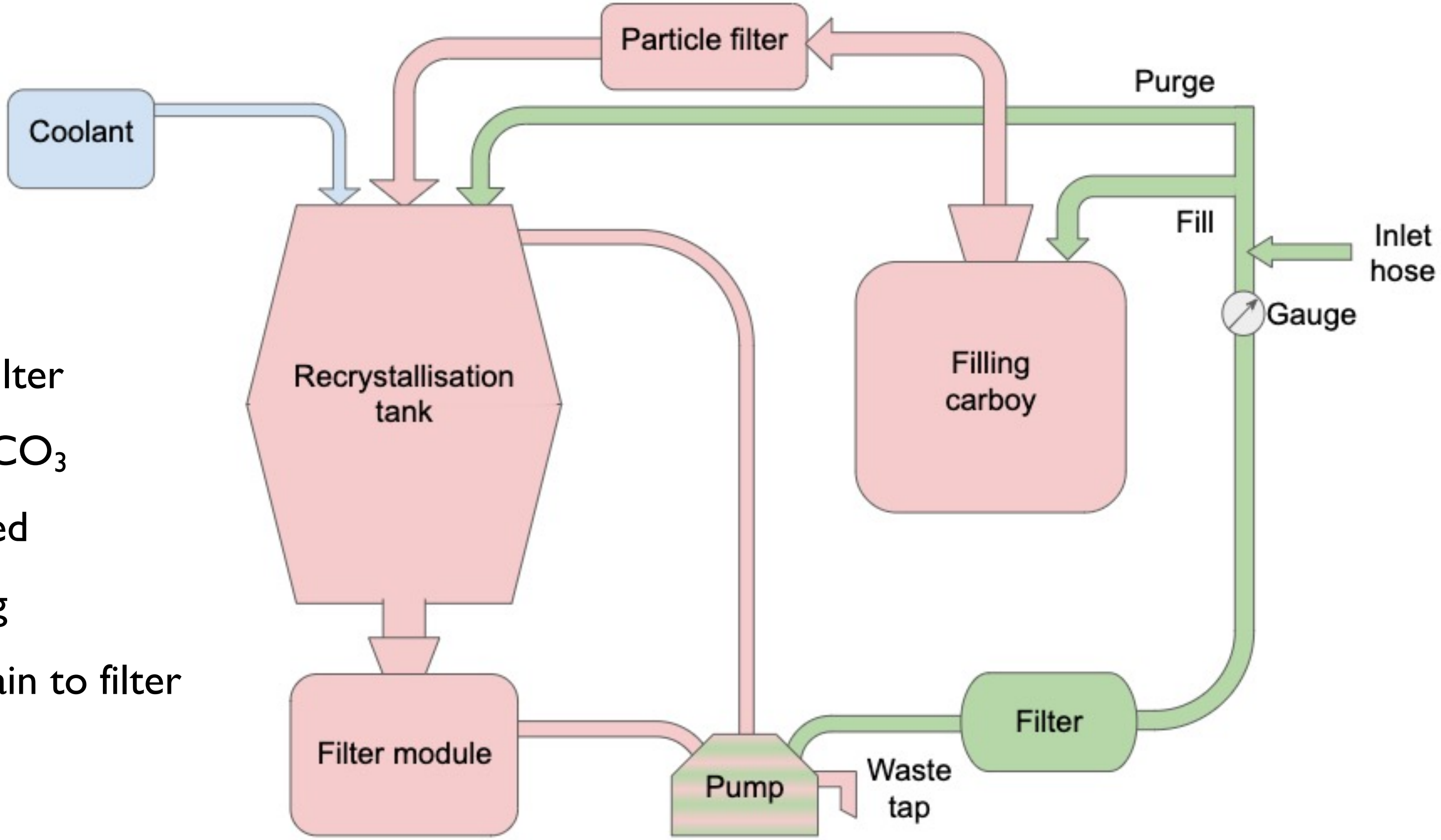

Method:

1. Pump 5 L DI water into tank via filter
2. Heat to 56℃ and stir in 1 kg Na_2CO_3
3. Cool to -5℃ for 24 hrs untouched
4. Kickstart crystallization by stirring
5. Leave for 18 hrs, then mix and drain to filter module

210PB REDUCTION

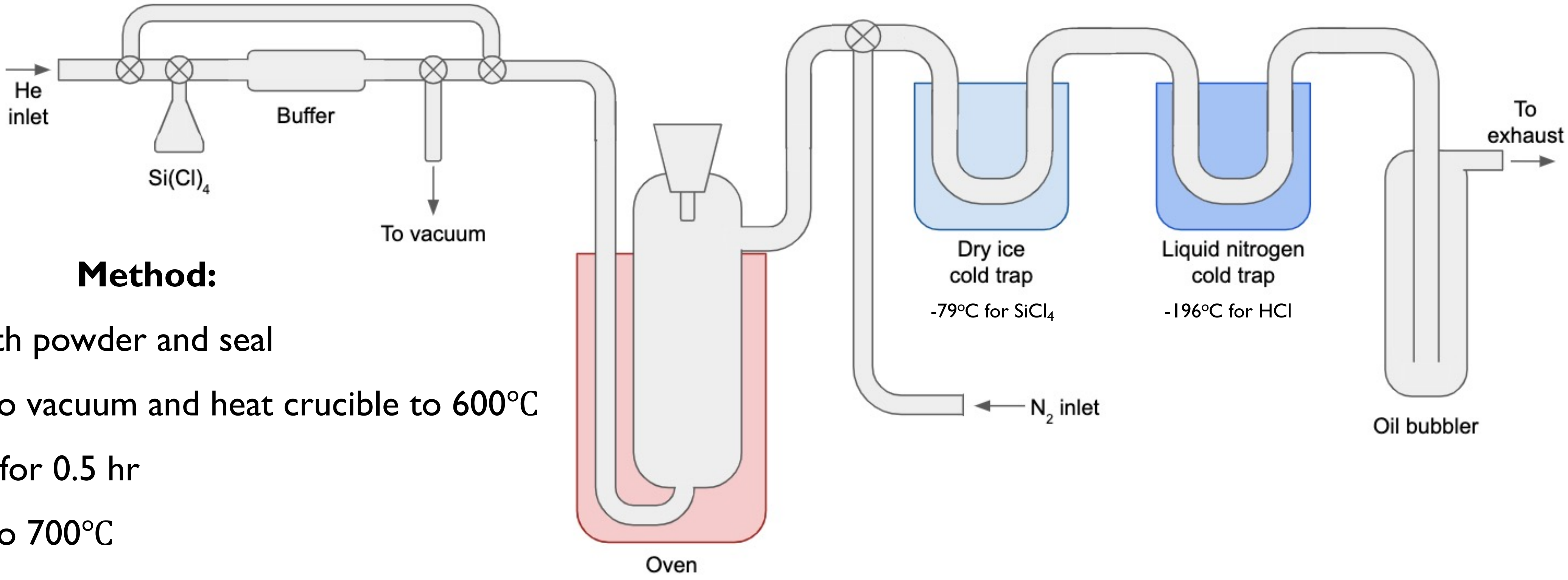

Method:

1. Fill crucible with powder and seal
2. Pump system to vacuum and heat crucible to 600°C
3. Bubble He gas for 0.5 hr
4. Increase heat to 700°C
5. Leave molten powder with He bubbling for 2.5 hrs
6. Turn of He, cool NaI to 20°C at rate of 5°C/min

TOTAL BACKGROUND MODEL

[1] SABRE South Collab. arxiv:2205.13849

Veto system not only reduces background but also allows for in situ measurements and particle ID.

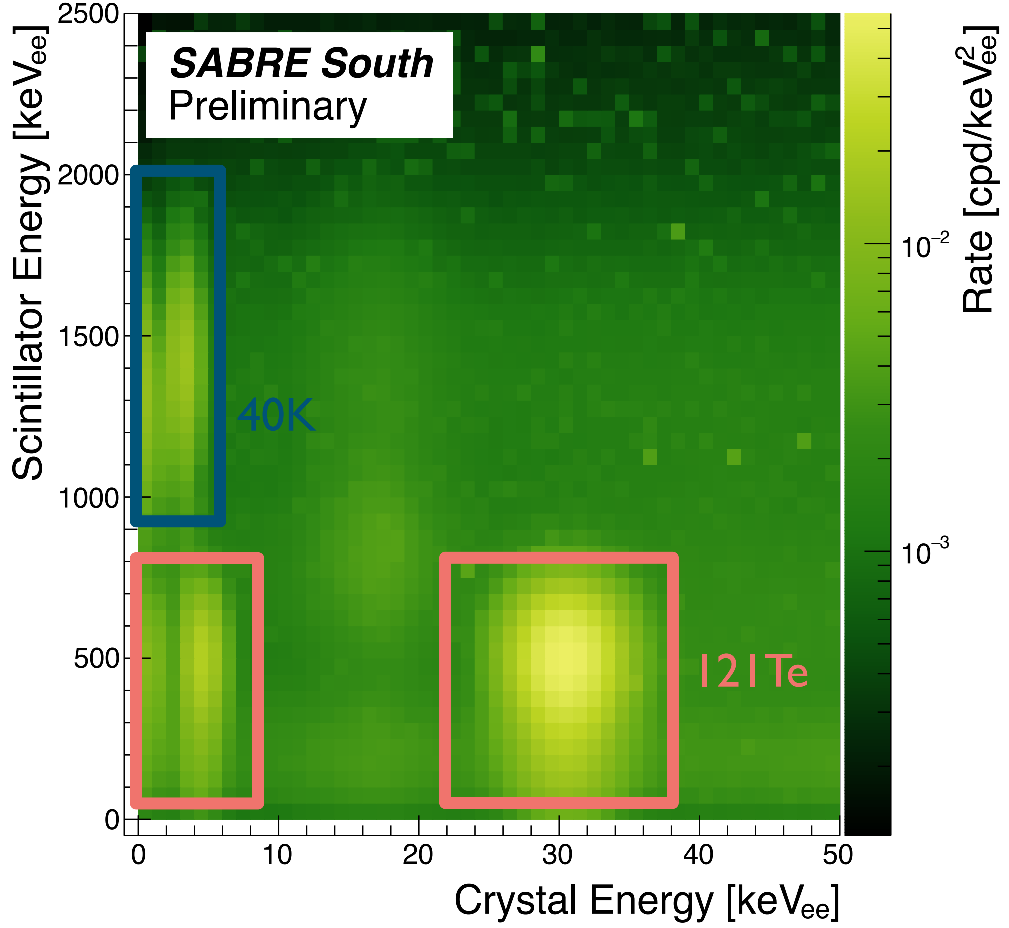

E.g., 40K and 121Te both have distinct islands in crystal-scint energy plane

Rate in crystals

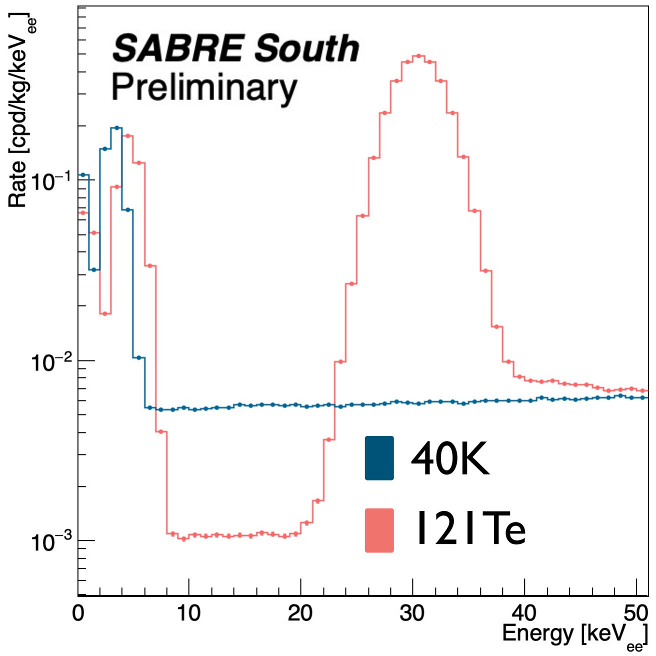

Rate in liquid scintillator

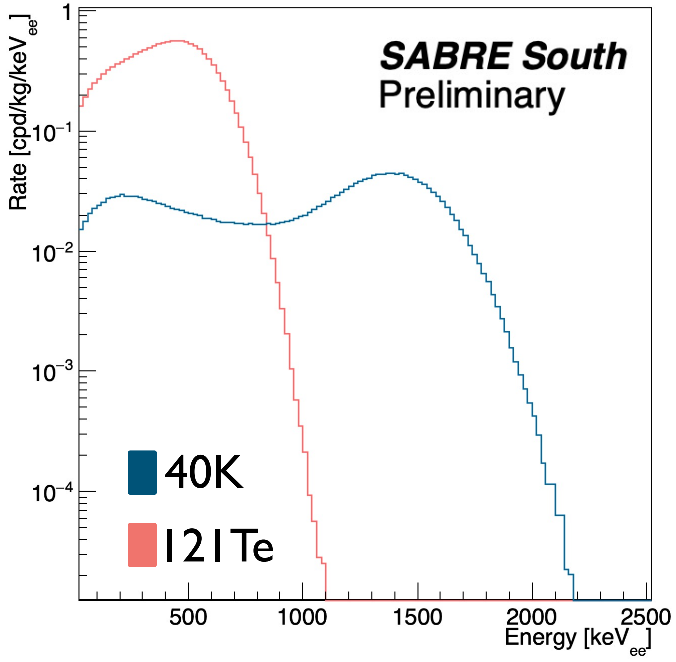

TOTAL BACKGROUND MODEL

[1] SABRE South Collab. arxiv:2205.13849

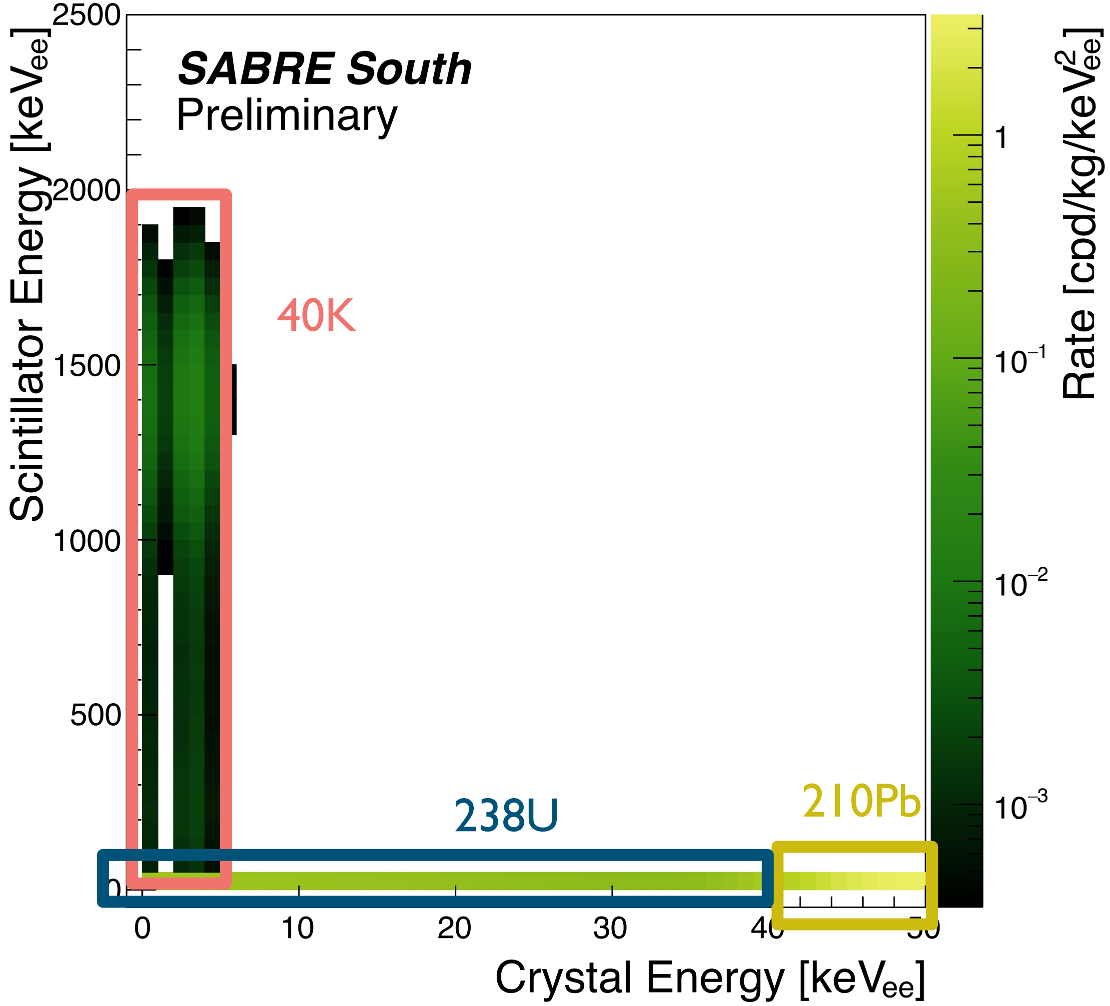

Contamination from intrinsic radiation of crystals

Deposition in crystal

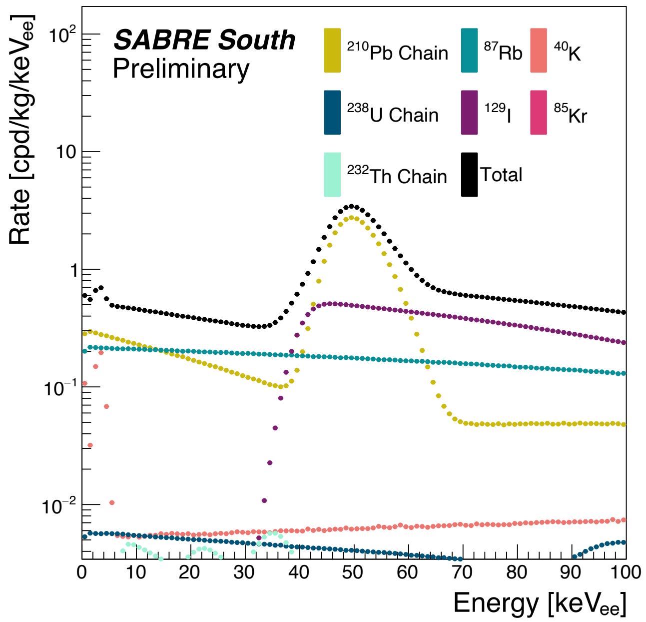

Deposition in veto

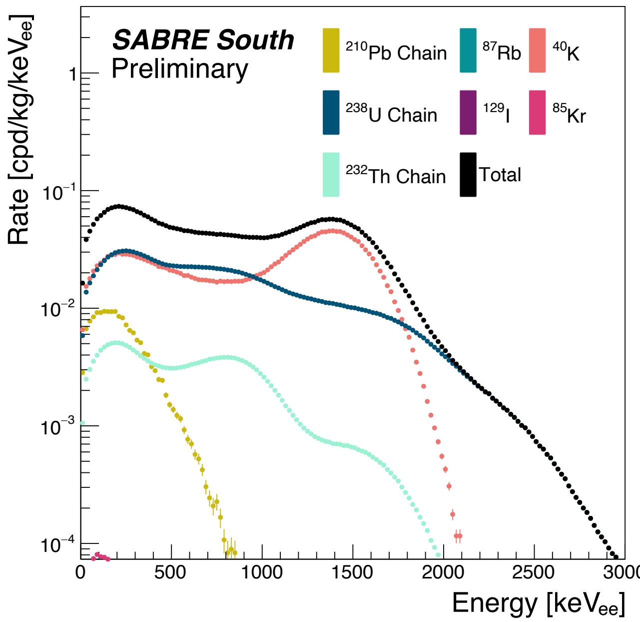

TOTAL BACKGROUND MODEL

[1] SABRE South Collab. arxiv:2205.13849

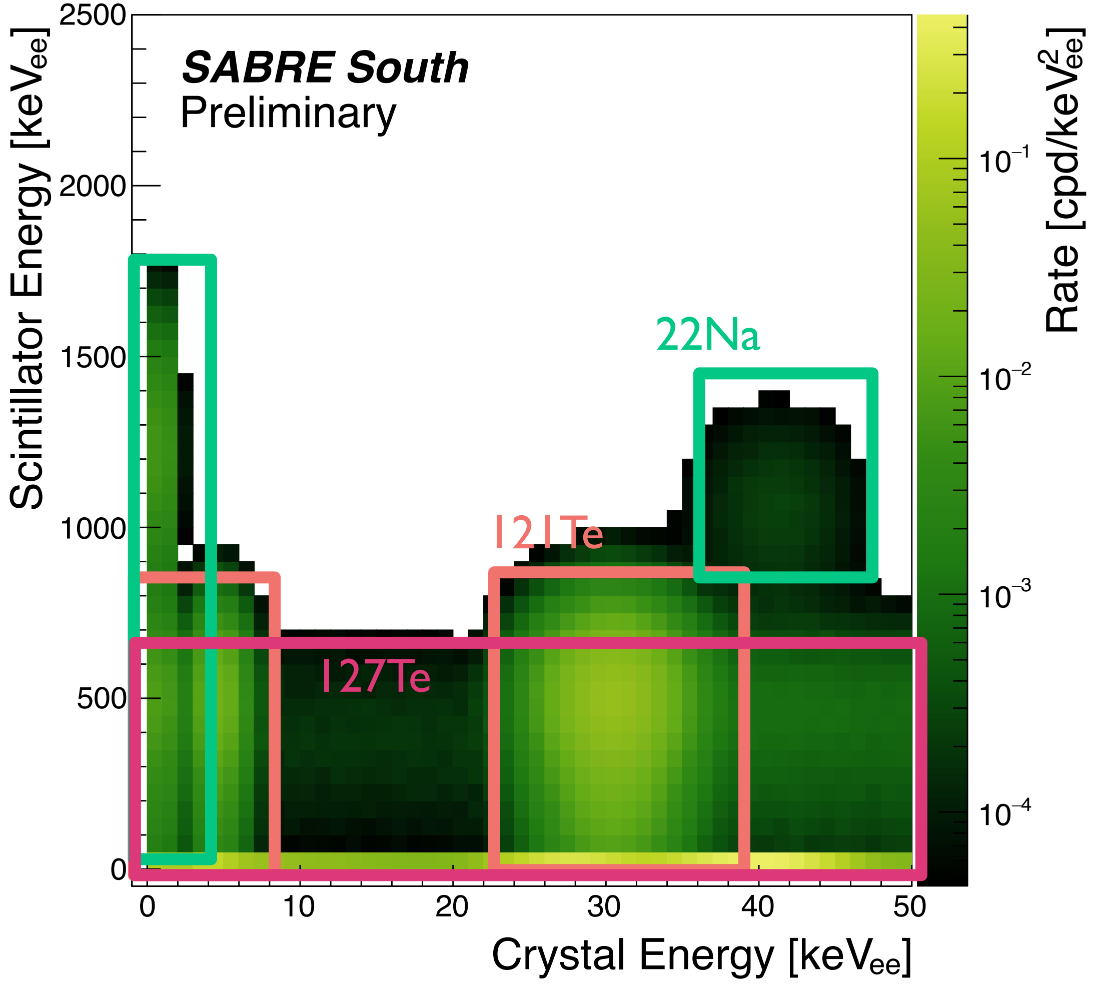

Contamination from cosmogenic activation of crystals

Deposition in crystal

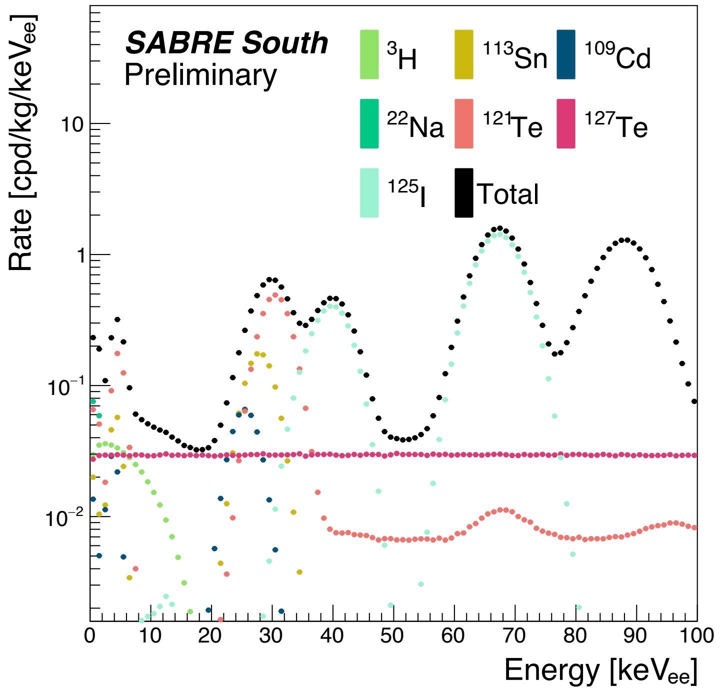

Deposition in veto

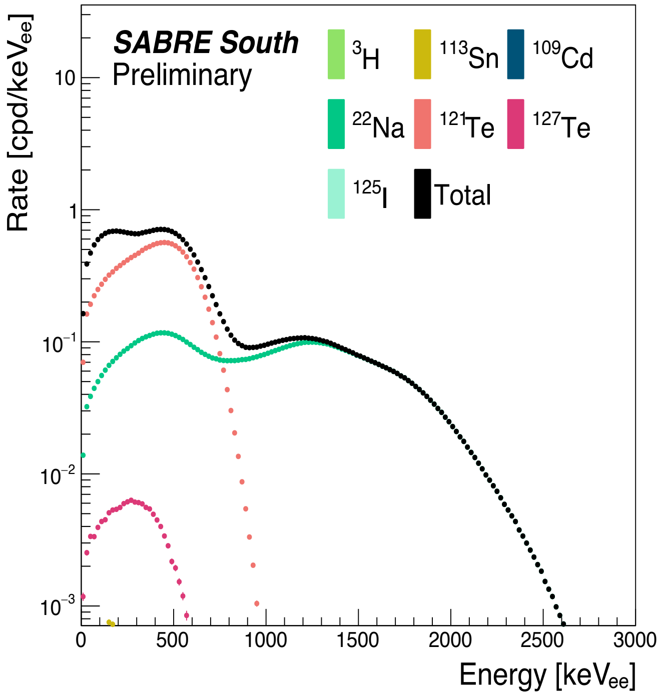

PROBABILITY RECONSTRUCTION

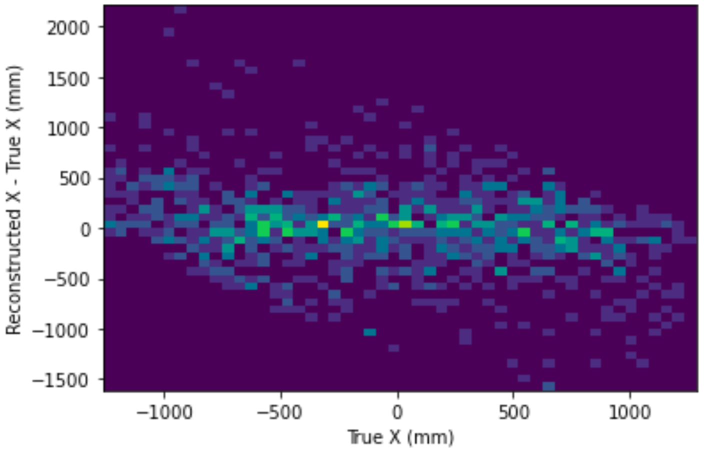

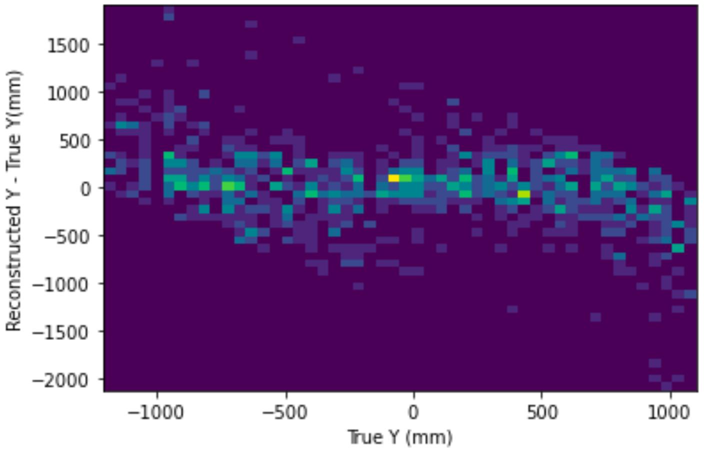

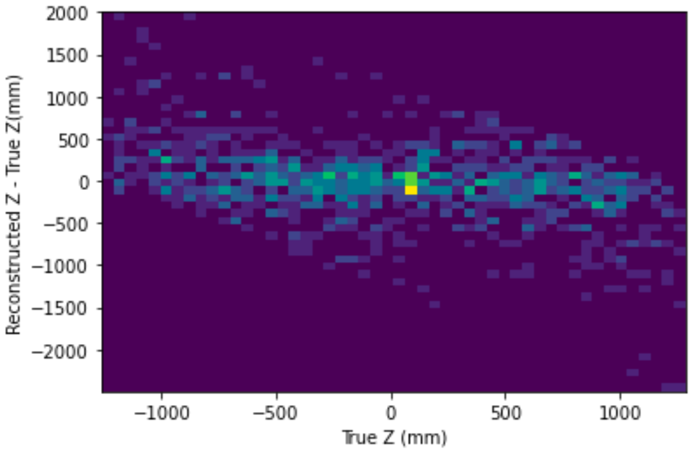

Av. uncertainty in position is ~30 cm

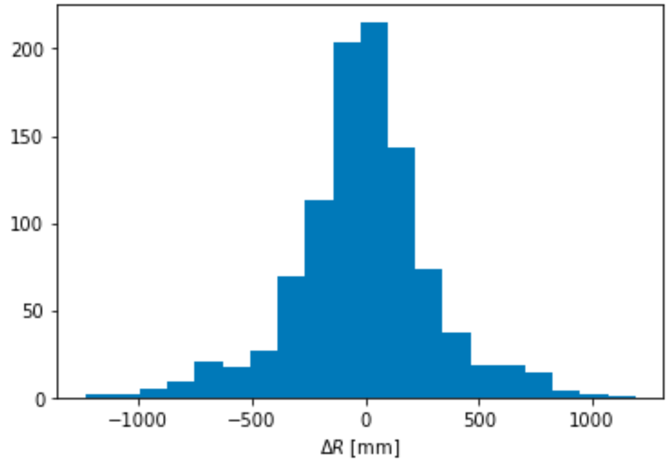

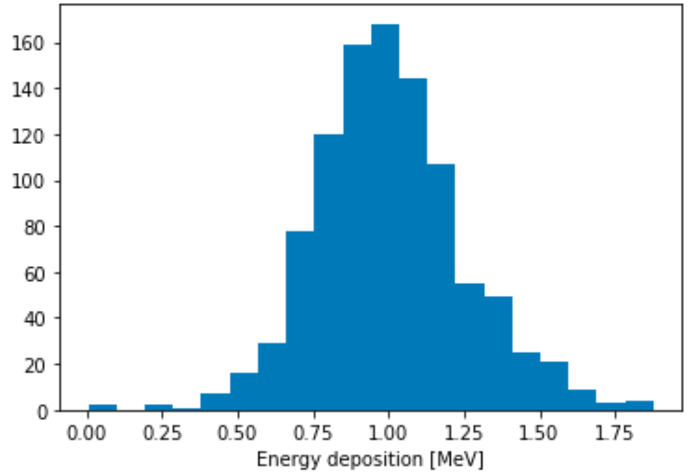

Av. uncertainty in energy is 0.25 MeV

WAVEFORM SIMULATION

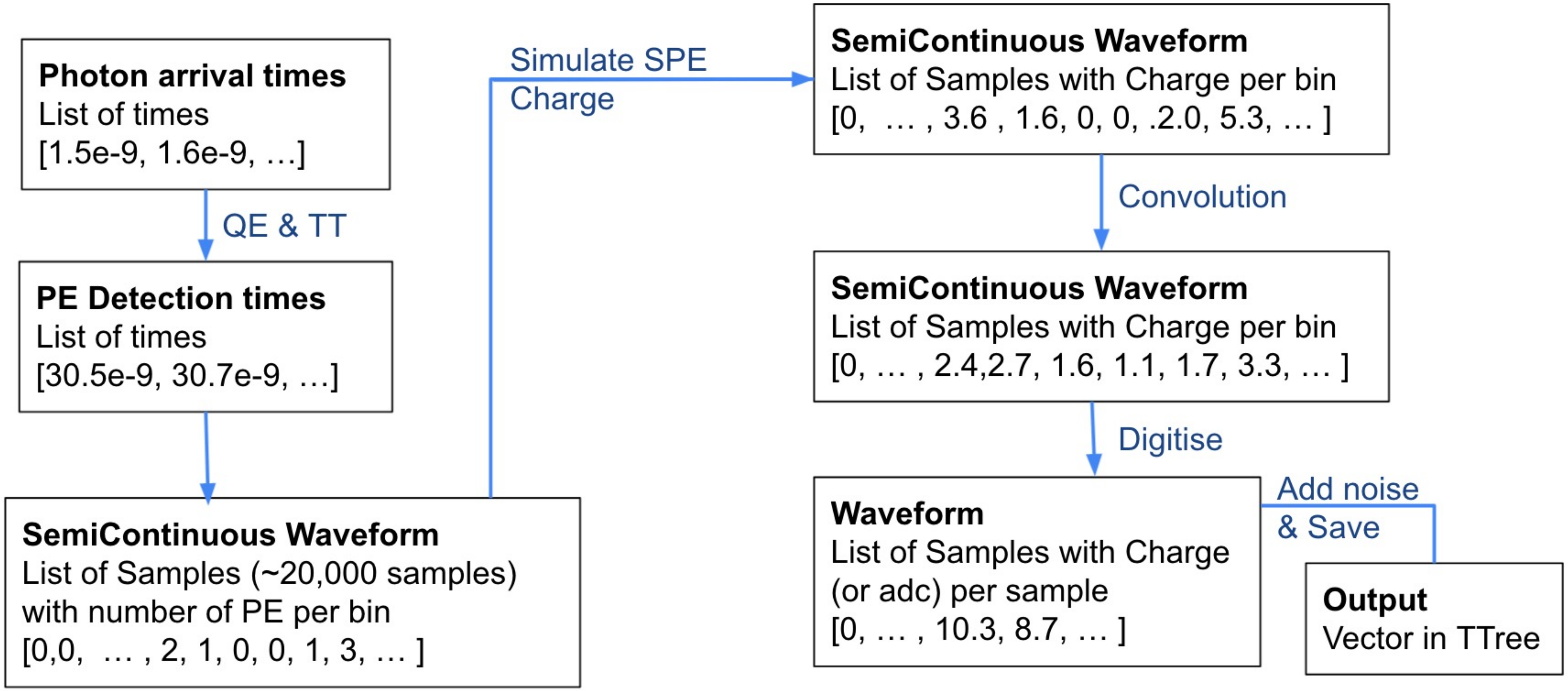

WAVEFORM SIMULATION

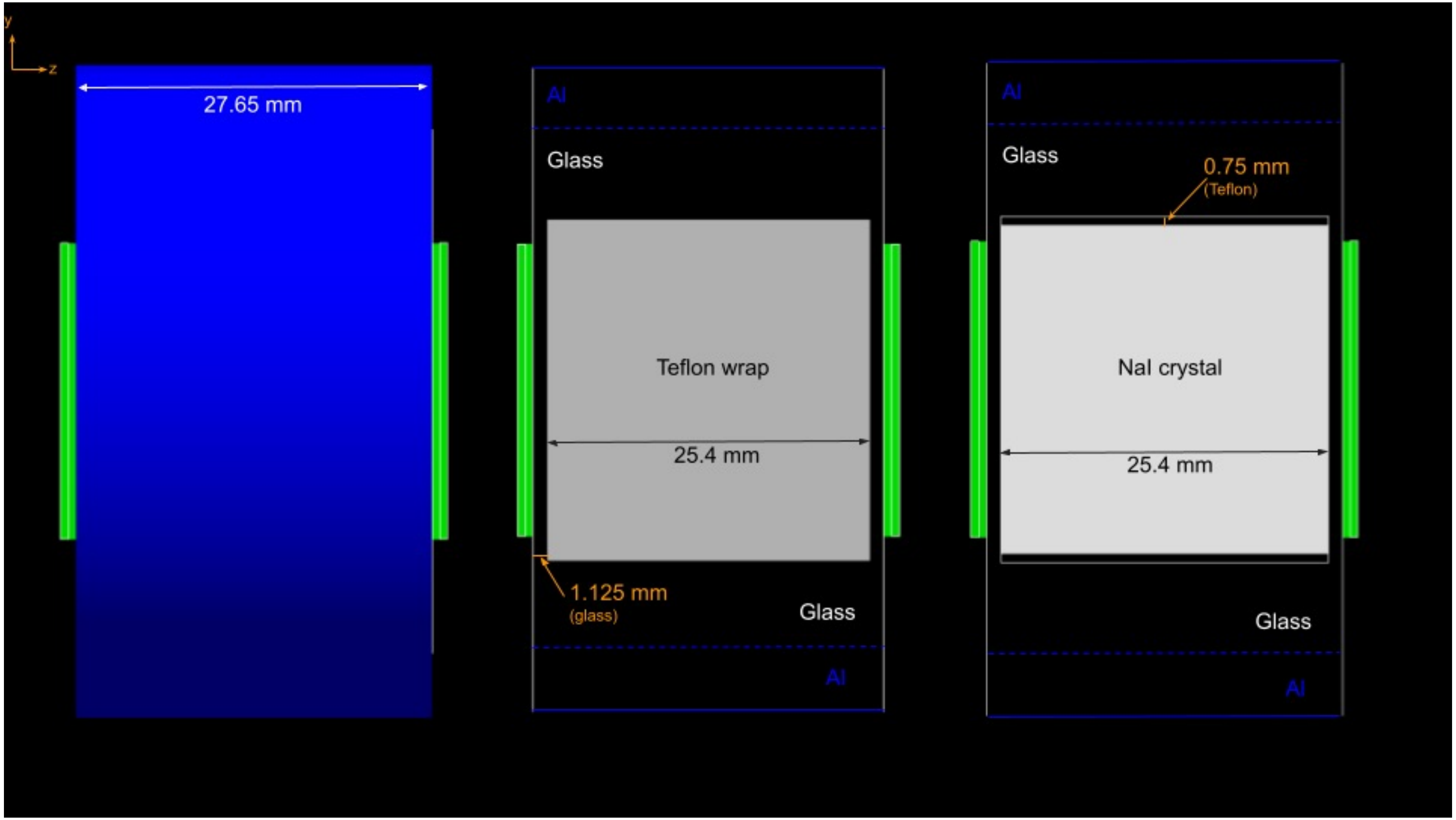

WAVEFORM SIMULATION